METABOLOMIC FINGERPRINTING OF PRODUCTION ANIMALS UNDER GENETIC SELECTION AND CHEMICAL EXPOSURE

A Dissertation

SUBMITTED TO THE FACULTY OF THE

UNIVERSITY OF MINNESOTA

BY

YUE GUO

IN PARTIAL FULFILLMENT OF THE REQUIRMENTS

FOR THE DEGREE OF

DOCTOR OF PHILOSOPHY

DR. CHI CHEN, ADVISOR

October 2022

Acknowledgments

First and foremost, I would like to express my gratitude to my advisor Dr. Chi Chen for his invaluable advice, continuous support, and patience during my Ph.D. study. His immense knowledge and plentiful experience have encouraged me all the time in my academic research. Without his advice, my studies and research projects would have never been accomplished over these past years.

I would like to thank the rest of my thesis committee, Drs. Xiaoli Chen, Daniel Gallaher, Brian Crooker, and Luciano Caixeta. I want to thank them for their insightful advice and generous help with my projects.

My sincere thanks also go to my previous and current lab members, Dana Yao for the countless help with instructions on the instrument and trouble-shooting; Dr. Lei Wang, Dr. Yiwei Ma, Dr. Yuyin Zhou, Dr. Jieyao Yuan, Wes Mosher, Qingqing Mao, Junwei Zhang, and Rachel Su for their help to my experiments. I would also like to thank Wanda Weber, who provided help with animal studies and statistical analysis.

Finally, I would be remiss in not mentioning my family and friends for providing me with unfailing support and continuous encouragement throughout my years of studying. Their belief in me has kept my spirits and motivation high during this process. I would also like to thank my cat for all the entertainment and emotional support.

Abstract

Metabolic performance contributes to the health and productivity of production animals through its associations with endogenous metabolic status and energy converting efficiency from feed to body mass. Genetic selection and chemical treatments are the common intrinsic and external approaches utilized in practice to improve the metabolic performance of production animals through altering their metabolic performance. These manipulations are expected to elicit diverse and unexpected metabolic events across different functional components of production animals, therefore posing challenges in the identification and characterization of the most significant metabolic changes as well as their underlying mechanisms. Metabolomics, as a high-throughput platform capable of detecting both subtle and extensive metabolic changes in a complex biological system, is being utilized to examine the altered metabolic performance of production animals. In this project, the most prominent metabolic events elicited by genetic selection and chemical exposure (rutin and oxidized oil) in dairy cows and pigs were examined by liquid chromatograph-mass spectrometry (LC-MS)-based metabolomic fingerprinting and biochemical analyses, resulting in the following novel knowledge: (1) The increased incidence of hepatosteatosis in Contemporary Holstein (CH) might be induced by the insufficient biotransformation of choline to phosphatidylcholine, instead of choline deficiency. The lack of phospholipids in the liver prevents the incorporation of triacylglycerols into very-low density lipoprotein (VLDL) for lipid export, causing fatty liver and lipid metabolism disorder primarily during the parturition or early lactation (2) Rutin, a health-promoting natural flavonol, undergoes extensive ruminal microbial metabolism in dairy cows, forming 4-methylcatechol as a dominant, bioavailable, and

bioactive metabolite. In addition, the biotransformation of rutin to 4-methylcatechol inhibits the microbial metabolism of tyrosine to *p*-cresol, a toxic and odorous compound in animal production. (3) Feeding oxidized oil selectively affects amino acid metabolism in pigs through transcriptional regulation and direct chemical reactions which results in changes in redox balance and compromises growth performance. Overall, these results demonstrate the capability of metabolomic fingerprinting as a highly efficient tool for examining the metabolic events induced by genetic selection and chemical exposure and provide guidance for developing new approaches and practices to enhance the productivity and health of production animals.

Table of Contents

List of Tables

List of Figures

Appendix

CHAPTER 1. LITERATURE REVIEW

1.1 ESSENTIAL ROLES OF METABOLISM IN PRODUCTION ANIMAL PERFORMANCE

1.1.1 Need for more efficient animal production

The global demand for food has increased dramatically in this new millennium since the human population in the world has increased from 6.5 billion in 2005 to 7.9 billion in 2021, and will further increase to around 9 billion by 2050 based on the prediction by the Food and Agriculture Organization (FAO) of the United Nations [1]. Meanwhile, raising incomes and urbanization are shifting the composition of human diet to a higher percentage of animal products, through the consumption of meat, milk, and egg. The FAO predicts that between 2005 and 2050, human consumption of animal products will double while human consumption of cereal grain will remain stable [1]. Nevertheless, animal consumption of cereal grain will increase dramatically since cereal grain is the staple ingredient in animal feed. Because energy loss is inevitable in the conversion from cereal grain to animal biomass in animal production, improving the metabolic performance of production animals will be crucial in the upcoming decades to meet the increased demands for animal products and the sustainability of world food supply.

1.1.2 Current status of metabolic performance of production animals

Dairy and beef cattle, swine, and poultry are the main sources of animal products in the United States, covering the demands on milk, meat, and egg in human diet. Industrialized operation system of production animals has been progressing with the innovations in animal breeding, nutrition, management, and husbandry systems, resulting in a dramatic increase in productivity in the last 40 years as the consequence of improved metabolic performance. The improvements in metabolic performance that occurred to the major species of production animals are summarized as follows.

1.1.2.1 Dairy cow

Technological innovations in genetics and management have dramatically increased the efficiency of milk production in the U.S. dairy industry over the past decades. A notable achievement is milk production which was 76 billion kilograms in 2000 and is 45% greater than that of 1950 (**Table 1.1**). Although the total milk production was comparable between 1975 and 1950, the number of dairy cows for milk production was almost half in 1975 thus milk production per cow was largely improved by around 2 times compared to the cow in 1950. This improvement in production efficiency continued to increase from 1975 to 2000 as an 18% decrease in dairy cow number was associated with a 76% increase in average milk production per cow (**Figure 1.1**). Overall, the average dairy cow produced 3.42 times more milk in 2000 compared to that in 1950 [2]. Moreover, current genetic selection (**Figure 1.5**) and improved nutrition also increased milk fat content associated with milk production per dairy cow per year. In comparison to 1950 (**Figure 1.2**), average milk production per cow largely increased to 10,000 kg in 2021 [3], while milk fat also increased by 300 kg in 2015 than in 1957 [4].

1.1.2.2 Swine

Significant productivity improvements have been achieved in the swine industry over the last 35 years (**Table 1.2**) [5]. For growth performance, the number of marketed pigs, average market weight, average daily gain, and carcass weight were significantly increased from 9.2 to 22 pigs per sow; from 242 to 283 lb at slaughter; from 1.27 to 1.61 lb/d average daily gain; and from 171 to 212 lb carcass weight, from 1980 to 2015, respectively. In addition, the feed conversion ratio during the grow-finishing phase decreased from 3.28 to 2.45 kg of feed per kg of animal body mass from 1998 to 2016 [6,7], suggesting an increase in feed efficiency. Notably, during this same interval, back fat content was largely decreased from 1.0 to 0.72 inches, while loin area increased

from less than 5.0 in^2 to large than 8.0 in^2. These decreased fat content and increased lean meat resulted in a 38% increase in pork production with only a 10% increase in the number of animals harvested.

1.1.2.3 Poultry

Egg and meat are major products of poultry, especially chicken, which comprise a large proportion of the poultry industry. Minnesota grows around 45 million turkeys per year, which composes 18% of the turkey supply in the U.S. The development of the modern poultry production system since the 1950s has led to dramatic improvements in animal numbers and growth performance. In 2019, approximately nine billion broiler chickens (chicken for meat production) were raised in the US [8]. Their growth rate has increased 3-fold from 25 to 100 g body weight per day since the 1950s [9] while breast muscle mass weight increased two-fold [10]. In addition, the average age at slaughter decreased from 112 to 47 days, while the average weight at slaughter increased from 2.5 to 5.8 lb from 1925 to 2021. These data reflect the tremendous increase in feed efficiency from 4.7 to 1.79 lb feed per lb eggs achieved from 1920 through 2020 (**Figure 1.3**) [11].

As for egg production, industrialization increased the annual number of eggs 3-fold from 1925 to 2015 (**Figure 1.4**). Reduced age is another improvement of productivity in the egg industry, as the average age of first egg production in laying hens decreased from 183 to 139 d from 1950 to 2000 with no influence on egg size [12]. At present, the number of eggs produced by a commercial hybrid breed laying hen developed through selectively cross-breeding is between 180 to 200 per year, and laying hens produce eggs from 147 d to 532 d [13,14]. Moreover, the feed efficiency of laying hens was greatly improved from 1960 to 2010, with a 26% decrease in daily feed usage

and a 42% increase in feed conversion from 3.44 to 1.98 lb feed per/lb egg (**Table 1.3**) [15].

Significant improvements in milk, meat, and egg production are the results of continuous improvements in animal growth, health, and the conversion of feed to animal products. These improvements have been achieved in the past decades through the manipulation of animal breeding and the optimization of nutrition and management. An indispensable contributor to these improvements is the metabolic system in production animals. The metabolic system is responsible for converting nutrients from feed to energy and metabolites and then transforming them into biomass that represents animal production. The metabolic system is also highly responsive to nutrients and environments through the modulation of genes, proteins, and metabolites (**Figure 1.6**). Therefore, understanding metabolic performance based on metabolic system and metabolic changes is essential for characterizing the mechanisms underlying and regulating the enhanced performance of production animals.

1.2 METABOLIC SYSTEM IN PRODUCTION ANIMALS

1.2.1 Components

To detect metabolic events and how they contribute to metabolic functions, major reactions and components of the metabolic system need to be delineated. Anabolic and catabolic reactions contribute to the transformation of energy and nutrients from the feed into a useable source for the animal. In the digestive tract and in the body, these biotransformations generate metabolites that can be used for animal maintenance and growth. Some of the major tissue compartments or organs involved in this process will be discussed.

1.2.1.1 Gastrointestinal tract

The gastrointestinal tract (GIT) is a series of open organs starting from the mouth to the anus, it contains all of the major organs for digestion and absorption. Gut health and its effective functionality are important factors to determine the performance of production animals because it is a place experiencing nutrient acquisition, metabolism, disease defense, microbiome homeostasis, and other physiological activities. Under the biological aspect, a large number group of physiological events and biochemical reactions happen in the GIT, which involves host energy metabolism, immune response, and protection of exogenous pathogens. Therefore, modulation of metabolism and physiological homeostasis to develop a healthy gut plays a key role in animal growth performance and health although it is not directly caused by an enhanced performance or productivity in animals.

1.2.1.2 GIT Microbiome

The microbiome is a microbial environment composed of an assortment of gut-colonized microbes and their metabolic products in the GIT of humans and other animals as well as the rumen of ruminants [16]. A highly diverse and complex microbiome plays a crucial role in host health, compositional changes in metabolic products or alternation in microbes are related to multiple metabolic events in the host, including energy metabolism, immunity, and physiological activities that might further induce both positive or negative effects on the host's health [17-20].

In production animals, extensive studies in sequencing the microbial composition and identifying the effects of nutrients on microbe metabolism had been conducted in cow rumen, pig large intestine, and chicken cecum [21-23]. In general, microbes can utilize nutrients in the GIT of the host, such as undigested or unabsorbed nutrients (carbohydrates or amino acids) for their metabolism

that could provide extra energy harvest for the host. For example, some plant polysaccharides, which are not able to be practiced by digestion enzymes, are fermented by microbes to produce the end fermentation product short-chain fatty acids (SCFAs). Acetic acid, propionic acid, and butyric acid are major SCFAs produced during carbohydrate fermentation with a ratio of 3:1:1, they can be absorbed by colonocytes mainly through monocarboxylate transporter 1 (MCT-1) or sodium-dependent monocarboxylate transporters 1 (SMCT) [24]. Among them, butyric acid is the primary energy source of colonocytes and it also functions in maintaining the homeostasis of colonocytes [25], while most of the acetic acid and propionic acid are transported through portal circulation and further used by hepatocytes [26]. In particular, propionic acid and butyric acid are resolutions for chronic diseases, including inflammatory bowel disorder, obesity, and diabetes through the activation of G-protein-coupled receptors (GPCRs) [27]. According to these research findings, diet and fiber content play important roles in regulating microbiota and therefore influence gut health as well as animal performance. Except for the diet, other factors can also initiate alternation of the microbiome, such as stress, regrouping, hygiene condition, and management [28,29].

1.2.1.3 Blood

Blood is composed of plasma, blood cells, and cell fragments called platelets, it is the major place responsible for maintaining the homeostasis of the body by regulating temperature, pH, osmotic pressure, and nutrient exchange. The plasma contains water, lipids, glucose, proteins, and salts that enable the carrying and exchanges of nutrients, signal molecules, and metabolic wastes across different organs, such as the liver, kidney, and intestine, to support endogenous metabolism. Hemoglobin in red blood cells is capable to circulate oxygen and carbon dioxide throughout the circulatory systems, while white blood cells involve in the immune response.

1.2.1.4 Liver

The liver functions as a communicator between the digestive tract and peripheral tissues, and it plays a central role in endogenous metabolism in humans and other animals by modulating functions of digestion, nutrient transport and storage, metabolism, cell detoxification, and immune function [30]. The most significant function of the liver is nutrient metabolism, covering carbohydrate, protein, and lipid metabolism. Nutrients absorbed by the digestive system are imported to the liver through the portal vein and exported to other tissues through the hepatic vein, meanwhile, nutrients are handled by the liver by a series of anabolic and catabolic reactions.

1.2.1.5 Mammary gland

The mammary gland is the functional organ designed to synthesize and produce milk, it plays a central role in lactating animals for dairy production, in particular dairy cows. Cow milk is recognized as a nutrient-dense food with enriched macronutrients and micronutrients. Generally cow milk contains 85-87% water, 5% lactose, 3.8-5.5% fat, 2.9-3.5% protein, and minerals [31]. Besides, it is also a good food source of protein, vitamin A, vitamin D, riboflavin, vitamin B12, calcium, phosphorus, and potassium [32].

1.2.2 Functions and regulations

1.2.2.1 Gastrointestinal tract

Carbohydrate digestion in the GIT. The primary function of GIT is for digesting a diet or feed into small molecules by endogenous digestive enzymes and microbiome fermentation before absorbing them into the body. Initial digestion of carbohydrates begins with α-amylase, an endosaccharidase in saliva, which is specific for breaking α-1,4 glycosidic bonds of complex carbohydrates [33]. Salivary α-amylase keeps digesting carbohydrates until food enters into the

stomach, where the digestive enzyme activity of salivary α-amylase is inactive by the acid environment. When food reaches the small intestine, pancreatic juice containing bicarbonate and pancreatic α-amylase neutralizes gastric acid from the stomach and continues to break down carbohydrates into di-, tri-, and oligosaccharides, which are further broken down by disaccharidases in the plasma membrane of the brush border of intestinal epithelial cells [33]. Disaccharides functions as membrane digestion of disaccharides to produce monosaccharides that are absorbed by membrane transporters of intestinal epithelial cells. D-glucose and D-galactose can be taken by Na+ - glucose transporter 1 (SGLT1) or glucose transporters (GLUTs) through active transport or facilitated diffusion [34].

Protein digestion in the GIT. Proteins from the diet or feed are broken down firstly in the stomach by the protease, pepsin. Pepsin is secreted by gastric chief cells in the form of pepsinogen, with the activation of gastric acid, pepsinogen is cleavaged to become active pepsin in the stomach that hydrolyzes proteins into smaller polypeptides. In addition to the enzymatic digestion by pepsin, gastric acid can also denature proteins, this step results in processing unfold proteins and providing better access locations for proteases attaching [35]. When the partially digested food enters into the small intestine, pancreatic proteases, including trypsin, chymotrypsin, elastase, and carboxypeptidase, cut polypeptides into oligopeptides and amino acids. Aminopeptidases located on the brush-border membranes can hydrolyze oligopeptides into free amino acids, di- and tripeptides, which are uptake by amino acid transporters in the membrane of absorptive enterocytes.

Lipid digestion in the GIT. Lipid digestion starts with lingual lipase in the month, the digestion process continues to the stomach with gastric lipase. In the small intestine, lipases in pancreatic

enzyme secretion retain digestion of dietary fats. Lipases hydrolyze lipids to release free fatty acids from the glycerol backbone and emulsify lipid droplets to missiles that stabilize lipids with coating bile salts, phospholipids, and cholesterols [34]. After this processing step, the lipid droplets increase their surface area, which provides them easily accessible to enzymes for further digestion and absorption. Later on, fatty acids enter into the intestine by diffusion across the bilayer membranes or infused into the cell membrane lipid. For long-chain fatty acids and cholesterol, its uptake is facilitated by transporters, fatty acid translocase (FAT) and Niemann-Pick C1-Like 1 (NPC1L1), located on the membrane of enterocytes.

Other functions of GIT. The importance of a healthy GI tract directly reflects on growth and development in all stages of animals, especially in young animals through the interaction between nutrient digestion and absorption from feed and GIT. Except for the major function of nutrient digestion and absorption, GIT also functions as a defensive system that protects the host against environmental antigens or pathogen infection through its barrier function. In addition, the immune function of GIT is observed since it harbors gut-associated lymphoid tissue, a major component of mucosal-associated lymphoid tissue that covers 70% of the entire immune system and 80% of plasma immunoglobulin A-bearing cells [36].

GIT, microbiome, and gut health. Gut mucosal is a specific structure composed of a single layer of epithelium and a layer of mucus spread over the surface of the epithelium, where the microbiome colonized on the surface of mucous, and it interacts with the GIT and diet that ensure the effective functions of the digestive system [37]. Therefore, the homeostasis of the microbiome, diet, and gut mucosa is critical for gut health and animal performance. Understanding the

interaction between these key factors will clarify the effect of a healthy gut on the performance and productivity of production animals.

Due to the key role of diet in the digestive system, the ingredient, nutrients, and additives of diet or feed can have a significant influence on the development and functions of the GIT through regulation of energy metabolism, microbial metabolism, and immune response. On one aspect, nutrient imbalanced diet or diet antinutrients, such as certain types of dietary fiber, phytate, lectins, mycotoxins, and pathogenic microorganisms, can reduce the performance of animals by suppressing nutrients digestion and absorption in the GIT and might further compromise gut integrity and function [38]. However, a fiber-enriched diet provides a better source for the gut microbiome to undergo the fermentation process that might covert unabsorbed compounds into energy or other health-promoting metabolites to the host. On the other aspect, supplementation of nutraceuticals in the diet has beneficial effects on maintaining animal health and performance. For example, antioxidants, are frequently supplemented in the diet of production animals in preventing negative effects of excessive reactive oxygen species (ROS) formation, significant improvement in milk and meat quality of ruminants was achieved by this strategy [39]. Moreover, other feed nutraceuticals, such as ZnO, vitamin, mineral, amino acids, organic acid, and plant source additives, were found to have significant benefits on animal performance and gut health through diminishing stress-induced gut inflammation[40-44] or by regulating gut microbiome to stimulate gut development and immunity [45,46].

1.2.2.2 GIT microbiome

Microbiome metabolism in ruminants. In ruminants, the microbiome in the rumen effectively converts plant polysaccharides, which are not able to be practiced by digestive enzymes in the

GIT, to SCFAs, microbial protein, and gases. Because the ruminal microbiome displays a high abundance of cellulolytic microbes containing diverse enzymes to hydrolyze the side chains of plant polysaccharides, such as cellulose, hemicellulose, pectin, and oligosaccharide [21]. Under this environment, a unique system for ruminants to produce energy and biofuels through the degradation of plant sources feed by microbial enzymes is created in which a significant amount of energy is produced by ruminal microbial fermentation. In particular, SCFAs are considered as a predominant energy source for ruminants compared to monogastric animals, it contributes 70% of the total energy requirement in ruminants versus 10% in humans, respectively [47,48].

Microbiome metabolism in monogastric animals. Different from ruminants, most of the microbes colonize in the large intestine of pigs, where the most abundant bacteria are *Firmicutes*, *Bacteroidetes*, *Proteobacteria*, *Actinobacteria*, and *Spirochaetes* [49]. Among these bacteria, *Firmicutes* and *Bacteroidetes* count for approximately 90% of all bacteria in the pig microbial genes fecal microbiome. According to the result of metagenomics analysis of the pig microbiome, the most abundant microbial species are involved in carbohydrate metabolism [50], suggesting the importance of the microbiome in the digestion of plant-sourced feed. In the chicken cecum, the dominant phylotypes of microbes are *Firmicutes*, *Bacteroidetes*, and *Proteobacteria* [23]. Previous microbiome studies in monogastric animals demonstrated that SCFA can improve growth performance and carcass quality of chicken [51], improve health and reduce intestinal inflammation in pigs [52]. In addition, the composition of pig intestinal microbiomes is consistent with chicken intestinal and cow ruminal microbiomes, suggesting the potential capacity of the metabolic system in production animals by utilizing fibers in conversion into energy.

1.2.2.3 Blood

The functions of blood in supporting growth are mainly the distribution of nutrients and hormones to other tissues as well as the elimination of cell-produced metabolic waste. Due to the diverse nutrient composition and functions of the blood, changes in blood parameters, such as protein, lipid, and glucose, are closely related to animal growth conditions [53-56]. Therefore, the characterization of blood nutrient status is a pivotal indicator to evaluate the metabolic system in production animals that further indicates their growth and health.

1.2.2.4 Liver

Carbohydrate metabolism in the liver. In carbohydrate metabolism, the primary function of the liver is stabilizing blood glucose levels under a narrow, normal range. If excess glucose enters into the blood after a meal, the liver can remove the blood glucose and store it as glycogen. On the contrary, the liver can also release glucose into the blood by breaking down hepatic glycogen under low blood glucose levels, which is critical for production animals.

Protein metabolism in the liver. The liver is a major organ that regulates amino acid metabolism. Through deamination and transamination, some amino acids are converted to other amino acids, glucose, or lipids by removing nitrogenous parts. Some enzymes involved in these metabolic reactions are commonly used as a diagnosis in serum to access liver damage, such as alanine aminotransferase or aspartate aminotransferase [57]. During the process of removal of nitrogenous parts from amino acids, a toxic compound called ammonia is produced, while liver cells can convert ammonia to urea, which is released into the blood and further excluded from the body with urine.

Lipid metabolism in the liver. The liver is also the major organ where fat metabolism predominantly happens. On one aspect, triacylglycerols (TAGs) intake from the digestive system or plasma non-esterified fatty acids (NEFA) are oxidized by the liver to produce energy. On the other aspect, *de novo* lipogenesis occurs in the liver, TAG is exported from the liver to other tissues through the incorporation of very-low-density lipoprotein (VLDL), this lipid dispensable mechanism regulates lipid and energy metabolism [58].

Due to the indispensable function of the liver in metabolism, liver dysfunction has been observed to reduce feed intake, growth, and development in production animals [59]. Hence, the characterization of metabolic changes in the liver is recognized as an effective method to access the metabolic performance and health of production animals.

1.2.2.5 Mammary gland

Milk biosynthesis in the mammary gland. Mammary epithelial cells are the location that transforms nutrients from the circulation system into milk through a series of biosynthesis reactions. Lactose is synthesized from UDP-galactose and glucose and catalyzed by lactose synthetase, which is composed by the conjunction of A and B proteins [60]. B protein also called α-lactalbumin (α-LA), is originally located in the endoplasmic reticulum that passes to the Golgi apparatus and regulates A protein, while, A protein catalyzes the lactose synthesis reaction [61]. Milk protein is constituted by casein 80% and whey protein 20% of total proteins in cow milk, in which casein is classified as αS1-, αS2-, β-, γ-, and κ-casein, while α-lactalbumin and β-lactoglobulin are the major whey proteins [62]. The predominant composition of cow milk lipid is triacylglycerol, approximately 98%, other lipids are also found including 0.5-1% of phospholipids, 0.5% cholesterol, and 0.1% free fatty acids [63].

During lactation periods, mammary gland epithelial cells synthesize and secrete these nutrients into milk through milk-lipid droplets. Firstly, lipids, such as triacylglycerols, are synthesized in the endoplasmic reticulum. Associating with the synthesized lipid assembly, a microlipid droplet (less than 0.5 μm) is released from the reticular membrane into the cytoplasm and further coated with bilayer phospholipids and protein [64]. Thereafter, lipid droplets further aggregate into large droplets (around 1 μm or larger) in the cytoplasm, however, some of the milk droplets don't change their size and it is secreted as microlipids [64]. Eventually, the droplet is secreted from the apical membrane of mammary gland epithelial cells. Milk-fat globule membrane plays an important role in the final droplet membrane formation and release. Overall, the mammary gland shows an indispensable role in transforming nutrients into milk components.

1.3 COMMON APPROACHES FOR IMPROVING THE METABOLIC SYSTEM IN PRODUCTION ANIMALS

To increase the productivity of production animals, diverse approaches had been applied to promote animal growth performance and health through manipulating metabolic systems that enhance productive traits, optimize energy transformation from feed, and reduce extra energy expenditure for diseases. These approaches can be classified as internal and external modifications for improving metabolic performance in production animals.

Intrinsic modifications, such as genetic selection for high productive traits in production animals, have been used in the modern animal industry that processes the selection of highly productive animals individuals with higher biotransformation of their metabolic system from the populations. Besides, some other external approaches, such as modulating feed composition by adding essential nutrients or non-nutrient compounds, to maintain a stable environment and reduce stress,

are also able to improve metabolic performance and decrease energy expenditure. Both intrinsic and external modifications will be discussed.

1.3.1 Intrinsic modification: Genetic selection in production animals

After the domestication of the ancestor of production animals, farm animals experience a series of selection managed by human beings, not only for manageability and docility but specifically for breeding purposes in improving production traits, including milk production, growth rate, and egg numbers. The original aims of selection focused on animal's phenotype in which their offspring was expected to inherit a superior phenotype from the ancestor. Until the mid-20th century, quantitative genetics occurred and was considered as an advanced method to promote animal selection practice because it was supported by modern statistical theory and principles of heredity [65]. Thus, the likelihood of an individual in transmitting the favorable set of alleles for the trait of interest and thereafter expressed as the phenotype is calculated by quantitative genetics and applied to production animal selection [66]. Animal breeding has been applied to many species, such as dairy cows, broiler chickens, egg-laying chickens, and pigs.

History of genetic selection in production animals. The breeding of dairy cows started with selecting purebred Holstein with high milk production trait, continuous selection activity ultimately resulted in Holstein cows carrying high milk yield character in the modern population [67], and the milk yield trait presents approximately 50% of the total index during selection [4]. Broiler chicken breeding was conducted by selecting specifically for growth-related production traits, for example, heavy body weight and massive breast size as well as fast growth [68]. The modern chicken experienced intensive artificial selection and resulted in a selected "Cornish Cross" breed chicken [69]. Laying hens improved breeding programs by selecting high-produced

laying species starting with Single Comb White Leghorn hens [70]. Unlike selecting purebred dairy cows, crossbreeding is a common practice in commercial pig production since heterosis plays a key role in many traits [71].

1.3.1.1 Genetic selection in dairy cows for high milk yield

To meet the demands of milk production in society, the selection of dairy cattle has proceeded with a primary focus on the production traits since the middle of the 20th century. In 1964, Dr. Charles Young at the University of Minnesota initiated a single trait selection study of dairy cattle for high milk yield [72]. Dr.Young split a herd of Holstein cows into two groups based on their genetic merit for milk production. From that time, cows in one group have been bred with semen from Holsteins sires with the highest predicted transmitting ability (PTA) for milk (4 best sires used each year). This group of cows was initially called the selection line [72] and more recently has been categorized as representing contemporary Holsteins [73,74]. Cows in the other group (originally called the control line) were bred with semen from 20 Holstein sires (4 sires per year in a 5-year rotation) that were breed average for PTA milk yield in 1964 (**Figure 1.5**). Since the early 1990s, semen from the sons of these original 20 sires has been used to maintain the control line (now called unselected Holsteins [73-75]). As expected, the milk yield of the UH cows is less than that of the CH cows. Currently, this 50-year of continuous selection has increased the difference in milk yield between UH and CH cows to more than 4,500 kg/year. Other phenotypic changes have also occurred as CH cows are more angular in appearance and have larger body size than UH cows [76]. A negative consequence of previous selection practices has been insufficient attention to health traits and SNP analysis has indicated this has inadvertently carried along with genetic polymorphisms that are detrimental to health and reproductive function [77]. Indeed, the greater incidence of metabolic issues, such as displaced abomasa, ketosis, and mastitis, occur in CH cows that could be associated with the phenotypic changes during the genetic selection process [78,79].

More recent work indicates immune function is compromised in CH cows relative to their UH herdmates [73,74].

1.3.1.2 Metabolic disorders as consequences of genetic selection

Although the continuous selection and breeding largely enhance the milk production in dairy Holsteins, health and fertility issues have also been observed, including impaired reproductive performance, prolonged calving time, disturbed hormone level, and compromised immune response as well as a variety of metabolic disorders [80-84].

Metabolic disorders are more prone to happen during the transition period from late pregnancy to early lactation (Grummer defined that time period as -3 weeks to +3 weeks of calving) which is a physiological phase critically important to the health and production of dairy cows [85]. Dramatic shifts in nutrient and energy metabolism occur during the transition period which can lead to metabolic disorders [86]. Especially, the nutrient requirement for fetus development peaks in the last 3 weeks of the prepartum period, but dry matter intake (DMI) declines by 10-30% during the same period [87]. Similarly, energy utilization in the first 3 weeks of lactation greatly exceeds the energy that can be obtained from consumed feeds because increases in DMI lag behind the rapid postpartum increase in milk production [88-90]. Therefore, late prepartum and early postpartum dairy cows experience negative energy balance (NEB). Negative energy balance for UH cows often is resolved by week 4 postpartum while it can extend to week 10 postpartum for CH cows. Cows require comprehensive adaption, regulation, and integration of tissue metabolism during the physiological stage of NEB. Under this situation, multiple metabolic processes might be disturbed that can increase the risk of metabolic disorders, such as ketosis, hepatic lipidosis, hypocalcemia, mastitis, and metritis [91-94].

1.3.2 External modification: Bidirectional interactions of chemical exposure to metabolic system

1.3.2.1 Positive influence of chemical exposure

Nutrients

Regardless of genetic selection and breeding as the intrinsic modifications in animals, the external factors, especially the nutritional modification in the diet, also have a significant influence on animal health and productivity with bidirectional functions through regulating the metabolic system. On one aspect, supplementation of some essential or non-essential amino acids, such as methionine, lysine, tryptophan, arginine, and histidine, are crucial for improving animal growth and productivity. For example, additional arginine in the basal diet increased muscle gain and reduced body fat accretion of finishing pigs [95] and growth of milk-fed young pigs [96]. A positive impact of glycine supplementation in laying hens was observed in improving feed intakes, egg weight, and fat digestibility [97]. Due to the fermentation function in the rumen, supplying encapsulated lysine and methionine to dairy cows effectively protected amino acid degradation in the rumen and had beneficial effects on feed intake and weight gain [98].

Non-nutrients: antioxidants

Except for the benefits of nutrient supplements, some non-nutrient compounds, such as vitamins, minerals, and plant extracts, also have substantial functions for animal health and performance.

Due to the high susceptibility to lipid oxidation, antioxidants are frequently used as additives to prevent lipid oxidation and oxidative rancidity in animal feed. Because lipid oxidation can cause a notable decrease of its nutritional value by increasing odor, free radicals, and peroxides that are

either reduced feed intake or toxic to animals, which further results in the reduced energy transformation from feed to animal products and stress-induced diseases.

Balance of reactive oxygen species and antioxidants. Production animals are exposed to various stressors when raised in commercial conditions that might influence their productivity, in which oxidative stress is the most common stress. Oxidative stress is defined as an imbalanced oxidant and antioxidant that interrupts the redox homeostasis through the promoted production of reactive oxygen species (ROS) and related elimination of antioxidants by the antioxidant system [99]. At the molecular level, the accumulation of ROS products, such as hydrogen peroxide (H_2O_2), superoxide, hydroxyl radical, and singlet oxygen, from the electron transport chain in the mitochondria induces lipid peroxidation, protein, and DNA damage. Lipid peroxidation is a predominant reaction through the ROS attacking polyunsaturated fatty acids (PUFAs) in the cell membrane. This process interrupts regular metabolic events and results in membrane disruption and cell death [100]. At the same time, endogenous antioxidants function to maintain the redox balance, which includes a series of antioxidant enzymes, superoxide dismutase (SOD), catalase (CAT), and glutathione peroxidase (GPX), non-enzyme oligopeptide, glutathione (GSH) as well as vitamins. Under normal conditions, ROS products interact with excessive antioxidants in a dynamic range to dismiss the occurrence of oxidative stress. However, when the homeostasis between ROS and antioxidants is disrupted with promoted production of ROS, oxidative stress happens with tremendous influence on regular physiological activities and the growth of animals.

An accessible way to avoid this situation is by supplying vitamins, mainly vitamins E, C, and A, into animal feed. Among them, vitamin E and vitamin A can stop the lipid peroxidation process by mitigating ROS, while vitamin C is a reluctance that can regenerate other antioxidants such as

GSH by donating electrons [101,102]. Numerous studies have found the preventive effects of supplying antioxidants on oxidative stress-induced negative effects in animal products. In particular, feeding vitamin E and selenium had been proven in some studies on reducing oxidized stress and increasing milk yield in dairy cows [103]. In pigs, supplementation of vitamin E improved oxidized lipid-induced negative effects and meat quality [104,105]. Besides, vitamin E improved egg production and eggy quality in laying hens [106].

Non-nutrients: plant extracts/flavonoids

The usage of plant extract in animal feed became more frequent due to the prohibition of using antibiotics. Several plant source feed additives have been found to have beneficial functions by improving digestibility, anti-oxidant, anti-inflammatory, and promoting immune function. Plants contain a wide range of low molecular weight secondary metabolites, which can work in the immune system against pathogens and stress from the environment [107]. Flavonoids are one of the largest groups of plants with active secondary plant metabolites that have been suggested to have antioxidant and antibiotic functions [108]. Rutin and quercetin are the most bioactive flavonoids that had been proven to have positive effects, including improvements in growth, reproduction, health, and metabolism when supplied in the feed of dairy cows, in particular, mitigation of hepatic steatosis during lactation [109].

1.3.2.2 Negative influence of chemical exposure

Oxidized lipids

Lipids, including fats and oils, are considered essential dietary nutrients for production animals. Adding lipids into animal feeds can improve feed efficiency and palatability, reduce dust, and

supply essential fatty acids and vitamins [110]. Due to the economical consideration, rendered fats or oils, for example, the animal-derived fats or the used frying oils from fast-food restaurants, are commonly used in the animal feed [111].

Lipid oxidation. High temperature and extensive time length during rendering and processing not only cause the physical properties of lipids but incur a series of chemical reactions to form a variety of peroxidation compounds [112,113]. In particular, vegetable oils enriched with polyunsaturated fatty acids (PUFAs), are extremely sensitive to oxidation [114]. As the result, numerous lipid oxidation products (LOPs) are generated, and those LOPs are further classified as primary LOPs including hydroperoxides, epoxyhydroperoxides, ketohydroperoides, cyclic peroxides, and their decomposition products as secondary LOPs, such as aldehydes, ketones, alcohols, furans, and lactones [115]. Except for oxidation reactions, polymerization and hydrolysis reactions also occur in lipids during processing to form polymers and other products [116].

Disposition of oxidized lipids. Similar to dietary lipid disposition, consumption of oxidized lipids can introduce and dispose of LOPs into the metabolic system in production animals. In general, most of the primary LOPs are excreted in feces due to the low absorption rate, which causes a limited distribution inside of the body [117]. Conversely, several secondary LOPs, such as hexenal, 4-hydroxy-2-noneal (4-HNE), and 4-hydroxy-2-hexenal (4-HHE), can enter the body and move through the circulation system to reach various organs [118]. Other large molecules, such as polymers, are resistant to being absorbed by enterocytes [119].

Oxidized lipid-induced metabolic effects. A large number of studies have reported that consuming oxidized lipids could potentially cause adverse effects on the growth performance and

health of production animals. In general, the inclusion of oxidized lipids reduces feed efficiency, including average daily gain (ADG) of 5%, average daily feed intake (ADFI) of 3%, and gain to feed ratio (G: F) of 2% in chicken and pigs [120]. Meanwhile, oxidative stress was observed after ingesting oxidized lipid-contained diets in pigs and chickens [121,122]. Oxidative stress is defined as increased oxidative markers and depletion of antioxidants, such as increased thiobarbituric acid, reactive substances (TBARS), malondialdehyde (MDA), and decreased vitamin E or glutathione, respectively. Under this situation, poor meat quality in production animals might be recognized as the consequence of oxidized lipid-induced oxidative stress [123]. Besides, negative effects of oxidized lipids on gastrointestinal functions were found by disrupting the intestinal redox system and immune system [124]. While the influence of oxidized lipids on intestinal integrity to defend the hostile environments is not well established.

Transcriptional regulation by oxidized lipid intake. One of the prevalent influences of oxidized lipid intake is directly affecting lipid metabolism through the activation of transcription factors, peroxisome proliferator-activated receptors (PPARs). PPARα is the major form of PPARs highly expressed in the liver to mediate fatty acid oxidation. Some of the LOPs in oxidized oil, such as hydroxyoctadenoic acids act as a ligand of PPARs, it stimulates PPARα and its downstream genes after consuming oxidized lipids by increasing a series of activities on fatty acid uptake and oxidation [125]. Except for PPARs, sterol regulatory element-binding proteins (SREBPs), another transcriptional regular responsible for modulating lipid synthesis and uptake, are inhibited by oxidized lipids [126]. With transcriptional regulation of these factors, reduced triacylglycerol (TAG) and cholesterol levels were observed in the plasma and liver of animals fed oxidized lipid [105,106] as responses to the activation of PPARα and inhibition of SREBPs for promoting lipid catabolism rather than anabolism.

In addition to the contribution to lipid metabolism, oxidized lipids also indirectly influence the absorption of carbohydrate and amino acid metabolism [127,128]. These changes in nutrient metabolism might result in more energy expenditure and fewer nutrients are used for growth performance in production animals.

1.4 CHALLENGES AND APPROACHES IN THE INVESTIGATION OF METABOLIC PERFORMANCE CHANGES

1.4.1 Challenges in the investigation of metabolic performance changes

Metabolic performance is closely related to the growth performance and health of the production animals, understanding changes in endogenous metabolic events is crucial in particular for improving productivity. Meanwhile, major challenges exist in investigations of metabolic events. Firstly, endogenous metabolic events are diverse and complex which include different metabolic reactions and metabolic pathways that increase the challenge of detecting those events. Under this situation, the detection methods need to cover all metabolites in the biological system. Secondly, subtle metabolic changes, such as low abundance molecules as a signal metabolite in transducing systematic metabolic events in multiple tissues, will need the current method to obtain a dynamic range that allows capturing delicate changes. Thirdly, high throughput and efficient methods need to take into consideration for discovering the systemic metabolic events.

1.4.2 Platforms for examining metabolic performances

For evaluating metabolic performance and addressing potential metabolic events modified by intrinsic or external factors in reproduction animals, effective approaches to determine metabolic performance need to be considered in current research. This chapter discusses the current methods for the measurements of metabolic performance in production animals.

1.4.2.1 Traditional method of detecting metabolic performance

Biochemical analysis

Changes in blood composition, such as electrolytes, enzymes, and metabolites, are commonly used as indicators to uncover metabolic events. Biochemical analysis is typically applied to examine metabolic changes by quantifying some specific metabolites, such as glucose, enzymes, or hormone. For example, insulin resistance acts as a biomarker of diabetes, obesity, and many metabolic disorders. Glucocorticoid and adrenergic stimulation result in a series of nutrient metabolism, including glycogenolysis, gluconeogenesis, and lipolysis, these metabolic events cause changes in blood glucose, lactate, and NEFA levels [129]. Animals experiencing stress could induce muscle damage that is identified by creatine kinase, a plasma biomarker correlated to meat quality [129]. However, only one parameter can be measured in a single test, multiple measurements need to be processed to cover all the blood parameters. Besides, blood includes a lot of small-molecule metabolites from other organs which might be a signal molecule for metabolic disorders, such as signal lipids or dipeptides. Current biochemical approaches cannot achieve screening of all classes of the metabolites.

Pathological analysis

The biopsy is a direct approach to characterize pathological changes under a specific tissue from animals. For example, using liver biopsy to determine fatty liver in dairy cows is capable because it is a moderately invasive procedure. Quantification of lipid droplet diameter is the most reliable method to discriminate the severity of fatty liver in dairy cows. However, preparing histological samples is a time-consuming process and it still cannot provide a full picture of metabolic events under a specific piece of the biological sample. Therefore, a new approach for characterizing metabolic changes in biological samples needs to be explored in evaluating the metabolic

performance in production animals, which should include a wide targeted parameter detection and a rapid workflow.

1.4.2.2 Metabolomics

Over the past decades, omics technologies, have been widely applied for the identification and quantification of molecules involved in multiple activities in complex biological systems that contribute to phenotypic changes. The omics studies include genomics, transcriptomics, proteomics, and metabolomics, which represent the study of gene, RNA transcripts, protein, and metabolites in different cellular-level processes reflecting processes from genotype to phenotype. Phenotypic changes might not be fully revealed even investigations of the state of genes, RNAs, and proteins in a biological system were conducted. Therefore, investigation of metabolome is essential because it is widely used to explore the interactions between gene and protein downstream products under endogenous or external factors stimulation, and metabolic changes present a unique approach to characterize the phenotypic changes [130].

Metabolites are some small chemical molecules transformed through metabolism that provide a functional end-product of cellular biochemistry. Metabolites function as a direct reflection of endogenous biochemical reactions that are further correlated to physiological events and phenotypic changes. Metabolomics is the investigation of metabolites composition of the cell, tissue, or organ to reveal mechanical metabolism to phenotype and discover biomarkers [131]. Due to high resolution and sensitivity, metabolomic-based analysis is extensively applied to biochemical, physiological, and pathophysiological research. Compared to traditional analytic techniques, metabolomic-based analysis is capable of detecting subtle changes of metabolites in chemical or biological reactions in the whole system using a small amount of sample.

Targeted and untargeted metabolomics

Metabolomics experiments are classified into two categories, untargeted analysis, and targeted analysis. The untargeted analysis is an unbiased analytical method that identifies the metabolite composition in a biological sample under a specific physiological status or given environmental condition [132]. The untargeted metabolomics enables to identify of all detected metabolites as novel markers, however, it also largely depends on the current analytical platform and sample preparation whether it covers most metabolites in an unbiased manner. Untargeted metabolomics was broadly used in epidemiological studies and disease characterization [133,134].

The targeted analysis is an approach to quantify known metabolites that might play important roles in biological reactions. The targeted analysis is a powerful approach for the understanding status of metabolic enzymes, intermediate metabolites, and final products in specific metabolic pathways through quantification of the set of metabolites [133]. The application of metabolomics in biological sample analysis is a good approach to characterize metabolic events in production animals.

Metabolomic fingerprinting

Metabolomics provides a powerful and high-throughput platform for the detection and identification of extensive small molecule compounds simultaneously by targeted or untargeted analytical approaches. Through this process, the endogenous and exogenous metabolites in a biological system can be identified, quantified, and characterized. Thus, these metabolites are directly regarded as end products that reflect the phenotype of the body or indirectly indicated the genotype. Metabolomic fingerprinting is an approach in metabolomics analysis that aims to identify the most relevant differences rather than defining all the metabolites in the samples used

for comparison [135]. The spectroscopic method is the most common analytical technique used for metabolic fingerprinting that characterizes samples based on their origin or biological relevance. This approach provides a detailed analysis that helps to reveal a complex reaction network and uncover potential biomarkers after specific treatments [136].

Instruments of metabolomics

NMR versus MS. Nuclear magnetic resonance (NMR) and mass spectrometry (MS) are the two most common data acquisition instruments for metabolomics analysis. The principle of NMR is based on energy absorption and re-mission of the atomic nuclei that depend on variations in an external magnetic field. Spectral data produced by NMR allows for characterization of chemical structure and quantification of the concentration of metabolites [137]. The data acquisition of MS is presented as a mass-to-charge ratio (*m/z*) and a relative signal intensity of total ionized compounds. The advantages of NMR based analytical platform are highly selective, reproducible, and fewer sample preparation steps [138], which provides a direct correlation of its spectra and compound concentration. However, relatively low sensitivity with detecting only high abundance compounds limits the capacity of metabolites in biological samples. While, MS-based metabolomics analysis allows the scanning of different sets of molecules at different times by a separation step, which largely reduces the complexity of biological samples [139]. Compared to the NMR platform, the MS platform combines effective chromatographic separation and sample preparation that result in high sensitivity, specificity, and a good dynamic range of analysis. These advantages make the MS platform prior for both targeted and untargeted metabolomics [140].

LC-MS versus GC-MS. Liquid chromatography (LC) and gas chromatography (GC) are the most common separation techniques prior to the MS detection, thus they are further classified as LC-

MS and GC-MS. GC-MS is only applicable to volatile compounds with sample derivatization, while non-volatile compounds or thermo-labile compounds cannot be detected by GC-MS analysis without appropriate derivatization for GC separation [141]. The most common biological samples used for metabolomics analysis are plasma, serum, and milk followed by urine, meat, and other tissue [142,143]. The water matrix of these samples is incompatible with GC without pretreatment but matches well with LC. Therefore, LC has advantages in metabolite coverage over GC since it can cover nonvolatile polar or nonpolar compounds without derivatization [141], and LC-MS has become the staple platform for providing comprehensive and high-resolution metabolomic analysis.

LC-MS-based metabolomics. LC-MS data is composed of retention time (RT), mass-to-charge ratio (*m/z*), and signal intensity. For untargeted metabolomics analysis, the chromatographic and spectral data need to be properly processed and deconvoluted into a data matrix prior to multivariate data analysis. According to the objective of a particular study, principal component analysis (PCA), principal least square (PLS), or orthogonal partial least squares (OPLS) can be applied for data processing [142]. When a clear separation among treatments is observed in the scores plot, metabolites that contribute to this separation can be identified in the loadings plot according to their interaction with the principal components. For marker identification, ions can be determined by database search, MS/MS fragmentation, accurate mass measurement, and elemental composition analysis (**Figure 1.7**). Moreover, metabolites and spectral databases can be searched on the Kyoto Encyclopedia of Genes and Genomes (KEGG), Human Metabolome Database (HMDB), Lipid MAPs, METLIN database, BioCyc, and Spectral Database.

Applications of metabolomics in studying production animals

Due to its diverse functions in metabolic phenotyping and characterization, metabolomics has been applied in a wide range of research disciplines, including biomedical research, food and plant analysis, and environmental monitoring, and it was under rapid growth in the past two decades [144,145]. Especially, the advantages of metabolomics in detecting subtle and extensive metabolic changes and dietary responses make it an ideal tool in production animal research for the assessments of feed efficiency, disease, fertility, milk, and meat quality [146,147]. The major applications of metabolomics studies in the production animals are to define the roles of metabolism in animal health, nutrition, production, reproduction, and physiology. Among them, a large number of studies focus on the growth of ruminants (cow and sheep) and monogastric (pig and poultry) by identifying metabolite biomarkers of pathological events, understanding animal responses to different stressors, and characterizing bioproduct quality [143]. In dairy cows, most metabolomics-based research was to evaluate the effects of nutrients or feed on their health and milk production [148], disease-related metabolite biomarkers [149], and metabolism-related production performance [150]. In addition to addressing the performance of production animals, the metabolome of pigs has been widely used as a model system for studying human disease due to the similarity in physiology between pigs and humans [151]. At present, the majority of metabolomics studies on production animals are solely dedicated to metabolic phenotyping without additional characterization of the mechanisms behind the identified metabolic changes and differences from metabolomics analysis. Therefore, the combination of metabolomics with biochemical analysis should produce a more in-depth understanding on how both intrinsic factors and external treatments affect the health and growth of production animals.

Table 1.1 Milk production, 1950-2000.

Year	Cow numbers (x1000)	Production per cow (Pounds)	Total production (Millions)	Changes in cow numbers (%)	Changes in production per cow (%)	Change in total production (%)
1950	21,994	5,314	116,602			
1955	21,044	5,842	122,945	-4.32	9.94	5.44
1960	17,515	7,029	123,109	-16.77	20.32	0.13
1965	14,953	8,305	124,180	-14.63	18.15	0.87
1970	12,000	9,751	117,007	-19.75	17.41	-5.78
1975	11,139	10,360	115,398	-7.18	6.25	-1.38
1980	10,799	11,891	128,406	-3.05	14.78	11.27
1985	10,981	13,024	143,012	1.69	9.53	11.37
1990	9,930	14,782	147,721	-9.00	13.50	3.29
1995	9,466	16,405	155,292	-5.27	10.98	5.13
2000	9,210	18,204	167,658	0.59	2.43	3.04

Table 1.2 Swine productivity, 1980 vs 2015.

Production Trait	1980	2015
Pig marketed (per sow per year)	9.2	22
Average market weight (lb)	242	283
Average daily gain (lb)	1.27	1.61
Feed conversion (lb feed/gain)	3.20	2.60
Carcass weight (lb)	171	212
Back fat at 10^{th} rib (inches)	>1.0	0.72
Loin area (inches^2)	<5.0	>8.0
Lean meat per carcass (lb)	< 80	>118
Pork produced (lb per sow)	1,770	4,200

Table 1.3 Laying hen productivity, 1960 vs 2010.

Production Trait	1960	2011
Daily feed use (lb/100 hens)	26.9	19.9
Hen-day egg production (%)	59.2	75.3
Feed conversion (lb of feed/egg)	3.44	1.98
Mortality (%)	15.8	6.7

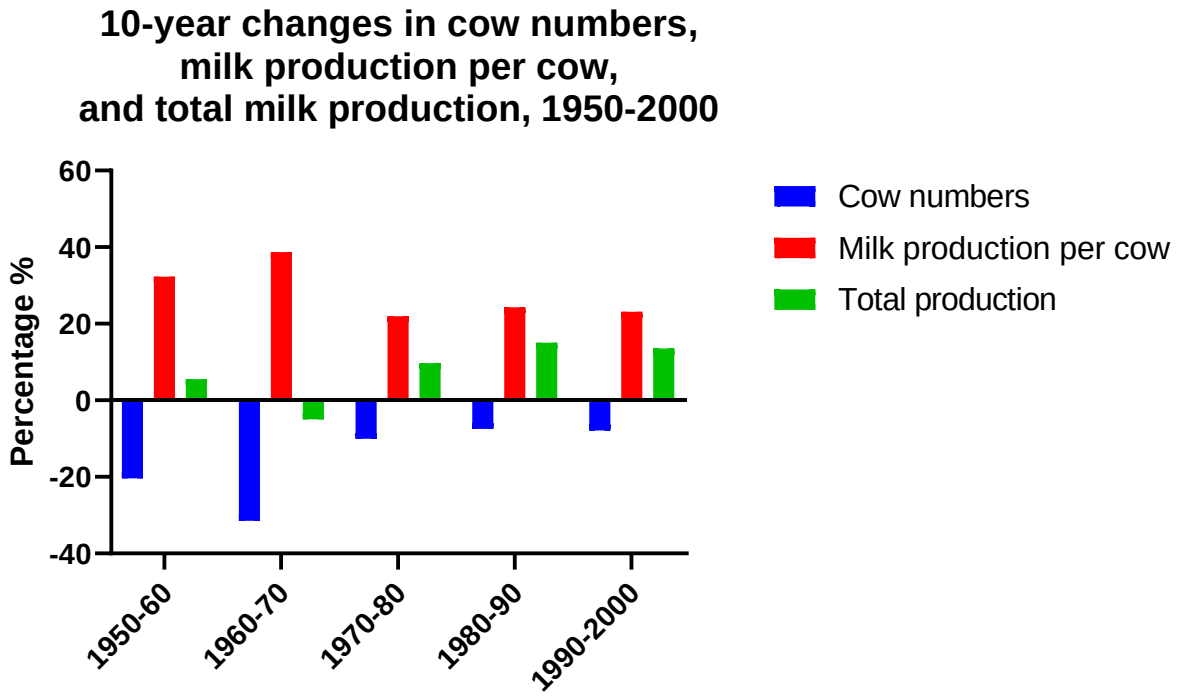

Figure 1.1 10-year changes in dairy cow industry from 1950 to 2000. Percentage change in average cow numbers, milk production per cow, and total production were plotted based on the data from USDA [2].

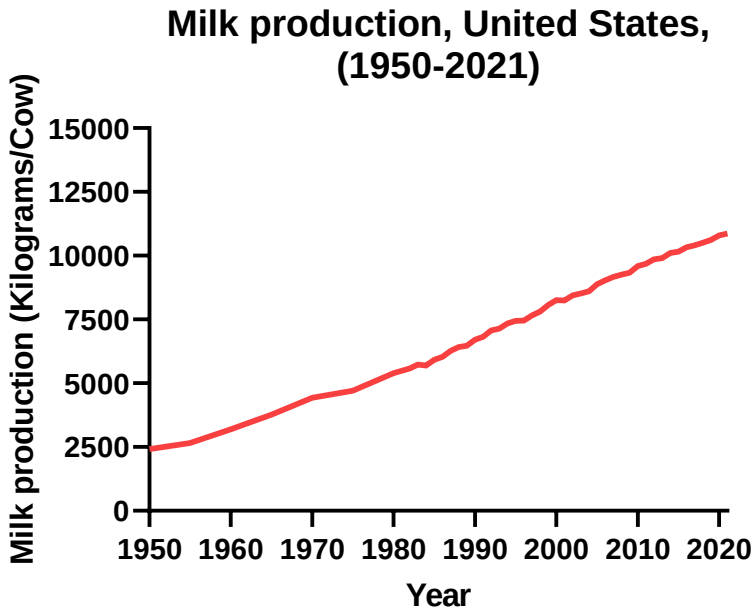

Figure 1.2 Average annual milk production in the United States from 1950 to 2021 (in kilograms per cow). The figure is plotted based on the data from the USDA-NASS [3].

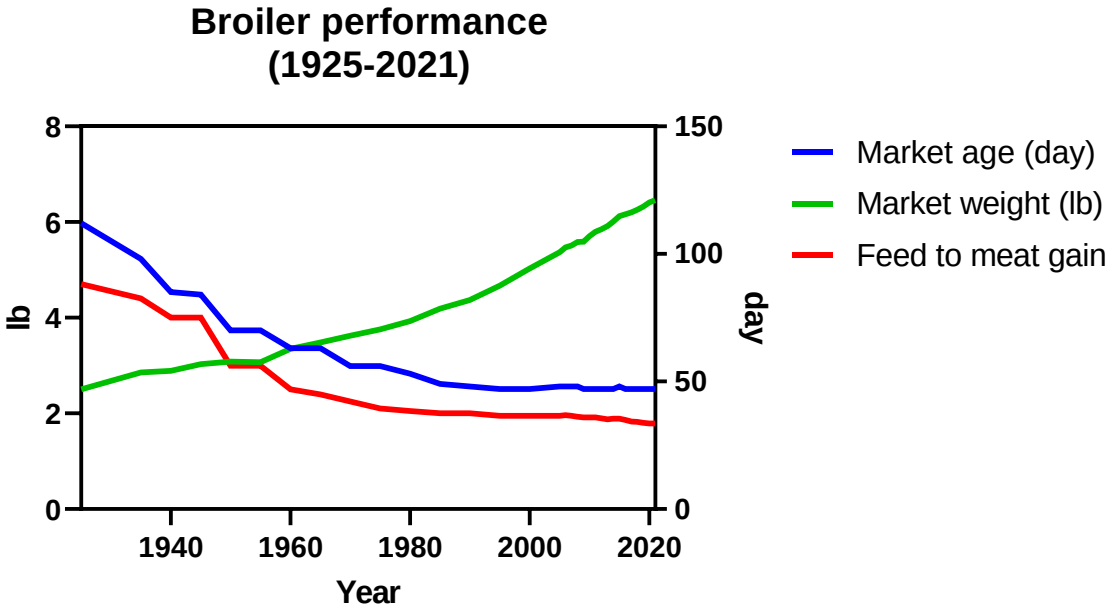

Figure 1.3 Broiler performance in the United States from 1950 to 2021. Average market age, market weight, and feed to meat gain. The figure is plotted based on the data from the National chicken council [11].

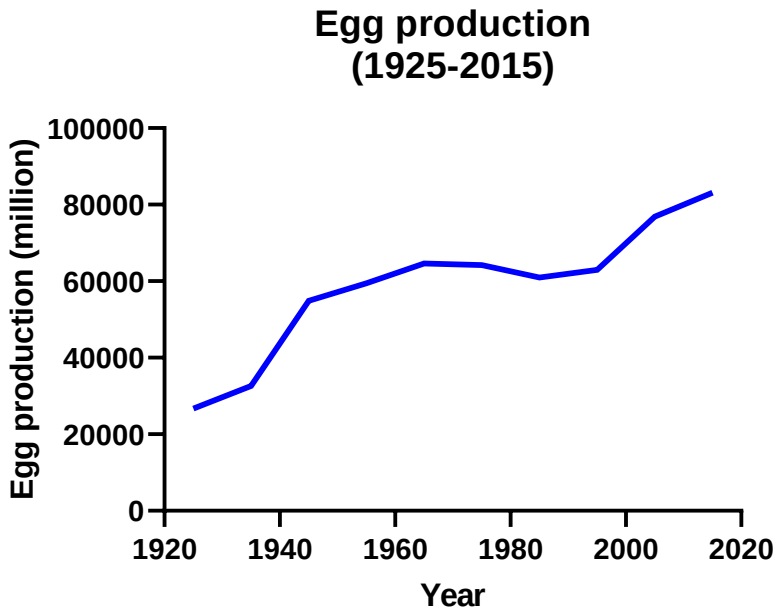

Figure 1.4 Average annual egg production in the United States from 1950 to 2019 (million).

The figure is plotted based on the data from Kidd and Anderson [12].

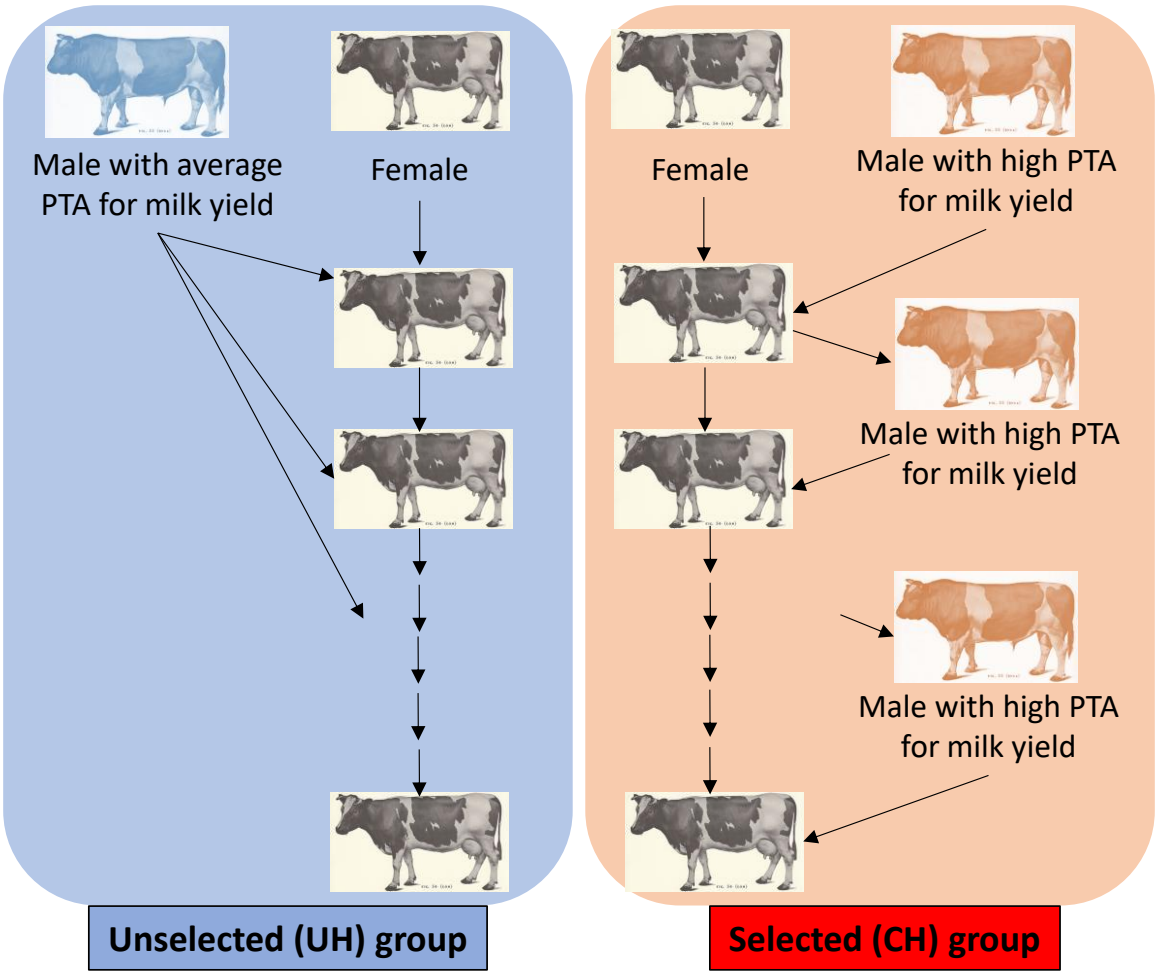

Figure 1.5 Contemporary Holstein (CH) vs unselected Holstein (UH). Genetic selection of dairy cattle was conducted in 1964. The linage of the selected group was mated with four Holstein sires of high predicted transmitting ability (PTA) in milk production for only one year. Every year, sires with high PTA in milk production were chosen from USDA sire summaries. During this genetic selection step, the milk production in the CH group improved significantly. The Unselected group was mated with Holstein sires of average PTA values in milk production since 1964. Their semen has remained at the Southern Search and Outreach Center. The milk production of the UH group remains the same since 1964. PTA: the predicted difference of a parent animal's offspring from average, due to the genes transmitted from that parent.

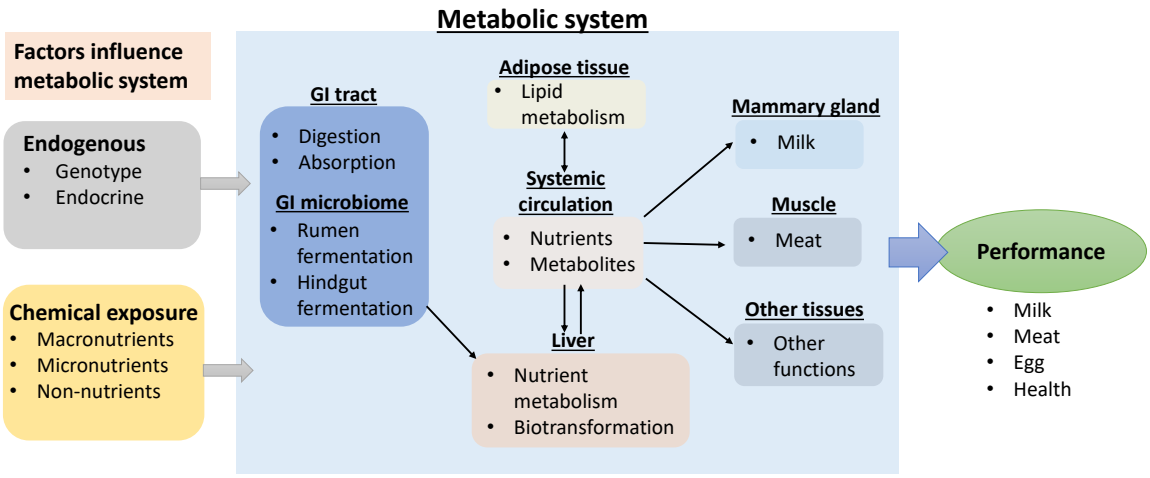

Figure 1.6 Interactions of feed, metabolic system, and performance in production animals. Endogenous factors, such as genotype or endocrine system, encode and regulate metabolic activities in the metabolic system. Feed containing macronutrients (carbohydrates, lipids, and proteins), micronutrients (vitamins and minerals), and non-nutrients can also influence activities in the metabolic system when they were consumed by animals. The metabolic system is composed of major tissues/organs, such as microbiome, GIT, blood, liver, rumen, adipose tissue, mammary gland, and muscle, where nutrient and metabolites exchanges and metabolic events happen. Modifications by changing endogenic and external factors, such as gene expression or chemical exposure can alter the metabolic system and further influence the performance of production animals.

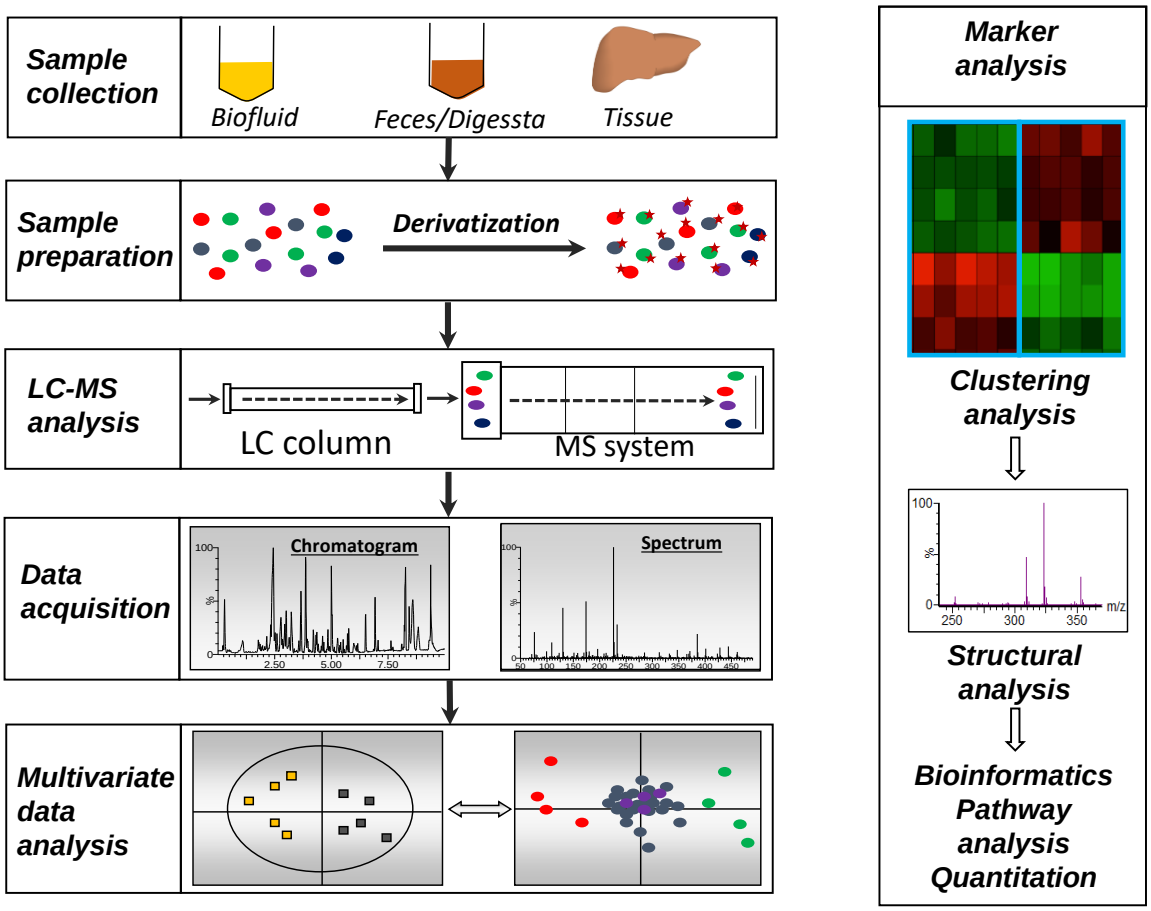

Figure 1.7 The workflow of metabolomics. Biological samples are processed appropriately to make them compatible with MS-based metabolic analysis. Chemical derivatization can be performed to facilitate the chromatographic separation of metabolites and increase metabolite detection in the LC-MS system. Spectral data acquired by MS needs to be deconvoluted to a data matrix compatible with multivariate data analysis. Markers analysis is based on clustering and structural analysis. The confirmed markers could be further used for bioinformatics, quantitation, and pathway analysis.

CHAPTER 2. METABOLOMIC FINGERPRINTING OF INTERNAL FACTOR-INDUCED METABOLIC CHANGES IN PRODUCTION ANIMALS: A CASE STUDY ON GENETIC SELECTION ALTERED HEPATIC LIPID METABOLISM IN TRANSITION DAIRY COWS

This chapter is modified from the unpublished manuscript:

Guo, Y.; Weber, W. J.; Crooker, B. A.; Chen, C. Inadequate hepatic biotransformation of choline to phospholipids contributes to lipid disorders in early lactation of contemporary Holstein cows.

2.1 SUMMARY

The contemporary Holstein (CH) dairy cows from decades of genetic selection are superior to their unselected Holstein (UH) counterparts in milk production, while more prone to hepatic steatosis and ketosis in transition and early lactation periods. Elevated negative energy balance (NEB) in the CH cows is widely accepted as the initial driving force of this phenotype, but the exact metabolic events underlying the susceptibility to lipid disorders remain to be fully defined. In this study, serum and liver metabolomes of periparturient CH and UH cows were compared by liquid chromatography-mass spectrometry-based metabolomics as well as biochemical and transcriptomic analyses. The examination of serum lipidome showed that CH cows underwent greater elevation of serum non-esterified fatty acids (NEFAs) from lipolysis in the transition period than UH cows, while two genetic lines had no differences in the concentration of total serum triacylglycerols (TAGs) and also comparable profiles in the composition of serum TAGs and phospholipids. The lipidomic analysis of the liver samples revealed the imbalance in the hepatic lipidome of CH cows during early phase of lactation, which was mainly caused by the accumulation of TAGs, together with the lack of parallel increase of phosphatidylcholines (PCs) that are needed for exporting TAGs through lipoproteins. Targeted analysis of the metabolites in PC biosynthesis showed that CH cows had similar levels of hepatic choline, but less phosphocholine and glycerophosphocholine compared to UH cows. Transcriptomic analysis indicated that the expression of CPT and CEPT genes in the CDP-choline pathway, the major PC biosynthesis pathway, were decreased, while the expression of BHMT and PEMT genes in the minor PC biosynthesis pathway, were increased in early lactation CH cows relative to those of UH cows. Overall, inadequate hepatic biotransformation of choline to phospholipids contributes to PC deficiency and hepatic steatosis in the CH cows. Effects to elevate PC synthesis could enhance hepatic very-low density lipoprotein (VLDL) export, reduce hepatic steatosis, and improve metabolic health of high-producing dairy cows in early lactation.

KEYWORDS: Choline, PC, lipid metabolism, VLDL, hepatic steatosis, dairy cow

ABBREVIATIONS: AA, amino acid; ACN, acetonitrile; AMP, adenosine monophosphate; BHMT, betaine-homocysteine S-methyltransferase; CDP-choline, cytidine diphosphate-choline; Cer, ceramide; CH, contemporary Hostein; CK, choline kinase; CEPT, choline/ethanolamine phosphotransferase; CPT, cholinephosphotransferase; DC, dansyl chloride; DPDS, 2-2'-dipyridyl disulfide; GPC, glycerophosphocholine; GSSG, oxidized glutathione; HCA, hierarchical clustering analysis; HMDB, human metabolome database; HQ, 2-hydrazinoquinoline; IACUC, institutional animals care and use committee; LC-MS, liquid chromatography-mass spectrometry; LysoPC, lysophosphatidylcholine; NEB, negative energy balance; NEFA, non-esterified fatty acid; PC, phosphatidylcholine; PCA, principal components analysis; PE, phosphatidylethanolamine; PEMT, phosphatidylethanolamine-N-methyltransferase; PhoC, phosphocholine; QTOFMS, quadrupole time of flight mass spectrometry; SCFA, short-chain fatty acid; SEM, standard error mean; SM, sphingomyelin; SREBP, sterol regulatory element binding protein; TAG, triacylglycerol; TPP, triphenylphosphine; UH, Unselected Holstein; UPLC, ultra-performance lipid chromatography; VLDL, very-low density lipoprotein.

2.2 INTRODUCTION

Contemporary Holsteins (CH), as the staple dairy cattle in the United States and many parts of the world, are derived from intensive genetic selection with a primary focus on milk production trait [152]. The genectic selection practices have led to multiple benefits to the producers, but also caused many challenges to CH cows, including decreased reproduction rate, prolonged calving interval, disturbed hormone level, compromised immune response, and higher incidence of metabolic disorders [80-84]. Among these challenges, metabolic disorders are a primary contributor to poor lactation performance, fertility, health, and longevity of CH cows [82]. Disrupted lipid metabolism, especially hepatic steatosis or fatty liver, is the most common form of metabolic disorders in high-producing CH cows during the periparturient period [153]. In the United States, up to 50% of dairy cows develop severe or moderate fatty liver in early lactation [153,154]. During these first few weeks postpartum, insufficient dry matter intake and high energy requirement for milk production lead to severe negative energy balance (NEB) [87], which triggers extensive lipolysis in the adipose tissue and continuous release of non-esterified fatty acids (NEFAs) into the blood [155]. The liver, as the central organ for lipid metabolism, can perform diverse functions to handle elevated NEFAs, including NEFA uptake, fatty acid oxidation, triacylglycerol (TAG) synthesis, and lipid export through very low-density lipoprotein (VLDL). However, when the load of NEFA uptake surpasses the capacity of the liver to perform oxidation and export, hepatic steatosis occurs [156]. The accumulation of TAGs in the hepatocytes further impedes regular metabolic functions of the liver, compromising the general performance of dairy cows.

The phenotypes of dyslipidemia, especially fatty liver, in the high-producing CH cows have been widely documanted [153]. However, due to the lack of suitable controls for comparison, the contribution of genetic selection to these lipid metabolic activities were not well elucidated. At the University of Minnesota, a herd of unselected Holsteins (UH) has been maintained at a stable and

unchanged level of milk production since 1964[77]. The annual milk yield of this UH herd is about 45,00 kg less than that of the UH herd that was selected from the same progenitors [75]. At the same time, these UH cows also experience less health issues and metabolic disorders than their UH counterparts. Therefore, this herd of UH cows can serve an ideal control to examine the physiological and metabolic impacts of the genetic selection for CH cows.

In the current study, comprehensive lipidomic, metabolomic, and transcriptomic analyses of serum and liver samples of CH and UH cows were conducted to define their metabolic status during the periparturient period. Differences between CH and UH cows in lipid metabolism and metabolic mobilization to meet the demand from milk production were identified and further characterized by comparing the scales and kinetics of both partuition- and genotype-responsive metabolites and genes. Our model focus on the alternations driven by genetic selection and thus likely is caused by differences in genetic polymorphisms in the UH and CH cows.

2.3 MATERIALS AND METHODS

2.3.1 Chemicals and reagents

The chemicals and reagents used in sample preparation, LC-MS analysis, structural confirmation, and quantification are enlisted in **Table 2.1**.

2.3.2 Animals and sample collection

The UH and CH cows in this study were maintained at the University of Minnesota Dairy Cattle Teaching and Research Center in St. Paul, MN, and managed uniformly. Animal care and experimental procedures were approved by the University of Minnesota Institutional Animal Care and Use Committee. Multiparous UH and CH cows (n = 12/genotype) were housed together for at

least 5 weeks prior to parturition and fed the same pre-and postpartum diets throughout the study. Diets were formulated as total mixed ration (TMR) designed to meet the nutritional requirements of Holsteins and cows were fed once daily. Classical measurements of cow performance and metabolism, including daily dry matter intakes, milk yields, weekly body weights, condition scores, circulating concentration of metabolites, and endocrine components are reported by Weber et al. (unpublished). Animals were observed daily for health abnormalities and treated when warranted. Blood samples were collected weekly from -4 through 8 wk of lactation and isolated serum stored at -80°C until analysis. Liver biopsies were collected at -14, 3, 14, and 42 d of lactation [157], snap-frozen and stored at -80°C until subsequent processing for metabolomic analysis.

2.3.3 Blood biochemical analysis

Serum non-esterified fatty acid (NEFA) concentrations were determined by a colorimetric assay (NEFA-HR (2), Wako Life Sciences, Mountain View, CA) with volumes modified for 96-well plates and read with a Perkin-Elmer HTS 7000 Plus, BioAssay Reader.

Serum TAG was determined using a respective colorimetric assay kits from Pointe Scientific (Canton, MI) in a Spectra Max 250 96-well plate reader from Molecular Devices (Sunnyvale, CA).

2.3.4 Metabolites extraction

Liver tissue samples were fractionated using a modified Bligh and Dyer method [158]. Briefly, 100 mg of liver sample was homogenized in 0.5 ml of methanol and mixed with 0.5 ml of chloroform and 0.4 ml of water. After 10-min centrifugation at 18,000 × *g*, the upper aqueous fraction was harvested while the lipid fraction in chloroform was dried with nitrogen gas and reconstituted in n-butanol. Serum samples were deproteinized and extracted by mixing 1 volume of serum with 19 volumes of 66% aqueous ACN and centrifuged at 18,000 × *g* for 10-min to obtain the supernatants.

2.3.5 Chemical derivatization

For detecting metabolites containing amino functional groups in their structure, samples were derivatized with dansyl chloride (DC) prior to the LC-MS analysis. Briefly, 5 µL of sample or amino acid standard was mixed with 50 µL of 10 mM sodium carbonate solution, 100 µL of 3 mg/ml DC solution, and 5 µL of 50 µM deuterated L-tryptophan-(indole-d_5) as an internal standard dissolved in acetone. The mixture was incubated at 60 °C for 15 min and centrifuged at 18,000 × g for 10 min, and the supernatant was transferred into an HPLC vial for LC-MS analysis. For detecting the metabolites containing the carboxyl group, the samples were derivatized with 2-2'-dipyridyl disulfide (DPDS), triphenylphosphine (TPP), and 2-hydrazinoquinoline (HQ) prior to the LC-MS analysis. Briefly, 2 µL of sample or standard was added into 100 µL of freshly prepared acetonitrile (ACN) solution containing 1 mM DPDS, 1 mM TPP, 1 mM HQ, and 100 µM deuterated *d4*-acetic acid as internal standard. The reaction mixture was incubated at 60 °C for 30 min, chilled on ice, and mixed with 100 µL of H_2O. This mixture was centrifuged at 18,000 × g for 10 min and the supernatant was used for LC-MS analysis.

2.3.6 LC-MS-based metabolomic analysis

A 5 µL of aliquot prepared from serum or hepatic extract sample was injected into an Acquity ultra-performance liquid chromatography-quadrupole time-of-flight mass spectrometry (UPLC-QTOFMS) system (Waters, Milford, MA), and separated by a UPLC column in a 10-min run at a flow rate of 0.5 mL/min. Detailed information on LC-MS acquisition conditions is provided (**Table 2.2**). The LC eluant was injected into a Xevo-G2-S QTOF mass spectrometry for accurate mass measurement and ion counting. Capillary voltage and cone voltage for electrospray ionization was maintained at 3 kV and 30 V for positive-mode detection, or at -3 kV and -35 V for negative-mode detection, respectively. Source temperature and desolvation temperature were set at 120 °C and 350 °C, respectively. Nitrogen was used as both cone gas (50 L/h) and desolvation gas (600 L/h), and argon was used as collision gas. For accurate mass measurement, the mass spectrometer was

calibrated with sodium formate solution range *m/z* 50-1000 and monitored by the intermittent injection of the lock mass leucine enkephalin ($[M + H]^+$ = *m/z* 556.2771 or $[M – H]^-$ = *m/z* 554.2615) in real-time. Additional structural information was obtained by tandem MS (MS/MS) fragmentation with collision energies ranging from 15 to 45 eV. Mass chromatograms and mass spectral data were acquired and processed by MassLynx^{TM} software (Waters) in centroided format.

2.3.6.1 Quantitative/Targeted analysis

The concentrations of choline, betaine, phosphocholine, glycerophosphocholine, short-chain fatty acids, and amino acids were determined by calculating the ratio between their individual peak areas and the peak area of internal standard and fitting with a standard curve using QuanLynx^{TM} software (Waters).

2.3.6.2 Untargeted multivariate data analysis

After data acquisition in the UPLC-QTOFMS system, chromatographic and spectral data of samples were deconvoluted by MarkerLynx^{TM} software. A multivariate data matrix containing information on sample identity, ion identity from retention time (RT) and *m/z*, and ion abundance, was generated through centroiding, deisotoping, filtering, peak recognition, and integration. The abundance of each ion was calculated by normalizing the single ion counts (SIC) vs. the total ion counts (TIC) in the entire chromatogram. The processed data matrix was exported into SIMCA-P^{+TM} software (Umetrics, Kinnelon, NJ) and transformed by *Pareto* scaling. Principal components analysis (PCA) was used to model the serum and liver samples from multiple time points of CH and UH cows. Major latent variables of the multivariate model were defined in a scores scatter plot. The potential metabolite markers were identified by analyzing ions contributing to the principal components and to the separation of sample groups in the loadings scatter plot. The chemical identities of interested compounds were determined by accurate mass measurement, elemental composition analysis, database search using Human Metabolome Database

(https://www.hmdb.ca/), and Metlin (https://metlin.scripps.edu/), MSMS fragmentation, and comparisons with authentic standards if available.

2.3.7 Transcriptomic analysis of liver samples

The transcriptomic data reported here are a sunset of data generated by Weber et al. (unpublished). High-quality total RNA was isolated (Qiagen miRNeasy; Germantown, MD) and subsequently processed using Illumina technologies by the University of Minnesota Genomics Center. Barcoded mRNA-Seq libraries of liver samples from 10 UH and 10 CH cows were prepared using the Illumina TruSeq RNA kit and the Illumina TruSeq RNA Library Preparation protocol (Illumina, San Diego, CA). Samples were multiplexed (20 samples/lane) and each sample was run on two lanes on HiSeq 2500 flow cells (24 total lanes). The transcriptome was sequenced using 50 bp paired-end reads. An average of 24.5 million raw reads per sample was obtained and aligned to the UMD3.1 bovine genome built with HISAT2 [159]. Alignment files were indexed and sorted using Samtools [160]. Transcript-level expression was estimated using kallisto [161] and UMD3.1 gene annotation from Ensembl release 81. The transcripts per million (TPM) values for the genes (n = 6) reported here were extracted from this analysis, and log10 transformed prior to statistical analysis.

2.3.8 Statistics

Cows were blocked (1 per genotype) by the actual calving date (< 21 d interval within any block). Effects of genotype, time relative to calving, and their interactions on metabolite concentration profiles as well as gene expression data were analyzed by repeated measure using PRO MIXED procedure of SAS with time relative to calving as the repeated effect. Multiple comparisons between data from UH and CH cows under the same time point were also conducted to indicate the difference on genotype at a certain time points. Experimental values were reported as mean ± standard error of the mean (SEM). Means were considered to differ when $P < 0.05$.

2.4 RESULTS

2.4.1 Status of serum lipids in UH and CH cows by proximate analysis

Examining the concentrations of serum NEFA from -4w to 8w of calving showed that both UH and CH cows had their serum NEFA increased from -2w and peaked at 1w of calving, but the scale of NEFA in CH cows was greater in scale and more prolonged than that in UH cows (**Figure 2.1A**). In contrast, serum triacylglycerol (TAG) concentrations at of UH and CH cows underwent sharp decreases at 1w of calving and then gradually increased, but no genotype-dependent differences were observed from -4w to 8w of calving (**Figure 2.1B**).

2.4.2 Status of serum lipids in UH and CH cows by lipidomic analysis

Periparturient UH and CH serum samples were further examined by the LC-MS-based lipidomic analysis. The kinetic profiles in the scores plot of the principal components analysis (PCA) model showed that UH and CH cows from -4w to 8w of calving shared a similar trajectory of time-dependent changes in the serum lipidomes, as reflected by the dramatic shift from -1 w to 1w along the principal component 2 and the gradual change from 1w to 8w along the principal component 1 of the model (**Figure 2.2A and Appendix A**). Nevertheless, the scale of changes in CH cows was greater than that in UH cows. The lipids contributing to this time-dependent separation of both UH and CH serum samples were identified in the loadings plot of the PCA model (**Figure 2.2B**) and further characterized by hierarchical clustering analysis that classified into 4 clusters as Cluster I_s, II_s, III_s, and IV_s, respectively (**Figure 2.2C**). The structural identities of major lipid markers in these 4 clusters of serum metabolites were defined by MSMS fragmentation and database search (**Table 2.3**). Cluster I_s comprises multiple TAGs and polyunsaturated fatty acid (PUFA)-containing phosphatidylcholines (PCs) that were decreased immediately after calving. Cluster II_s comprises mostly the PCs that were decreased after 1w of calving. Cluster III_s comprises the PCs that peaked at 1w or 2w of calving. Cluster IV_s comprises mostly the sphingomyelins (SMs), and lysophosphatidylcholine (LPCs) that were increased gradually after calving (**Figure 2.2C**).

Overall, periparturient UH and CH cows have similar time-dependent changes in their serum lipidomes with subtle differences on the time courses of individual lipid species.

2.4.3 Status of hepatic lipidome in UH and CH cows

Periparturient UH and CH liver samples from 4 time points were also examined by the LC-MS-based lipidomic analysis. Their kinetic profiles between -14d and 42d of calving in the scores plot of the PCA model showed that the hepatic lipidome of CH cows underwent more dramatic changes than that of UH cows (**Figure 2.3A and Appendix B**). The genotype-dependent differences are clearly visible in the representative chromatograms from the LC-MS analysis of hepatic lipids, in which polar lipids, mainly phospholipids, eluted between 3-5 min while neutral lipids, mainly TAGs, eluted between 6-8 min (**Figure 2.3B**). The lipids contributing to this genotype-dependent separation were identified in the loadings plot of the PCA model (**Appendix B**), and further characterized by MSMS fragmentation for their structural identities and the hierarchical clustering analysis for their kinetic profiles (**Table 2.4**). Among 3 clusters of genotype-dependent lipid markers defined by the clustering analysis, Cluster I_L comprises mostly the TAGs that became highly abundant in CH cows on 3d and 14d of calving but less so in UH cows; Cluster II_L comprises the PUFA-containing PCs that were abundant prepartum but decreased dramatically postpartum in CH cows; Cluster III_L comprises the PCs that were more abundant in UH cows (**Figure 2.3C**).

Considering that the PCA model, the kinetic profiles, and the clustering of UH and CH liver samples were all based on the relative abundance of hepatic lipids, the concentrations of TAG(18:1/18:1/18:1) and PC(18:1/18:1), two common TAG and PC species associated by their biosynthesis, were further quantified using their authentic standards. The results showed that UH and CH cows had comparable concentrations of hepatic TAG(18:1/18:1/18:1) and PC(18:1/18:1) on -14d and 42d of calving, but time- and genotype-dependent differences occurred on 3d and 14d of calving (**Figure 2.3D-E**). TAG(18:1/18:1/18:1) increased transiently on 3d, while it was greatly elevated on both 3d and 14d of calving in CH cows (**Figure 2.3D**). In contrast, PC(18:1/18:1)

increased gradually after calving in UH cows, while it underwent transient increase on 3d and then decreased afterward in CH cows (**Figure 2.3E**). These differences in the post-calving concentrations of TAG(18:1/18:1/18:1) and PC(18:1/18:1) led to different profiles of hepatic TAG (18:1/18:1/18:1) to PC(18:1/18:1) ratio between UH and CH cows, mainly caused by the more dramatic increase of TAG relative to PC in the liver of CH cows (**Figure 2.3F**). This imbalance of hepatic TAGs and PCs indicated that the PC biosynthesis in the liver of CH cows was not on pair with the dramatic increase of TAGs.

2.4.4 Status of hepatic metabolome in UH and CH cows

To examine hepatic hydrophilic metabolites in UH and CH, an untargeted metabolomic analysis was conducted. Similar to the lipidomic model, a clear separation between UH and CH in early lactation was observed in the scores plot of a PCA model (**Figure 2.4A and Appendix C**). The distribution of metabolite markers was illustrated in a loadings plot (**Figure 2.4B**). Ions contributed to the difference between UH and CH cows were identified (**Table 2.5**). Markers with high abundance in CH cows included β-hydroxy butyrate, carnitine, hypoxanthine, inosine, and dihydrothymine. High abundance markers in UH groups included choline, phosphocholine, dimethylamine, oxidized glutathione (GSSG), adenosine monophosphate (AMP), and spermine.

2.4.5 Choline and its related metabolites in the liver and serum of UH and CH cows

The causes underlying the lack of parallel increase of PC synthesis with TAG accumulation in post-calving CH cows were examined by measuring the concentrations of choline, betaine, phosphocholine (PhoC), and glycerophosphocholine (GPC) in the liver and serum, the core metabolites in PC biosynthesis and turnover. Hepatic choline and betaine decreased after calving but did not differ between UH and CH cows (**Figure 2.5A-B**). In contrast, hepatic PhoC and GPC had genotype-dependent differences as their concentrations were better recovered on 14d and 42d of calving in UH cows than that in CH cows after early postpartum decreases (**Figure 2.5C-D**).

Moreover, no genotype-dependent differences were observed on these metabolites in serum while time-dependent changes were observed on serum choline, betaine, and PhoC (**Figure 2.5E-H**).

2.4.6 Status of lipid metabolism-related genes in the hepatic transcriptomes of UH and CH cows

The influences of genetic selection on lipid metabolism were further examined by comparing the transcriptional levels of major enzymes and transporters involved in fatty acid synthesis, desaturation, elongation, and oxidation; NEFA uptake; TAG synthesis; PC synthesis; and VLDL assembly in CH and UH cow. Their transcript numbers in the liver of UH and CH cow were extracted from a RNAseq-based transcriptomic analysis and compared by hierarchical cluster analysis (**Figure 2.6**) revealing both calving-induced time-dependent changes and genotype-dependent differences in the expression of these lipid metabolism-related genes. Two major clusters, Cluster a and b, represented the higher expression of genes in the liver of CH and UH cows, respectively. In particular, genes that had statistical significance on genotype were further classified, from which genes involved in the hepatic VLDL assembly-related pathways were selected (**Figure 2.7A**). Most of the genes had higher expression levels in the liver CH cow than UH cow, including *AGAPT2*, *CD36*, and *DGAT1* that function for NEFA uptake and TAG synthesis; *APOC2*, *CIDEB*, *PLIN2*, and *MTTP* in VLDL assembly; *PEMT* and *BHMT*, and CKβ in PC synthesis (**Figure 2.7B-K**). The exceptions to this trend were *CPT* and *CEPT*, two enzymes responsible for converting CDP-choline to PC since their expression levels were lower in the liver of CH cows (**Figure 2.7L-M**).

Besides that, genes involved in other lipids metabolism events, such as fatty acid synthesis, elongation, desaturation, long-chain fatty acid transport and oxidation, were also examined and the result was shown by the hierarchical clustering analysis (**Figure 2.7**). For fatty acid synthesis,

elongation, and desaturation, expressions of *FADS1*, *FADS2*, *FADS6, ELOVL5*, and *SCD5* were higher in UH cows, which implied less FA synthesis and desaturation activities happened in the liver of CH cows. Expressions of *CPT1A, CPT1B, MLYCD*, and *ABCD3* in fatty acid oxidation were elevated in CH cows .

2.4.7 Correlation analysis of metabolites and genes in the serum and liver of UH and CH cows

Considering the genotype-dependent changes from lipidomic, transcriptomic, and metabolic analyses, the correlation analysis on metabolites and genes in the serum and liver of UH and CH cows were examined by Pearson correlation (**Figure 2.9**). The concentrations of hepatic TAG(18:1/18:1/18:1) and PC(18:1/18:1) were positively correlated to most of the genes in PC biosynthesis, TAG synthesis, and VLDL assembly, including *CKβ*, *PEMT*, *BHMT*, *AGAPT2*, *APOC2*, *CD36*, *CIDEB*, *DGAT1*, *MTTP*, and *PLIN2*, while negatively correlated to hepatic metabolites PhoC, GPC, and hepatic genes *CPT* and *CEPT*. Choline and betaine concentrations had positively correlation with PhoC and GPC, but they did not show strong correlation with hepatic gene expression in TAG synthesis or VLDL assembly. The intermediate metabolites, PhoC and GPC showed negatively correlation with most of the examined genes except for *CPT* and *CEPT*. For the correlation of hepatic genes, *CPT* and *CEPT* showed negatively correlated with other genes; while other genes examined in PC biosynthesis, TAG synthesis and VLDL assembly were positively correlated.

2.5 DISCUSSION

Hepatic steatosis, also called hepatic lipidosis or fatty liver, is a common early postpartum metabolic disorder in high-producing dairy cows. Postpartum alternations in lipid metabolism can lead to the formation of hepatic steatosis. The current study compared genetic selection-induced changes through a comparison of the lipidome, metabolomes, and transcriptomes, and identified

potential causes of hepatic steatosis in high-yield dairy cows. Inhibited hepatic PC biotransformation from choline and significant hepatic TAGs accumulation in the early lactation of CH is the most prominent observations that contribute to the development of hepatic steatosis. The causes and significance of genetic selection-induced metabolic changes in high milk yield dairy cows are summarized (**Figure 2.10**).

2.5.1 Profiling changes of lipids in serum

During early lactation, the NEB initiates lipid mobilization from adipose tissue to induce a high blood NEFA concentration. Serum NEFA concentrations increased sharply in CH cows at -1w of calving but peaked higher (250 vs 500 mEq/mL at 1 w) and remained higher in CH cows through 8w of calving (**Figure 2.1A**). Serum NEFA concentrations > 290 mEq/mL prepartum or > 600 mEq/mL postpartum are recognized as a risk for hepatic steatosis development [92], and our results indicate some of the CH cows had a greater risk of fatty liver development. Serum total TAG did not provide evidence of lipid metabolic changes between genotypes (**Figure 2.1B**), which suggest that major serum lipoprotein - VLDL concentration (not measured) might not have differed between these genotypes.

Through further comprehensive lipidomic analysis, subtle changes in PC, LPC, and SM species between genotypes were observed (**Figure 2.2C**). Previous research indicated lipid biomarkers for metabolic disorders-included increased serum PC C30:2 or PC C32:2 concentrations for fatty liver [162] and increased serum LPC and SM for hepatic steatosis, cardiovascular diseases, and diabetes [163-165]. In our study, most of the identified PC species contained 34-38 carbons further analysis is needed to determine whether they could be considered as biomarkers of metabolic disorders.

Compared to UH cows, CH cows had slightly higher levels of LPC and SM in postpartum suggesting a high possibility of generating hepatic steatosis.

2.5.2 Influence of genetic selection on hepatic lipidome and metabolome

In the current study, hepatic accumulation of TAGs in early lactation and inadequate PCs through all sampling time points in CH cows as the major lipid metabolic events (**Figure 2.3**). Hepatic hydrophilic metabolites with high abundance in early lactation CH cows included, β-hydroxybutyrate and carnitine (**Figure 2.4, Table 2.5**), which have been associated with the development of ketosis, hepatic steatosis, and increased lipid oxidation [153]. Moreover, the reduced PC and PhoC in the liver of CH cows guide the following investigation on choline metabolism and VLDL assembly. VLDL is the primary vehicle for hepatic TAGs export to other tissues. During this process, TAGs are incorporated into VLDL with apolipoprotein, phospholipids, bile salts, and cholesterols from hepatocytes. Among phospholipid species, PC accounts for 70% of total phospholipids in rodent VLDL, while minor components, PE and LPC are 4% and 3%, respectively [166]. Insufficient hepatic PC has been shown to impair the assembly and export of VLDL and contribute to the development of hepatic steatosis in rodents [167-169]. Therefore, the decreased PC in the current study might be relevant to a high risk of fatty liver formation in CH cows due to the impaired function of VLDL.

2.5.3 Influence of genetic selection on hepatic choline metabolism

Liver is the major location for choline metabolism, in which choline predominantly converts to PC and other choline-containing phospholipids, such as LPC, SM, and plasmalogen [170]. In the CDP-choline pathway, also called the Kennedy pathway, choline is converted to PhoC, CDP-choline, and PC catalyzed by choline kinase (CK), CTP: phosphocholine cytidylyltransferase (CT), CDP-

choline:1,2-diacylglycerol cholinephostransferase (CPT), and choline-ethanolamine phosphotransferase (CEPT) [171,172]. Concentrations of hepatic PhoC and GPC decreased at early lactation in both UH and CH (**Figure 2.5C-D**), while, their levels in CH remained much lower than UH although hepatic and serum choline concentrations were comparable (**Figure 2.5A and 4E**). This phenomenon suggests the inhibited PC synthesis of the CDP-choline pathway in the liver of CH rather than deficiency of choline intake.

CDP-choline pathway. CK catalyzes the first step in the CDP-choline pathway through phosphorylation of choline to PhoC. Three types of isozymes were found in mammals as CKα1, CKα2, and CKβ [173]. CK functions as a dimeric protein through the formation of either homodimer or heterodimer, the most active to less active forms are α/α homodimer, α/β heterodimer, and β/β homodimer, respectively [173]. In the current study, although a higher *CKβ* level was observed in CH (**Figure 2.7K**), *CKα* might be the majior enzymatic form with higher transcripts compared to *CKβ* (**Figure 2.8A**). Besides, the total transcripts in cluding CKα and CKβ maintained stability (**Figure 2.8B**) indicates the promoted expression of CKβ might not provide sufficient enzymatic quantity or activity for PC biosynehsis. CT is the rate-limiting enzyme of the CDP-choline pathway that can be regulated by sterol regulatory element-binding proteins (SREBPs) [174], however, no significant difference was found in our current study. *CPT* and *CEPT* levels (**Figure 2.7L-M**) were lower in CH compared to UH which limits the last step of PC synthesis in the liver. Inhibitions of *CPT* and *CEPT* in CH were not fully understood, it might be influenced by thyroid hormone [175].

PEMT pathway. Choline also serves as the major dietary source of methyl groups in one-carbon metabolism through oxidation to betaine [176], which recycles methionine and S-adenosylmethionine (SAM) in the PEMT-mediated PC synthesis [35,40]. *PEMT* and *BHMT* expression increased in

postpartum of UH and CH cows, especially in CH (**Figure 2.7I-J**). BHMT and PEMT catalyze the methyl group transformation from betaine and PC synthesis from PE in the PEMT pathway, respectively. When the CDP-choline pathway was defective, supplementation of choline and betaine reduced hepatic steatosis due to the role as methyl donors of choline and betaine that stimulated transmethylation of PE to PC through the PEMT pathway [177]. Correspondingly, our study observed the suppressed CDP-choline pathway and promoted the PEMT pathway, which was shown as the slight increased PC concentration (**Figure 2.3E**) postpartum associated with the dramatic increased TAG concentration. This phenomenon might be a compensational mechanism of PC biosynthesis in the liver of CH cows. In rodents, 70% of hepatic PC is synthesized through the CDP-choline pathway, and this pathway can mobilize 95% of choline in the total choline pool [178]. The other 30% of hepatic PC derives from the PEMT pathway, of which the liver is the only tissue that contains PEMT activity [179]. However, the contribution of these two metabolic pathways to PC biosynthesis in dairy cattle needs to be further investigated.

2.5.4 Influence of genetic selection on hepatic lipid synthesis

VLDL assembly. Apolipoprotein B-100 (ApoB100), apolipoprotein C (ApoC), and apolipoprotein E (ApoE) are the main structural protein for VLDL stabilization and assembly [180,181]. Microsomal triglyceride transfer protein (MTP) and low-density lipoprotein receptor (LDLR), two assistant proteins, function for the incorporation of TAGs into the VLDL [182,183]. CIDEB and PLIN2 (also called adipocyte differentiation-related protein, ADRP) are two major proteins associated with cytosolic lipid droplet formation in the liver. Overexpression of *PLIN2* is associated with increased accumulation of hepatic cytosolic lipid droplets and a corresponding decrease in VLDL secretion [184]. The negative correlation of VLDL assembly and secretion with hepatic steatosis in dairy cows had been observed in clinical research [185]. In our current study, high level expressions of *APOC2*,

CIDEB, *MTTP*, and *PLIN2* were observed in the liver of CH cows (**Figure 2.7**), suggesting more TAG transported into VLDL but impeded VLDL distribution from the liver to other tissues.

TAG synthesis. As responses of enhanced blood NEFA concentration in the serum, CH cows had increased gene expression related to TAG synthesis in the liver, which is reflected as promoted fatty acid transport protein cluster of differentiation 36 (CD36) and TAG synthesis enzyme diacylglycerol acyltransferase 1 (DGAT1) (**Figure 2.7**). These phenomena indicate more TAG was synthesized and accumulated in the liver of CH cows. A high concentration of NEFA also associated with the reduced VLDL assembly and secretion in bovine hepatocytes was found in a previous study [186].

2.5.5 Influence of genetic selection on hepatic lipid oxidation

Lipid metabolism in the liver is largely regulated by PPARα and SREBP, in which the former gene regulates a series of enzymes involved in fatty acid oxidation and ketogenesis, including carnitine palmitoyl transferase 1A (CPT1A), CPT2, fatty acid-binding protein 1 (FABP1), acyl-CoA oxidase 1 (ACOX1), mitochondrial long and medium-chain acyl-CoA dehydrogenase (LCAD, MCAD), and mitochondrial-3-hydroxy-3-methylglutaryl-CoA (HMGCS2) [187,188]. Conversely, SREPB-1 plays an important role in the regulation of hepatic lipid synthesis through activating lipogenic enzymes, such as acetyl-CoA carboxylase 1 (ACC1), fatty acid synthase (FAS), stearoyl-CoA desaturase-1 (SCD1), DGAT1, and DGAT2 [189,190]. Fatty acid oxidation and TAG export through VLDL are two major factors regulating TAG content in the liver. Dairy cows with mild fatty liver showed increased expressions of PPARα and its regulated genes compared to individuals without fatty liver [191,192], implying that the lack of fatty acid oxidation might not be the crucial reason behind the development of hepatic steatosis. Therefore, inadequate VLDL in exporting extra TAG from

the liver contributes more to hepatic steatosis development. The overexpression of SREBP-1c is capable to induce hepatic steatosis in transgenic mice [193]. In our current study, we observed the elevated expression of *DGAT1*, *CPT1A*, *CPT1B* (**Figure 2.6**), which suggests the promotion of TAG synthesis and oxidation. Meanwhile, reduced expression of *FADS*, *FADS2*, *FADS6*, and *SCD5* was also observed in the liver of CH cows (**Figure 2.6**), indicating more saturated fatty acid incorporated into hepatic lipids of CH cows than UH cows, this phenomenon was consistent with the results on the composition of fatty acid profiles in serum and hepatic lipidome (**Figure 2.2C** and **Figure 2.3C**). These results indicate that robust lipid metabolism occurred in the liver of CH cows than UH cows with the persistent stimulation in PPARα and SREBP-regulated metabolic events, but CH cows had high risk to obtain more saturated fat in their liver that might contribute to the fatty liver development.

2.5.6 Practice and significance of choline supplementation in high-producing dairy cows

It is well established that choline is needed for hepatic VLDL assembly and export [176], and choline deficiency contributes to hepatic steatosis [194-197]. Supplementation of rumen-protected choline (RPC) has become a widely adopted practice in dairy cow husbandry to alleviate the extent of hepatic lipid infiltration, especially in the transition period [153,198-200]. Relatively consistent observations in numerous RPC feeding trials were the increased milk production by RPC supplementation, but its effects in reducing hepatic steatosis were inconsistent and contradictory in many cases [198,201-203]. The mechanisms behind the selective effects of RPC supplementation are not fully investigated. Our current study might reveal the potential cause of hepatic steatosis in CH due to the reduced biotransformation PC from choline rather than the insufficient choline supplementation as a response for handling excessed NEFAs in the liver of CH cows. Meanwhile, the enhanced choline through PEMT pathway metabolism using choline as precursor might be a compensatory mechanism for insufficient PC synthesis in the CDP-choline pathway. Considering

that PC biosynthesis and one-carbon metabolism are two major usages of choline, it is likely that RPC supplementation may greatly enhance the anabolic metabolism for milk production through its methyl donor function, but its influence on PC biosynthesis through the CDP-choline pathway might be very limited. Results from this study can contribute to novel approaches for alleviating and managing metabolic disorders in the transition period of dairy cows.

2.5.7 Utilization of metabolomics and lipidomics platform

Previous efforts on examining the metabolites and metabolic events contributing to the lipid metabolism disorders of dairy cows mainly focused on measuring classes of lipids, such as total free fatty acids and total lipids, and were not able to identify specific lipid species effectively. Comprehensive profiling of the complex and diverse metabolic events in lipidomes of dairy cows using metabolomics platforms is required. In our current study, lipid species that contribute the genetic selection-induced difference were identified, especially the hepatic lipidome, in which increase of TAGs and decrease of PCs were the main observations (**Figure 2.3**). The LC-MS-based metabolomics and lipidomic analyses revealed novel information on metabolic disorders in dairy cows.

2.6 CONCLUSIONS

Overall, our current study examined the serum and hepatic lipidomes, in which the imbalanced lipid profile in the liver was observed as dramatically increased TAG associated with insufficient PC as well as suppressed choline to PC biosynthesis pathway in CH cows. Compared to UH cows, the deficient hepatic PC for VLDL synthesis and assembly inhibited TAG export from the liver to other tissues, causing lipid accumulation in the liver and the development of hepatic steatosis in

CH cows. These observations warrant further investigations on the mechanisms of genetic selection-induced lipid metabolic disorders.

Table 2.1 Source of chemicals and reagents used in chemical analysis, LC-MS analysis, structural confirmation, and quantification.

Chemicals and reagents	**Vendor**
Acetonitrile (LC-MS grade), Formic acid (LC-MS grade), Water (LC-MS grade)	Fisher Scientific (Houston, TX)
Amino acid mixture (acidic), Amino acid mixture (basic), *n*-Butanol, Dansyl chloride (DC), Phosphocholine	Sigma-Aldrich (St. Louis, MO)
Betaine	USB Corporation (Cleveland, OH)
Choline	Acros Organics (Fair Lawn, NJ)
3,4-Dihydroxyphenylacetic acid (DHPAA), 2-Hydrazinoquinoline (HQ), Triphenylphosphine (TPP)	Alfa Aesar (Tewksbury, MA)
2-2′-Dipyridyl disulfide (DPDS)	MP Biomedicals, LLC (Irvine, CA)
Fatty acids standards (C4-C22)	Nu-Chek Prep, Inc. (Elysian, MN)
Glycerophosphocholine	Chem-IMPEX international (Wood Dale, IL)
Methanol (LC-MS grade)	Avantor performance materials (Radnor, PA)
1,2-Dioleoyl-sn-glycero-3-phosphocholine/PC(18:1,18:1)	Sigma-Aldrich (St. Louis, MO)
Triolein/TAG(18:1, 18:1, 18:1)	Nu-Chek Prep (Elysian, MN)

Table 2.2 LC-MS data acquisition condition in a 10-minute run.

Target compounds	Column type	Mobile phase	MS detection mode
Lipidome	BEH C8	A: 0.1% formic acid and 10 mM NH_4HCO_2 in 60% H_2O and 40% ACN B: 0.1% formic acid and 10 mM NH_4HCO_2 in methanol	Positive
Amino acids (dansylated)	BEH C18	A: 0.1% formic acid in H_2O B: 0.1% formic acid in ACN	Positive
Fatty acids (HQ derivatization)	BEH C18	A: 2 mM NH_4OAc in H_2O with 0.05% CH_3COOH B: 2 mM NH_4OAc in 95% ACN and 5% H_2O with 0.05% CH_3COOH	Positive
Hydrophilic metabolites	BEH C18	A: 0.1% formic acid in H_2O B: 0.1% formic acid in ACN	Positive and negative
Choline metabolites	BEH Amide	A: 10 mM ammonium formate (pH = 5) in H_2O with 10% ACN B: 95% ACN with 5%A	Positive

Table 2.3 Identification of lipid species in serum lipidome in CH and UH cows.

Cluster	Detection mode	*m/z*	Structural ID	Cluster	Detection mode	*m/z*	Structural ID
I_s	$[M+H]^+$	806.5696	PC(18:2/20:4)*	II_s	$[M+H]^+$	812.6163	PC(18:2/20:1)*
I_s	$[M+H]^+$	804.5659	PC(18:2/20:5)*	III_s	$[M+H]^+$	758.5656	PC(16:0/18:2)*
I_s	$[M+H]^+$	671.5743	CE(20:5)*	III_s	$[M+H]^+$	760.5861	PC(16:0/18:1)*
I_s	$[M+H]^+$	780.5553	PC(18:2/18:3)*	III_s	$[M+H]^+$	786.6025	PC(18:0/18:2)*
I_s	$[M+H]^+$	808.5345	PC(18:1/20:4)*	IV_s	$[M+H]^+$	756.5540	PC(16:1/18:2)
I_s	$[M+H]^+$	700.5287	PC(12:0/18:3)	IV_s	$[M+H]^+$	689.5570	SM(d18:1/15:0)
I_s	$[M+H]^+$	678.5785	PE(14:0/17:0)	IV_s	$[M+H]^+$	801.6844	SM(d18:1/23:0)
II_s	$[M+NH_4]^+$	904.8314	TAG(18:0/18:1/18:1)*	IVs	$[M+H]^+$	675.5444	SM(d18:1/14:0)
II_s	$[M+NH_4]^+$	906.8447	TAG(18:0/18:0/18:1)*	IV_s	$[M+H]^+$	520.3407	LPC(18:2)*
II_s	$[M+NH_4]^+$	838.7852	TAG(16:0/16:0/17:0)	IV_s	$[M+H]^+$	542.3220	LPC(20:5)
II_s	$[M+NH_4]^+$	912.7965	TAG(15:0/18:1/22:4)	IV_s	$[M+H]^+$	546.3561	LPC(20:3)*
II_s	$[M+NH_4]^+$	908.8598	TAG(18:0/18:0/18:0)*	IV_s	$[M+H]^+$	524.3733	LPC(18:0)*
II_s	$[M+NH_4]^+$	876.8010	TAG(16:0/18:1/18:1)*	IV_s	$[M+H]^+$	703.5760	SM(d18:1/16:0)
II_s	$[M+H]^+$	832.5850	PC(18:2/22:5)*	IV_s	$[M+H]^+$	731.6000	SM(d18:1/18:0)
II_s	$[M+H]^+$	834.6000	PC(18:2/22:4)*	IV_s	$[M+H]^+$	742.5749	PC(O-16:0/18:3)*

*: confirmed by MSMS fragmentation.

Table 2.4 Identification of lipid species in hepatic lipidome of CH and UH cows.

Cluster	Detection mode	*m/z*	Structural ID	Cluster	Detection mode	*m/z*	Structural ID
I_L	$[M+NH_4]^+$	846.7561	TAG(16:0,/16:1/18:2)*	I_L	$[M+NH_4]^+$	836.7726	TAG(15:0/16:0/18:1)*
I_L	$[M+NH_4]^+$	874.7856	TAG(16:0/18:1/18:2)*	I_L	$[M+NH_4]^+$	828.7136	TAG(15:1/17:2/17:2)*
I_L	$[M+NH_4]^+$	902.8165	TAG(18:1/18:1/18:1)*	II_L	$[M+H]^+$	834.5992	PC(18:1/22:5)*
I_L	$[M+H]^+$	562.6341	Cer(d18:2/18:1)	II_L	$[M+H]^+$	838.6321	PC(18:1/22:3)*
I_L	$[M+H]^+$	551.5030	DAG(14:0/18:1)	II_L	$[M+H]^+$	810.6014	PC(16:0/22:4)*
I_L	$[M+NH_4]^+$	796.7431	TAG(14:0/16:0/16:0)*	III_L	$[M+H]^+$	774.6041	PC(17:0/18:1)*
I_L	$[M+NH_4]^+$	824.7721	TAG(16:0/16:0/16:0)*	III_L	$[M+H]^+$	808.5878	PC(18:1/20:4)*
I_L	$[M+NH_4]^+$	853.8062	TAG(15:0/18:3/18:3)	III_L	$[M+H]^+$	808.5878	PC(16:0/22:5)
I_L	$[M+NH_4]^+$	794.7271	TAG(14:0/16:0/16:1)	III_L	$[M+H]^+$	836.6161	PC(18:1/22:4)*
I_L	$[M+NH_4]^+$	822.7553	TAG(14:0/16:0/18:1)*	III_L	$[M+H]^+$	858.5867	PC(20:3/22:5)*
I_L	$[M+NH_4]^+$	878.8142	TAG(16:0/18:0/18:1)*	III_L	$[M+H]^+$	647.5593	DAG(18:3/20:0)
I_L	$[M+NH_4]^+$	820.7424	TAG(16:0/16:1/16:1)	III_L	$[M+H]^+$	788.6172	PC(18:0/18:1)*
I_L	$[M+NH_4]^+$	884.7736	TAG(17:1/18:2/18:2)	III_L	$[M+H]^+$	786.6000	PC(18:1/18:1)*
I_L	$[M+NH_4]^+$	848.7734	TAG(16:1/16:1/18:0)	III_L	$[M+H]^+$	758.5704	PC(16:0/18:2)*

*: confirmed by MSMS fragmentation.

Table 2.5 identification of metabolites in hepatic metabolome of UH and CH cows

Ions	Modes of Ion detection	*m/z* of detection	Identity	Formula	Δppm	Database ID
I	$[M+HQ]^+$	270.1349	Dihydrothymine	$C_5H_8N_2O_2$	-0.4	HMDB0000079
II	$[M+H]^+$	137.0466	Hypoxanthine	$C_5H_4N_4O$	2.2	HMDB0000157
III	$[M-H]^-$	267.0698	Inosine	$C_{10}H_{12}N_4O_5$	-7.8	HMDB0000195
IV	$[M+HQ]^+$	246.1238	β-Hydroxy butyrate	$C_4H_8O_3$	-1.2	HMDB0000011
V	$[M+H]^+$	162.1132	Carnitine	$C_7H_{15}NO_3$	1.2	HMDB0000062
VI	$[M+H]^+$	203.2235	Spermine	$C_{10}H_{26}N_4$	-0.5	HMDB0001256
VII	$[M+DC]^+$	279.1168	Dimethylamine	C_2H_7N	0.4	HMDB0000087
VIII	$[M-H]^-$	611.1454	Glutathione, oxidized	$C_{20}H_{32}N_6O_{12}S_2$	-1.2	HMDB0003337
IX	$[M+H]^+$	104.1077	Choline	$C_5H_{13}NO$	1.9	HMDB0000097
X	$[M+H]^+$	348.0707	Adenosine monophosphate	$C_{10}H_{14}N_5O_7P$	-0.6	HMDB0000045
XI	$[M+H]^+$	184.0741	Phosphocholine	$C_5H_{14}NO_4P$	4.4	HMDB0001565

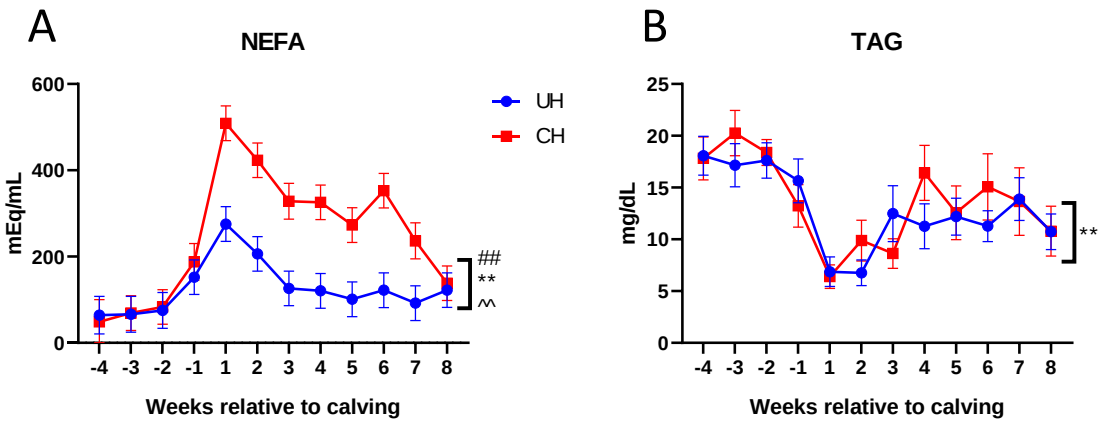

Figure 2.1 Biochemical analysis of serum lipids in transition UH and CH cows from -4w to 8w of calving. UH and CH cows (n =12/genotype) were fed the same TMR throughout the study. (A) Concentrations of serum NEFA. (B) Concentrations of serum TAG. The symbols of #, *, ^, and ##, **, ^^ indicate $0.01<P\leqslant 0.05$ and $P \leqslant 0.01$ for statistical differences by genotype, time (week), and genotype-time interaction, respectively. The NEFA data are from Weber et al., unpublished.

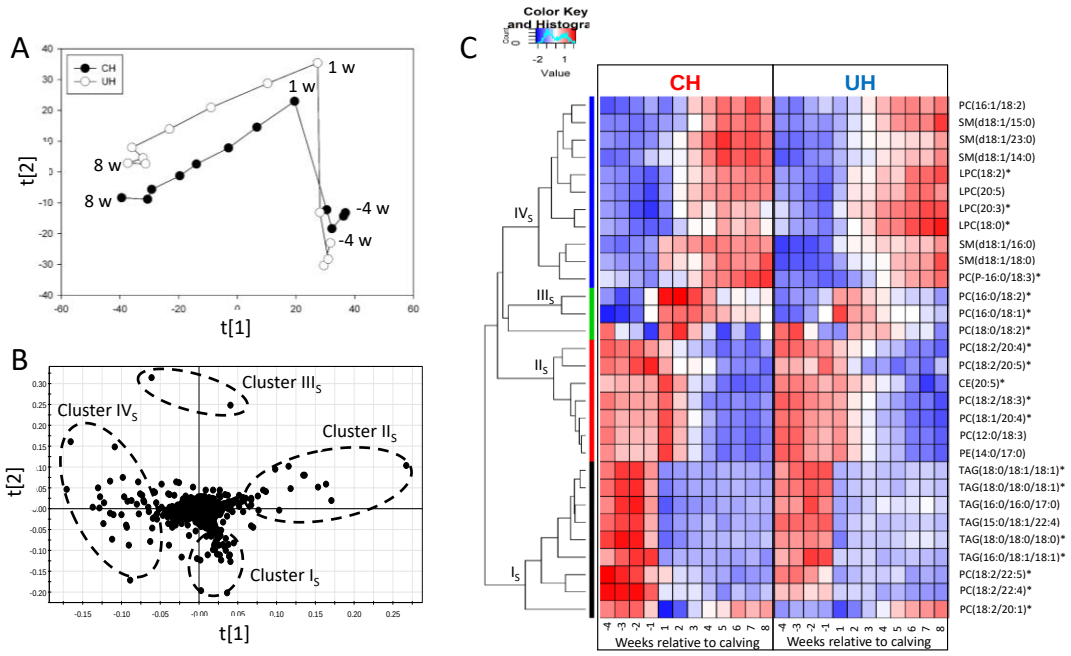

Figure 2.2 Characterization of time-dependent changes in the serum lipidomes of transitional UH and CH cows. (A) The scores plot of a PCA model on serum lipidome from -4w to 8w of calving. Each data point is the means of 12 samples at each time point in principal components 1 and 2. (B) The loadings plot of the PCA model. (C) HCA-based heat map on the serum lipid species in CH and UH cows. *: confirmed by MSMS fragmentation.

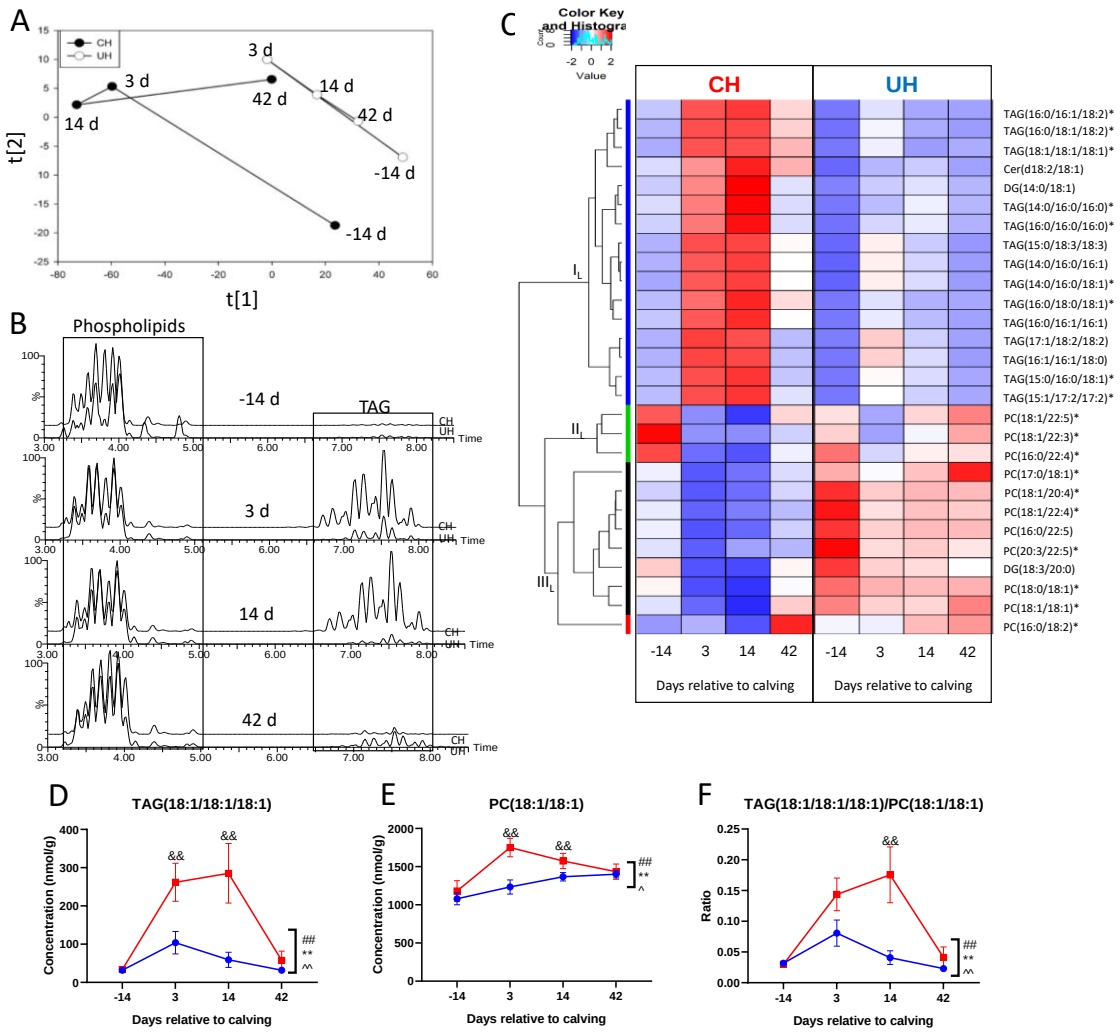

Figure 2.3 Genetic selection-induced difference in hepatic lipidome. (A) The scores plot of a PCA model on hepatic lipidome at -14d, 3d, 14d, and 42d of lactation. Each data point is the means of 12 samples at each time point in the principal components 1 and 2. (B) Extracted chromatography of UH and CH cows in comparison of phospholipid (PL) and TAG groups. (C) HCA-based heat map on the serum lipid species in CH and UH cows. *: confirmed by MSMS fragmentation. One TAG and one PC species from hepatic multivariate modeling were quantified. (D) Concentrations of hepatic TAG(18:1/18:1/18:1). (E) Concentrations of hepatic PC(18:1/18:1). (F) Ratio of TAG(18:1/18:1/18:1) vs PC(18:1/18:1). The symbols of #, *, ^, & and ##, **, ^^, && indicate

$0.01<P\leq 0.05$ and $P \leq 0.01$ for statistical difference by genotype, time (day), genotype-time interaction, and genotype under a specific time point, respectively.

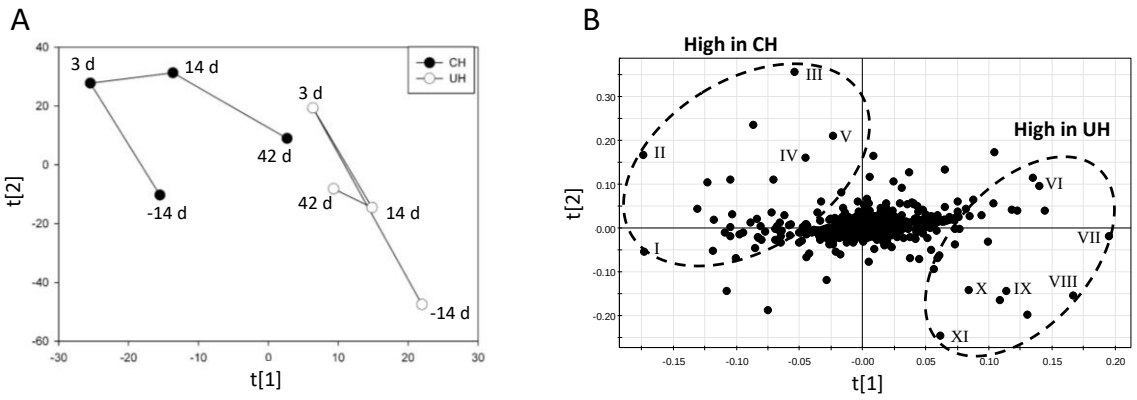

Figure 2.4 Genetic selection-induced difference in hepatic hydrophilic metabolites. The metabolome of hepatic aqueous extraction was conducted. (A) The scores plot of a PCA model on hepatic metabolome -14d, 3d, 14d, and 42d of lactation. Each data point is the means of 12 samples at each time point in principal components 1 and 2. (B) The loadings plot of the PCA model.

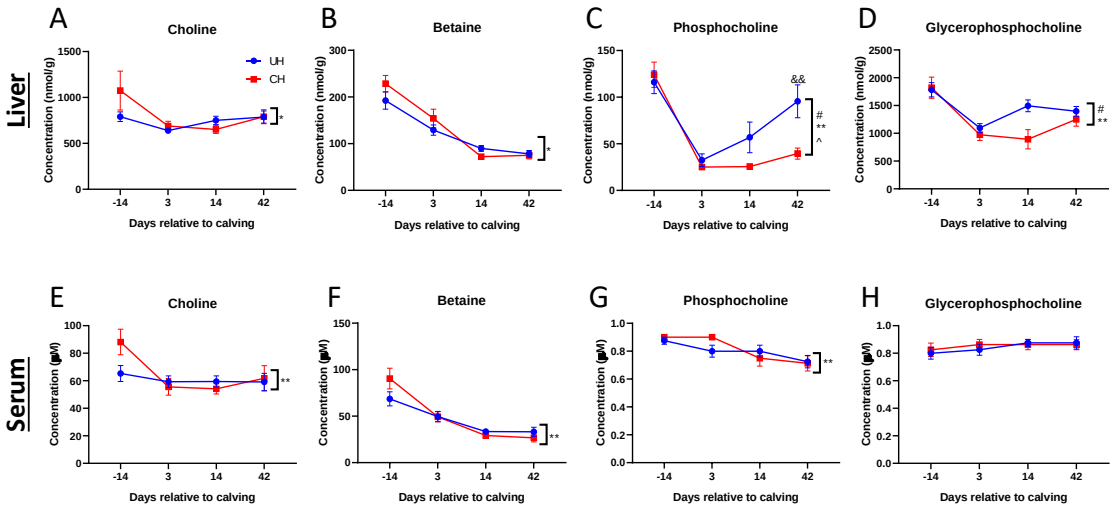

Figure 2.5 Genetic selection-induced difference in choline-related metabolites in the liver and serum. (A) Concentrations of hepatic choline at -14d, 3d, 14d, and 42d of lactation. (B) Concentrations of hepatic betaine. (C) Concentrations of phosphocholine. (D) Concentrations of glycerophosphocholine. (E) Concentrations of serum choline. (F) Concentrations of serum betaine. (G) Concentrations of serum phosphocholine. (H) Concentrations of serum glycerophosphocholine. The symbols of #, *, ^, & and ##, **, ^^, && indicate $0.01<P\leq 0.05$ and $P \leq 0.01$ for statistical difference by genotype, time (day), genotype-time interaction, and genotype under a specific time point, respectively.

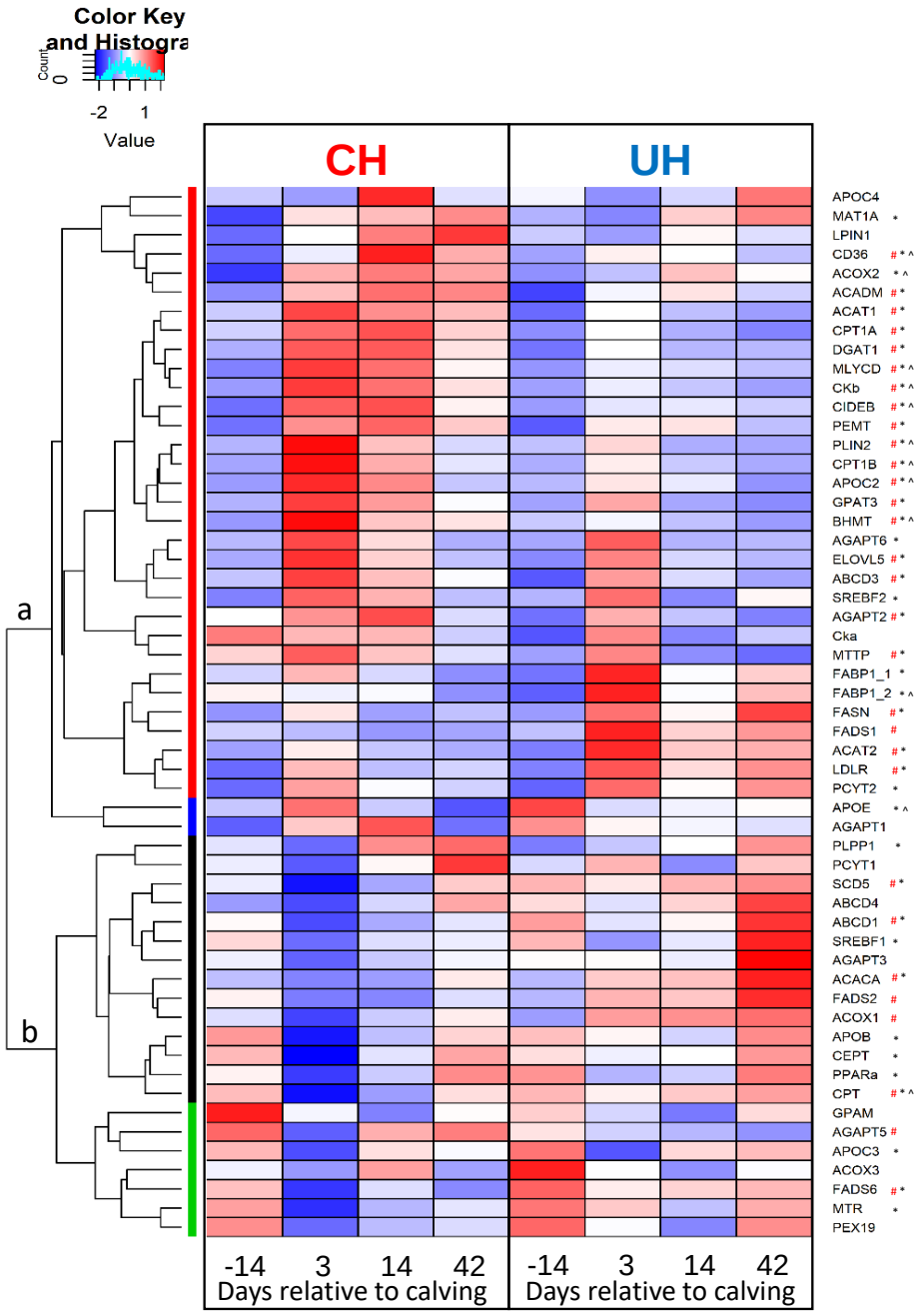

Figure 2.6 Cluster analysis of genes involved in hepatic lipid metabolism. Transcript numbers of hepatic lipid metabolism-related genes in the liver of CH and UH at -14d, 3d, 14d, and 42d of lactation were quantified and recorded as transcripts per million. Gene expression levels were grouped by HCA. Gene expression levels of each amino acid at different time points and genotypes were compared with their mean value and are presented according to inlaid color keys. The symbols of #, *, ^ indicate $0.01<P\leq 0.05$ for statistical difference by genotype, time (day), and genotype-

time interaction, respectively. ABCD1: ATP binding cassette subfamily D member 1; ABCD3: ATP binding cassette subfamily D member 3; ABCD4: ATP binding cassette subfamily D member 4; ACACA: acetyl-CoA carboxylase alpha; ACADM: medium-chain acyl-CoA dehydrogenase; ACAT1: acetyl-CoA acetyltransferase 1; ACAT2: acetyl-CoA acetyltransferase 2; ACOX1: acyl-CoA oxidase 1; ACOX2: acyl-CoA oxidase 2; ACOX3: acyl-CoA oxidase 3; AGAPT1: 1-acylglycerol-3-phosphate O-acyltransferase 1; AGAPT2: 1-acylglycerol-3-phosphate O-acyltransferase 2; AGAPT3: 1-acylglycerol-3-phosphate O-acyltransferase 3; AGAPT5: 1-acylglycerol-3-phosphate O-acyltransferase 5; AGAPT6: 1-acylglycerol-3-phosphate O-acyltransferase 6; APOB: apolipoprotein B; APOC2: apolipoprotein C2; APOC3: apolipoprotein C3; APOC4: apolipoprotein C4; APOE: apolipoprotein E; BHMT: betaine homocysteine methyltransferase; CD36: cluster of differentiation 36; CEPT: choline/ethanolamine phosphotransferase 1; CIDEB: cell death-inducing DFFA-like effector b. CKα: choline kinase alpha; CKβ: choline kinase beta; CPT: choline phosphotransferase 1; CPT1A: carnitine palmitoyl-transferase 1a; CPT1B: carnitine palmitoyl-transferase 1b; DGAT1: diacylglycerol O-acyltransferase 1; ELOVOL5: fatty acid elongase 5; FABP11: fatty acid binding protein 1, transcript 1; FABP12: fatty acid binding protein 1, transcript 2; FADS1: fatty acid desaturase 1; FADS2: fatty acid desaturase 2; FADS6: fatty acid desaturase 6; FASN: fatty acid synthase; GPAM: glycerol-3-phosphate acyltransferase; GPAT3: glycerol-3-phosphate acyltransferase 3; LDLR: low-density lipoprotein receptor; LPIN1: lpin 1; MAT1A: methionine adenosyltransferase 1A; MLYCD: malonyl-CoA dehydrogenase; MTR: 5-methyltetrahydrofolate-homocysteine methyltransferase; MTTP: microsomal triglyceride transfer protein; PCYT1: phosphate cytidylyltransferase 1; PCYT2: phosphate cytidylyltransferase 2; PEMT: phosphatidylethanolamine N-methyltransferase; PEX19: peroxisomal biogenesis factor 19; PLIN2: perilipin 1; PLPP1: phospholipid phosphatase 1; PPARa: peroxisomal proliferator-activated receptor alpha; SCD5: stearoyl-CoA desaturase 5; SREBF1: sterol regulatory element-binding transcription factor 1; SREBF2: sterol regulatory element-binding transcription factor 2.

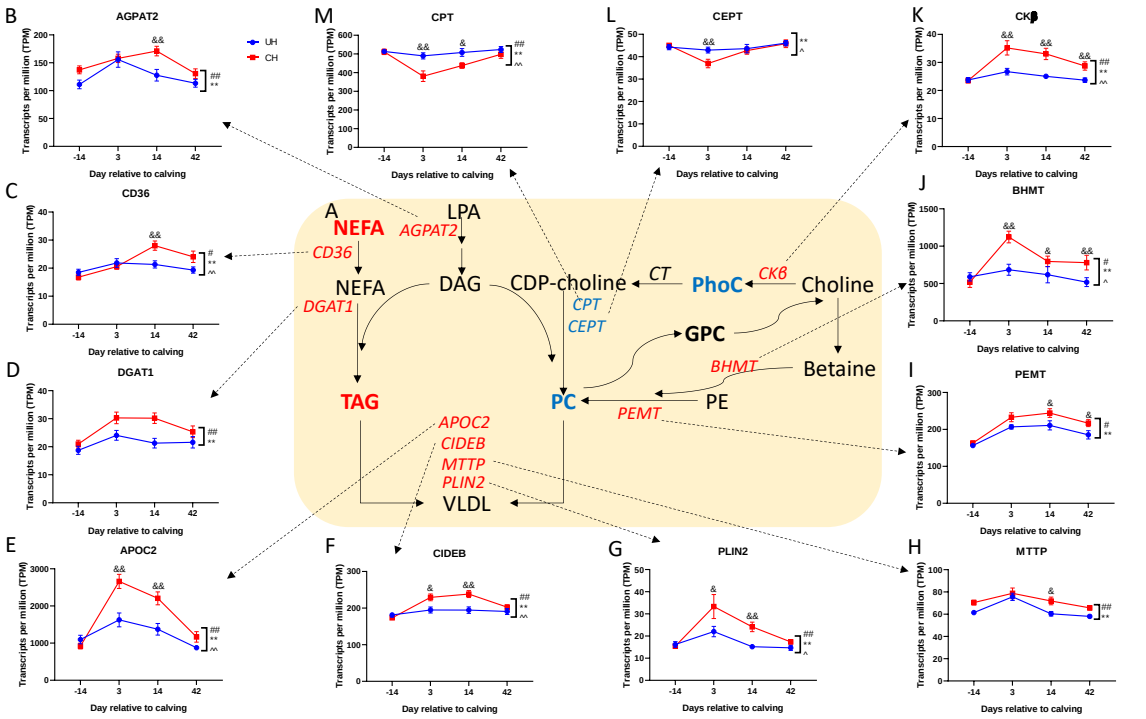

Figure 2.7 Hepatic gene expression of lipid metabolism in UH and CH cows. Transcript numbers of lipid metabolism-related genes in the liver of CH and UH at -14d, 3d, 14d, and 42d of lactation were quantified and recorded as transcripts per million. (A) Major pathway in hepatic lipid metabolism. (B) Gene expression level of *AGPAT2*. (C) Gene expression level of *CD36*. (D) Gene expression level of *DGAT1*. (E) Gene expression level of *APOC2*. (F) Gene expression level of *CIDEB*. (G) Gene expression level of *PLIN2*. (H) Gene expression level of *MTTP*. (I) Gene expression level of *PEMT*. (J) Gene expression level of *BHMT*. (K) Gene expression level of *CKβ*. (L) Gene expression level of *CEPT*. (M) Gene expression level of *CPT*. The symbols of #, *, ^, & and ##, **, ^^, && indicate $0.01<P\leq 0.05$ and $P \leq 0.01$ for statistical difference by genotype, time (day), genotype-time interaction, and genotype under a specific time point, respectively. AGAPT2: 1-acylglycerol-3-phosphate O-acyltransferase 2; CD36: cluster of differentiation 36; DGAT1: diacylglycerol O-acyltransferase 1; APOC2: apolipoprotein C2; CIDEB: cell death-inducing DFFA-like effector b; PLIN2: perilipin 2; MTTP: microsomal triglyceride transfer protein; PEMT:

phosphatidylethanolamine N-methyltransferase; BHMT: betaine homocysteine methyltransferase; CKβ: choline kinase beta.

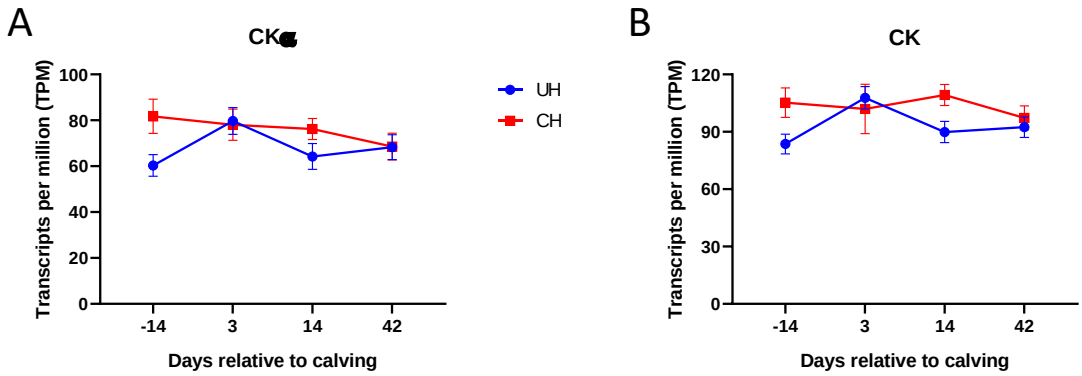

Figure 2.8 Hepatic CK gene expression in UH and CH cows. Transcript numbers of CK genes in the liver of UH and CH at -14d, 3d, 14d, and 42d of lactation were quantified and recorded as transcripts per million. (A) Gene expression level of CKα. (B) Gene expression level of CK (combined transcript number from CKα and CKβ).

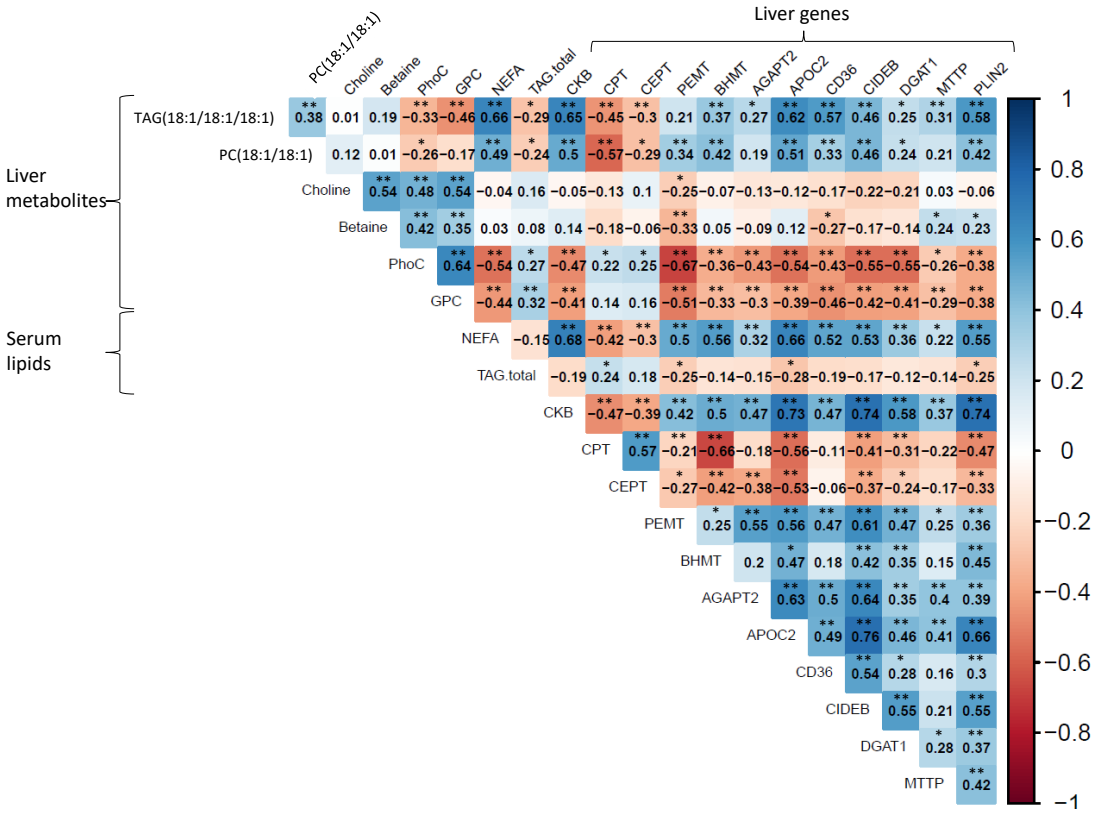

Figure 2.9 Interactions of serum lipids, hepatic metabolites, and hepatic genes. Concentrations of hepatic metabolites, serum lipids, and transcripts of hepatic gene expression in CH and UH at -14d, 3d, 14d, and 42d of lactation were analyzed by Pearson correlation. R-value of two factors was labeled on the plot indicating either a positive correlation or a negative correlation. The symbols of * and ** indicate 0.01<P≤ 0.05 and P ≤ 0.01 for statistical difference. TAG.18.1.18.1.18.1: TAG(18:1/18:1/18:1); PC.18.1.18.1: PC(18:1/18:1); PhoC: phosphocholine; GPC: glycerophosphocholine; NEFA: non-esterified fatty acid; TAG total: total serum TAG; CKb: choline kinase beta, CKβ; CPT: choline phosphotransferase 1; CEPT: choline/ethanolamine phosphotransferase 1; PEMT: phosphatidylethanolamine N-methyltransferase; BHMT: betaine homocysteine methyltransferase; AGAPT2: 1-acylglycerol-3-phosphate O-acyltransferase 2; APOC2: apolipoprotein C2; CD36: cluster of differentiation 36; CIDEB: cell death-inducing DFFA-like effector b; DGAT1: diacylglycerol O-acyltransferase 1; MTTP: microsomal triglyceride transfer protein.

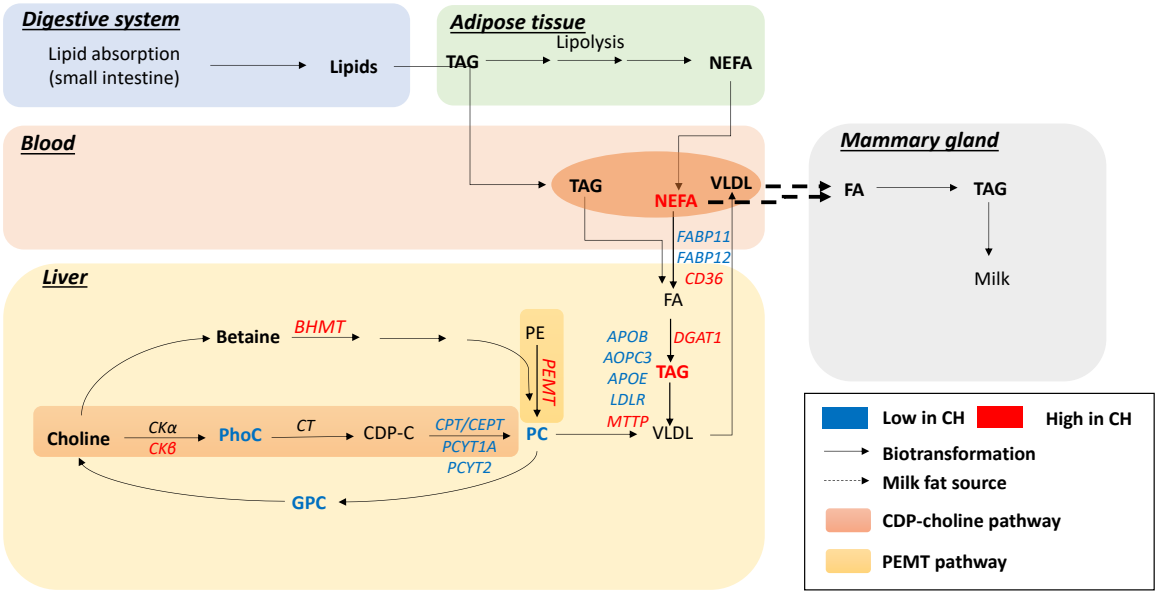

Figure 2.10 Summary of genetic selection-induced lipid metabolic disorder in dairy cows. Elevated serum NEFA from lipolysis in adipose tissue happened due to the high demand for milk production in the transition period of CH cows. Imbalanced TAG and PC in the liver were the prominent markers in the lipidome of CH cows due to the insufficient PC biosynthesis from the CDP-choline pathway, meanwhile, the PEMT pathway was promoted as a response to PC deficiency. Under this situation, TAG accumulation and PC deficiency might further suppress lipid export from the liver through VLDL in CH cows. These genetic selection-induced metabolic events disturb lipid metabolism and cause hepatic steatosis in CH cows.

CHAPTER 3. METABOLOMIC FINGERPRINTING OF CHEMICAL EXPOSURE IN PRODUCTION ANIMALS: A CASE STUDY ON RUMINAL RUTIN TREATMENT AND ITS INTERACTION WITH MICROBIAL METABOLISM IN DAIRY COWS

This chapter is modified from the manuscript:

Guo, Y.; Weber., W. J.; Yao, D.; Caixeta, L.; Zimmerman, N. P.; Thompson, J.; Block, E.; Rehberger, T. G.; Crooker, B. A.; Chen, C. Forming 4-methylcatechol as the dominant bioavailable metabolite of intraruminal rutin inhibits *p*-cresol production in dairy cows. *Metabolites* 2021 12(1): 16.

3.1 SUMMARY

Rutin, a natural flavonol glycoside, elicits its diverse health-promoting effects from the bioactivities of quercetin, its aglycone. While widely distributed in the vegetables and fruits of the human diet, rutin is either absent or inadequate in common animal feed ingredients. Rutin has been supplemented to dairy cows for performance enhancement, but its metabolic fate *in vivo* has not been determined. In this study, plasma, urine, and rumen fluid samples were collected before and after the intraruminal dosing of 100 mg/kg rutin to 4 Holsteins, and then characterized by both targeted and untargeted liquid chromatography-mass spectrometry (LC-MS)-based metabolomic analysis. In plasma and urine, 4-methylcatechol sulfate was identified as the most abundant metabolite of rutin, instead of quercetin and its flavonol metabolites, and its concentration was inversely correlated with the concentration of *p*-cresol sulfate. In rumen fluid, the formation of 3,4-dihydroxyphenylacetic acid (DHPAA) and 4-methylcatechol after rapid degradation of rutin and quercetin concurred with the decrease of *p*-cresol and the increase of its precursor, 4-hydroxyphenylacetic acid. Overall, the formation of 4-methylcatechol, a bioactive microbial metabolite, as the dominant bioavailable metabolite of rutin and quercetin, could contribute to their beneficial bioactivities in dairy cows, while the decrease of *p*-cresol, a microbial metabolite with negative biological and sensory properties, from the competitive inhibition between microbial metabolism of rutin and tyrosine, has the potential to reduce environmental impact of dairy operations and improve health of dairy cattle.

KEYWORDS: Rutin, quercetin, 4-methylcatechol, p-cresol, microbial metabolism, dairy cow

ABBREVIATIONS: AA, amino acid; ACN, acetonitrile; tBHQ, tert-butyl hydroxyquinone; DC, dansyl chloride; DHPAA, 3,4-dihydroxyphenylacetic acid; DPDS, 2-2'-dipyridyl disulfide; HCl, hydrochloride acid; HMDB, human metabolome database; HQ, 2-hydrazinoquinoline; IACUC, institutional animals care and use committee; LC-MS, liquid chromatography-mass spectrometry; QTOFMS, quadrupole time of flight mass spectrometry; SCFA, short-chain fatty acid; SEM, standard error mean; TPP, triphenylphosphine. UPLC, ultra-performance lipid chromatography;

3.2 INTRODUCTION

Flavonoids, as a large group of ubiquitous polyphenolic compounds in plants [204], are well known for their health-promoting and disease-preventing effects in humans and production animals, mainly through their anti-inflammatory and anti-oxidative properties [205]. Quercetin is one of the most bioactive flavonoids. It is widely distributed in the fruits and vegetables of human diet as the aglycone of rutin (quercetin-3-O-rutinoside), but lacking in common plant-derived feed ingredients of monogastrics and ruminants, such as corn, soybean, and alfalfa [108]. Therefore, the use of quercetin in animal feed, commonly through rutin supplement, has been extensively explored for alleviating the morbidities under pathophysiological challenges. In dairy cows, positive effects of quercetin and rutin on growth, health, reproduction, metabolism, and milk production have been observed [109,206-208]. In young calves, feeding quercetin decreased splanchnic glucose oxidation, increased glucose absorption, and increased antioxidative capacity [207,209]. In lactating cows, intraduodenal supplementation of quercetin enhanced insulin release and sensitivity [210], and mitigated the hepatic disorders from lipid accumulation and metabolic stress [109]. Furthermore, the modulation of rumen microbiota was observed after rutin supplementation in dairy cows, as shown by the decrease of methane production [208] and the increases of short-chain fatty acids (SCFAs) and crude protein from fermentation [206]. All these beneficial effects on health and metabolism can be further translated into the enhancement of energy utilization and production in dairy cows.

Many proposed mechanisms on the health- and growth-promoting effects of quercetin and rutin, such as anti-inflammatory and antioxidant activities, are largely based on the results of *in vitro* studies [211-215], in which the concentrations of quercetin chosen for unraveling its intracellular mechanisms might not be physiologically relevant. Therefore, whether these mechanisms are applicable to the *in vivo* biological processes depends on the disposition of quercetin and rutin *in vivo*, mainly through their bioavailability and biotransformation. In monogastric animals, quercetin

is mostly absorbed in the small intestine with 17% bioavailability in pigs [216] and 59% in dogs [217], whereas rutin is more absorbable in the large intestine after its glycoside bonds are cleaved by bacterial α-rhamnosidase and β-glucosidase to release quercetin [218,219]. In ruminants, ruminal bacteria-mediated degradation occurs prior to the absorption. The bioavailability of intraruminal quercetin and rutin in nonlactating cows was only 0.1 and 0.5%, respectively [220]. The *in vitro* incubation of quercetin with the ruminal fluid of nonlactating cows showed that almost 90% of quercetin was degraded during the first 5 hours of incubation, producing 3,4-dihydroxyphenylacetic acid (DHPAA) and 4-methylcatechol as the major metabolites from fermentation [221]. However, the formation of these microbial metabolites *in vivo* and their metabolic fates in dairy cows have not been examined.

In this study with dairy cows, both targeted metabolite and untargeted metabolomic analyses were conducted to determine rutin and quercetin metabolites in plasma, urine, and rumen fluids after intraruminal dosing of rutin, as well as the associated metabolic changes in these biological fluids. The distribution of these metabolites was defined by the quantitative analysis.

3.3 MATERIALS AND METHODS

3.3.1 Chemicals and reagents

The chemicals and reagents used in sample preparation, LC-MS analysis, structural confirmation, and quantification are enlisted in the supplementary material (**Table 3.1**).

3.3.2 Animals, experimental design, and sample collection

Animal care and experimental procedures were approved by the University of Minnesota Institutional Animal Care and Use Committee. Four multiparous rumen-cannulated Holstein cows

in mid-to-late lactation were fed a standard total mixed ration (TMR) formulated to meet the nutritional needs of Holsteins in late lactation (**Table 3.2**). Cows had *ad libitum* access to feed and water throughout the day except for the periods of feed change and milking (< 30 min, twice per day). Cows had no clinical signs of disease or metabolic disorders and appeared healthy throughout the study. On the day of experiment, each cow received a 100 mg/kg BW intraruminal dose of rutin. Rutin was suspended in 300 mL of deionized water and dosed into the rumen through the cannula. The container of rutin suspension was rinsed twice with 200 mL deionized water, which was also added to the rumen. Rumen fluid samples were collected at 0, 0.5, 1, 2, 4, and 6 h of the rutin administration, and immediately placed on ice. Blood samples were collected via jugular catheter using heparinized tubes at 0, 0.25, 0.75, 1.0, 1.5, 2, 3, 4, and 6 h after the rutin administration, and immediately placed on ice until centrifuged at 2000 × *g* for 10 min to separate plasma. Urine samples were collected in 19 L plastic pails and then pooled within 3 periods, including -3 to 0, 0 to 3, and 3 to 6 h of rutin administration, to form 3 urine samples per cow. Urine samples were immediately placed on ice after the collection. The aliquots of rumen, plasma, and urine samples were stored at -80 °C prior to analysis.

3.3.3 Metabolite extraction

Rumen fluid samples were prepared by mixing with 50% aqueous acetonitrile (ACN) in 1:10 (v/v) ratio; plasma samples were deproteinized by mixing with 50% aqueous ACN in 1:5 (v/v) ratio; urine samples were prepared by mixing with 50% aqueous ACN in 1:4 (v/v) ratio. The mixtures were centrifuged at 16,000 × *g* for 10 min to precipitate the particles and insolubles. The supernatants were used in sample analysis.

3.3.3.1 Acid hydrolysis of conjugated metabolites

Glucuronide and sulfate metabolites in plasma or urine samples were hydrolyzed following a modified method [222]. Briefly, 120 µL of plasma or urine sample was mixed with 200 µL of 2 mg/ml *tert*-butyl hydroxyquinone (tBHQ) methanol solution and 80 µL of 10 M HCl, and then incubated in a water bath at 90 °C for 2 h. After cooling, the mixture was further mixed with 400 µL of 2 mg/ml tBHQ methanol solution, and then centrifuged at 16000 × *g* for 10 min. To measure hydroxyl group contained metabolites, a similar procedure for hydrolysis using methanol without tBHQ was conducted as described above. After cooling, the mixture was neutralized ammonia hydroxide, and then centrifuged at 16000 × *g* for 10 min. The supernatant was used in the subsequent sample preparation and analysis.

3.3.3.2 Chemical derivatization

For detecting the metabolites containing amino group (amino acids) and the ones containing hydroxyl group (*p*-cresol), samples were derivatized with dansyl chloride (DC) prior to the LC-MS analysis [223]. Briefly, 5 µL of sample or standard was mixed with 50 µL of 10 mM sodium carbonate solution, 5 µL of 50 µM deuterated L-tryptophan-(indole-d_5) as an internal standard, and 100 µL of 3 mg/ml DC solution dissolved in acetone. The mixture underwent the incubation at 60 °C for 15 min, cooling on ice, and then centrifugation at 16000 × *g* for 10 min, and the supernatant was used for LC-MS analysis. For detecting the metabolites containing carboxyl group, the samples were derivatized with 2-2'-dipyridyl disulfide (DPDS), triphenylphosphine (TPP), and 2-hydrazinoquinoline (HQ) prior to the LC-MS analysis [224]. Briefly, 2 µL of sample or standard was added into 100 µL of freshly prepared ACN solution containing 1 mM DPDS, 1 mM TPP, 1 mM HQ, and 100 µM deuterated d_4-acetic acid as internal standard. The reaction mixture was incubated at 60 °C for 30 min, chilled on ice, and mixed with 100 µL of H_2O. This mixture was centrifuged at 16000 × *g* for 10 min and the supernatant was used for LC-MS analysis.

3.3.4 LC-MS analysis

A 5 μL of aliquot prepared from rumen fluid, plasma, or urine was injected into an Acquity ultra performance liquid chromatography-quadrupole time-of-flight mass spectrometry (UPLC-QTOFMS) system (Waters, Milford, MA), and then separated in a UPLC column in a 10-min run at a flow rate of 0.5 mL/min. Detailed information on LC-MS acquisition conditions is provided (Table 3.3**)**. The LC eluant was injected into a Xevo-G2-S QTOF mass spectrometry for accurate mass measurement and ion counting. Capillary voltage and cone voltage for electrospray ionization was maintained at 3kV and 30 kV for positive-mode detection, or at -3 kV and -35 V for negative-mode detection, respectively. Source temperature and desolvation temperature were set at 120°C and 350°C, respectively. Nitrogen was used as both cone gas (50 L/h) and desolvation gas (600 L/h), and argon as collision gas. For accurate mass measurement, the mass spectrometer was calibrated with sodium formate solution (range *m/z* 50–1,000) and monitored by the intermittent injection of the lock mass leucine enkephalin ($[M+H]^+$ = *m/z* 556.2771 or $[M-H]^-$ = *m/z* 554.2615) in real time. Additional structural information was obtained by tandem MS (MS/MS) fragmentation with collision energies ranging from 15 to 45 eV. Mass chromatograms and mass spectral data were acquired and processed by MassLynx^{TM} software (Waters) in centroided format.

3.3.4.1 Targeted quantitative analysis

The concentrations of rutin, quercetin, methylated quercetin, kaempferol, DHPAA, 4-methylcatechol, *p*-cresol, short-chain fatty acids, and amino acids were determined by calculating the ratio between their individual peak areas and the peak area of internal standard and fitting with a standard curve using QuanLynx^{TM} software (Waters).

3.3.4.2 Untargeted multivariate data analysis and marker characterization

After data acquisition in the UPLC-QTOFMS system, chromatographic and spectral data of samples were deconvoluted by MarkerLynx^{TM} software. A multivariate data matrix containing

information on sample identity, ion identity from retention time (RT) and *m/z*, and ion abundance, was generated through centroiding, deisotoping, filtering, peak recognition, and integration. The intensity of each ion was calculated by normalizing the single ion counts (SIC) versus the total ion counts (TIC) in the whole chromatogram. The processed data matrix was exported into SIMCA-P+^{TM} software (Umetrics, Kinnelon, NJ), transformed by *Pareto* scaling, and then analyzed by partial least squares discriminant analysis (PLS-DA) on multiple time points of samples after rutin administration. Major latent variables of the multivariate model were defined in a scores scatter plot. The potential metabolite markers were identified by analyzing ions contributing to the principal components and to the separation of sample groups in the loadings scatter plot. The chemical identities of compounds of interest were determined by accurate mass measurement, elemental composition analysis, database search using Human Metabolome Database (https://www.hmdb.ca/), and Metlin (https://metlin.scripps.edu/), MSMS fragmentation, and comparisons with authentic standards if available.

3.3.5 Kinetic analysis

The kinetic parameters of rumen and plasma samples were determined by the extravascular input non-compartmental analysis (Module 101) of SOLVER in Microsoft Excel 2016 version 16.0.5173.1000 (Redmond, WA) [225].

3.3.6 Statistical analysis

Experimental values were reported as mean ± standard error of the mean (SEM). The statistical significance among samples at different time points was analyzed by one-way ANOVA followed by Tukey's post hoc test, Pearson correlation, or linear regression using GraphPad Prism version 8.0.2 (GraphPad, Inc. La Jolla, CA). A value of $P < 0.05$ was considered significant.

3.4 RESULTS

3.4.1 Identification of plasma metabolites affected by intraruminal rutin

Targeted analysis was conducted to determine the presence as well as the concentrations of rutin, quercetin, and their known flavonol metabolites, including kaempferol (a dehydroxylated metabolite of quercetin), isorhamnetin, and tamarixetin (two methylated metabolites of quercetin), in both unhydrolyzed and hydrolyzed plasma samples. Rutin (I), isorhamnetin, and tamarixetin were not detected in the samples (data not shown). Quercetin (II) and kaempferol (III) were detected in hydrolyzed samples but not in unhydrolyzed samples (**Table 3.4**), indicating extensive conjugation. Moreover, the concentration of kaempferol was more than one order lower than that of quercetin, indicating its status as a minor metabolite (**Figure 3.1A-B**). The pharmacokinetics analysis on the time course of quercetin revealed its low plasma concentration (C_{max} = 1.70 μmol/L), short half-life ($t_{1/2}$ = 12 min), high clearance (Cl = 0.97 L/min/kg), and large volume of distribution (V_d = 129.63 L/kg) (**Table 3.5**).

To determine whether other quercetin metabolites were also present, an untargeted metabolomics analysis was conducted on the plasma LC-MS data. In the scores plot of a PLS-DA model, the time-dependent separation of plasma samples is observed along with the principal component 1 of the model (**Figure 3.2A** and **Figure 3.3**). Two ions (IV-V) contributing to the sample separation through their high values in the principal component 1 were identified in the loadings plot of the model (**Figure 3.2B**), and then determined as 4-methylcatechol sulfate (IV) and *p*-cresol sulfate (V) by elemental composition analysis and MS/MS fragmentation (**Figure 3.2C-D**, **Table 3.4**). After removing the sulfate group from these two metabolites by acid hydrolysis, the concentrations of 4-methylcatechol (VI) and *p*-cresol (VII) in plasma samples were quantified. The results showed that, after the intraruminal dosing of rutin, the concentration of 4-methylcatechol increased gradually and peaked at 240 min, whereas the concentration of *p*-cresol decreased through 240 min

(**Figure 3.2E-F**). The Pearson correlation analysis showed a significant inverse correlation between these two metabolites (**Figure 3.2G**), implying that the formation of 4-methylcatechol sulfate (IV) might negatively affect the production of *p*-cresol sulfate (V).

3.4.2 Identification of urinary metabolites affected by intraruminal rutin

The metabolomic analysis of pre-dosing (-3 to 0 h) and post-dosing urine samples (0 to 3 h and 3 to 6 h) showed the time-dependent separation in the scorings plot of a PLS-DA model, mainly along with the principal component 1 (**Figure 3.4A**). Three most prominent metabolites (IV-V, VIII) contributing to this separation were identified in the loadings plot of the model through their high values in the principal component 1 (**Figure 3.4B**) and then determined as 4-methylcatechol sulfate (IV), *p*-cresol sulfate (V), and hippuric acid (VIII) (**Table 3.4**). Consistent with the results of plasma analysis, the analysis of hydrolyzed urine samples showed that the concentration of 4-methylcatechol (VI) increased dramatically while the concentration of *p*-cresol (VII) decreased after the intraruminal rutin dosing (**Figure 3.4C-D**). In addition, hippuric acid (VIII) in urine was also decreased by the rutin treatment (**Figure 3.4E**).

3.4.3 Investigation of ruminal degradation of rutin and quercetin

The sources and causes of observed metabolic changes in plasma and urine were further examined by the metabolomic analysis of the rumen fluid samples collected at multiple time points after the rutin administration. A distinctive time-dependent separation was observed in the scores plot of a PLS-DA model, in which the trajectory of sample groups showed the reversible metabolic changes in rumen fluid after the rutin administration (**Figure 3.5A**). The metabolites contributing to these time-dependent changes were further identified in the loadings plot (**Figure 3.5B**), and determined as rutin (I), quercetin (II), DHPAA (IX and IX' from its in-source fragment), and 4-hydroxyphenylacetic acid (X) (**Figure 3.6**). Quantitative analyses of these metabolites in rumen fluid showed that the concentration of rutin (I) decreased rapidly after 30 min and disappeared at 2

h (**Figure 3.5C**), while the concentration of quercetin (II) peaked at 1 h and disappeared at 4 h (**Figure 3.5D**). Compared to rutin and quercetin, the time course of DHPAA (IX) was further delayed since its concentration peaked at 2 h around 200 μM and returned to its basal level at 6 h (**Figure 3.5E**). The targeted analysis of 4-methycatechol (VI) showed a profile similar to DHPAA but in much lower concentrations (**Figure 3.5F**). The half-life ($t_{1/2}$) of rutin (I), quercetin (II), DHPAA (IX), and 4-methycatechol (VI) were determined as 10.89 min, 14.62 min, 60.65 min, and 48.22 min, respectively (**Table 3.6**). All these profiles indicate rapid degradation of rutin and quercetin followed by the gradual formation of DHPAA and 4-methylcatechol in the rumen.

3.4.4 Influence of rutin on ruminal tyrosine metabolism

In addition to rutin and quercetin metabolites, 4-hydroxyphenylacetic acid (X), the intermediate metabolite in the microbial conversion of tyrosine to *p*-cresol, was identified as a prominent ruminal metabolite affected by the rutin treatment (**Figure 3.5B**). The quantitative analysis showed that the concentration of 4-hydroxyphenylacetic acid continuously increased in the first 4 h of rutin administration and then plateaued afterward (**Figure 3.7A**). In contrast, the concentration of *p*-cresol (VII) gradually decreased in the first 4 h of rutin treatment (**Figure 3.7B**). Moreover, the concentration of tyrosine (XI) was not altered by ruminal rutin (**Figure 3.7C**). All these observations indicated that the decrease in *p*-cresol might be caused by the inhibition of the conversion from 4-hydroxyphenylacetic acid to *p*-cresol, instead of the deficiency in tyrosine.

3.4.5 Ruminal short-chain fatty acids (SCFAs)

The influences of rutin treatment on rumen fermentation were further examined by measuring the concentrations of SCFAs in the rumen fluid. The results showed that intraruminal rutin had limited effects on acetic acid (**Figure 3.8A**), while it consistently increased the concentrations of propionic acid and butyric acid (**Figure 3.8B-3.8C**).

3.5 DISCUSSION

The identification of 4-methylcatechol, a microbial metabolite, as the dominant bioavailable metabolite of intraruminal rutin, and the inhibitory effect of the rutin→quercetin→DHPAA→4-methylcatechol degradation route on the microbial production of *p*-cresol, are the two most notable observations from the intrarumial rutin treatment in the current study. The metabolic events associated with these observations occurred either in sequence or in parallel through both microbial and endogenous metabolism at different physiological sites (**Figure 3.8**). The causes and significances of these metabolic events are discussed in the following sections.

3.5.1 4-methylcatechol as the most bioavailable metabolite of rutin and its significance

Both 4-methylcatechol (3,4-dihydroxytoluene) and its immediate precursor, DHPAA, are known microbial metabolites of rutin [226]. However, our data are the first to demonstrate 4-methylcatechol as the most bioavailable metabolite from microbial metabolism of rutin in dairy cows.

Bioavailability of rutin, quercetin, and their derivatives. Previous bioavailability studies on rutin and quercetin, which were mainly conducted in human and monogastric animals, focused on the post-absorption presence of quercetin and its flavonol metabolites produced via methylation (isorhamnetin and tamarixetin) or dehydroxylation (kaempferol). In dairy cows, the peak plasma concentration of total flavonols, which included quercetin, isorhamnetin, tamarixetin, and kaempferol, was around 1 μM from intraruminal administration of 100 mg rutin/kg BW [220]. With the same dose of rutin, the peak plasma concentration of quercetin (1.7 μM) in our study was in the comparable range. In contrast, concentrations of 4-methylcatechol (50 μM) in plasma and urine (3000 μM) were much greater than any other metabolite of rutin. This observation clearly indicates that 4-methylcatechol is the most abundant bioavailable metabolite of intraruminal rutin in dairy cows. In addition, this phenomenon might not occur solely in ruminants because the plasma and

urinary concentrations of 4-methylcatechol sulfate and catechol sulfate, another microbial metabolite of flavonols, in human subjects were also 1-3 orders greater than the concentrations of their flavonol precursors [227]. Therefore, more studies are needed to determine the status of 4-methylcatechol and other microbe-derived phenolics as the bioavailable metabolites of flavonoids in ruminants and non-ruminants.

Significance of 4-methylcatechol as the dominant bioavailable rutin metabolite. A direct implication of this observation is to provide additional explanations for the documented bioactivities of rutin and quercetin, such as antioxidant and other health- and performance-promoting activities, in dairy cows [109,206-208]. A previous comparison on the antioxidant activities of quercetin and its metabolites indicated that 4-methylcatechol performed as a robust radical scavenger in the 2,2-diphenyl-1-picrylhydrazyl (DPPH) assay and was equally effective as quercetin for suppressing malondialdehyde production in a cell-based lipid peroxidation assay [228]. Therefore, 4-methylcatechol might alleviate the oxidative stress occurred in the metabolic disorders of periparturient cows, such as hepatosteatosis and ketoacidosis [153,229]. In addition to its antioxidant activity, 4-methylcatechol has been shown to possess strong antiplatelet and hypotensive activities [230,231] and thus could function prophylactically against circulatory morbidities in dairy cows, such as pulmonary artery hypertension-elicited right-heart failure in neonatal calves [232]. It will be interesting to examine whether rutin supplementation might decrease the mortality associated with pulmonary artery hypertension in calves and improve the performance of adult cows.

In the current study, 4-methylcatechol was primarily detected as its sulfate conjugate in plasma and urine. This observation is expected since sulfation is the most common conjugation reaction for absorbed catechols and phenols (**Figure 7**). If the non-conjugated form is required for the aforementioned bioactivities, then hydrolysis of 4-methylcatechol sulfate to release 4-methylcatechol is required prior to or at the site of action. One possible route of deconjugation is

through the activity of lysosome sulfatase [233]. Further examination on the status of 4-methylcatechol in bovine tissue may provide more insight on this issue.

3.5.2 Rutin degradation pathway and its interactions with tyrosine degradation in the rumen

The stepwise degradation of rutin→quercetin→DHPAA→4-methylcatechol in ruminal fermentation has been shown *in vitro* [221]. The results of our *in vivo* study provide solid evidence on this pathway through the kinetic profiles of these 4 compounds (**Figure 4** and **Table 3**). More importantly, this degradation pathway inhibited the degradation of tyrosine to *p*-cresol in rumen (**Figure 5**). These metabolic reactions and interactions derived from ruminal microbes and their enzymes can have significant impacts on the performance of dairy cows.

Reactions and bacteria responsible for rutin degradation. Rapid degradation of rutin to quercetin in the rumen is expected since many ruminal bacteria, such as *Selenomonas*, *Butyrivibrio*, and *Peptostreptococcus* species, contain glycosidases, a family of enzymes capable of hydrolyzing two glycosidic bonds in rutin [234]. The sugars released by this hydrolysis, including rhamnose, glucose, and rutinose, are available for ruminal fermentation to produce SCFAs, such as *Butyrivibrio*-mediated butyric acid production [235], which might partially contribute to the selective increase of ruminal SCFAs in this study. Quercetin can undergo the hydrolytic cleavage of its heterocyclic C ring, a reaction conducted by *Butyrivibrio* and *Clostridium* species [236,237], to form phloroglycinol, an A ring-derived metabolite, and DHPAA, a B ring-derived metabolite (**Figure 7**). Phloroglucinol can go through a series of reduction and oxidation reactions to produce butyric acid and acetic acid, which has been observed in *Eubacterium oxidoreducens* [238], while DHPAA undergoes a decarboxylation reaction to form of 4-methylcatechol, a terminal product from the microbial degradation of rutin [239].

Influence of rutin degradation on p-cresol production and its potential mechanism. As an end product of microbial tyrosine degradation, *p*-cresol can be formed directly by cleaving the Cα–Cβ bond of tyrosine, a reaction catalyzed by tyrosine lyase, or by the decarboxylation of 4-hydroxyphenylacetic acid, which is formed by the transamination of tyrosine and oxidation of 4-hydroxyphenylpyruvic acid [240]. After absorption, *p*-cresol is conjugated to its sulfate or glucuronide forms by colonocytes or hepatic cells [241]. The inverse correlation between 4-methylcatechol and *p*-cresol observed in this study (**Figure 2G**) indicates the potential competition between rutin degradation and *p*-cresol production, especially in the decarboxylation step. This conclusion is supported by the fact that the conversion of DHPAA to 4-methylcatechol and the conversion of 4-hydroxyphenylacetic acid to *p*-cresol occur through the same decarboxylation reaction and therefore likely share the same decarboxylases. More importantly, the decrease of *p*-cresol in rumen fluid was coincident with the increase of 4-hydroxyphenylacetic acid (**Figure 5A**), which can be considered as a direct consequence of inhibiting the 4-hydroxyphenylacetic acid→*p*-cresol biotransformation. In fact, 4-hydroxyphenylacetic acid decarboxylase, a glycyl radical enzyme, has been purified and cloned from *Clostridium difficile*, a pathogenic bacteria, and other *Clostridium* species [242]. The substrate affinity analysis showed that DHPAA had higher affinity (K_m = 0.5 mM) than 4-hydroxyphenylacetic acid (K_m = 2.8 mM) for this decarboxylase, and DHPAA inhibited the decarboxylation of 4-hydroxyphenylacetic acid with K_i = 0.4 mM [242]. This decarboxylase activity is likely present in many bacterial species since *p*-cresol is produced as a degradation product of tyrosine by diverse anaerobic bacteria, such as *Clostridium*, *Faecalibacterium*, *Eubacterium*, *Anaerostipes*, *Ruminococcus*, *Bacteroides*, *Bifidobacterium* and *Coriobacteriaceae* [240,243]. In rumen of dairy cows, multiple strains of a *Lactobacillus sp*. have been shown to catalyze the formation of *p*-cresol and 4-methylcatechol [244-246].

As with *p*-cresol, urinary hippuric acid was also decreased by rutin administration (**Figure 3E**). This observation is similar to the results of our recent study, in which urinary hippuric acid, together

with indoxyl sulfate and phenylacetylglutamine, were decreased by the supplement of green tea polyphenols in human subjects [247]. Benzoic acid, the precursor of hippuric acid, originates from the microbial metabolism of tyrosine, phenylalanine, phenolics and quinic acid in plants. Therefore, a similar competitive inhibition mechanism could be responsible for the inhibitory effect of rutin on the biosynthesis of hippuric acid.

Significance of inhibiting p-cresol production. Unlike other beneficial metabolites produced by bacterial fermentation, *p*-cresol is known for its negative bioactivities, mainly its inhibitory effects on epithelial cell proliferation, mitochondrial bioenergetic activity, and T helper 1 cell-regulated immune response [248,249]. It has also been considered as a uremic toxin due to the correlation between serum *p*-cresol sulfate and endothelial damage in kidney disease [250]. In addition, *p*-cresol is widely considered as a prominent volatile organic compound responsible for the odor of concentrated cattle and dairy operations [251]. Therefore, decreased *p*-cresol in rumen fluid and decreased *p*-cresol sulfate in plasma and urine should be considered as beneficial effects of rutin consumption.

3.6 CONCLUSIONS

Overall, our current study examined the *in vivo* ruminal rutin degradation process and identified 4-methylcatechol, an end product of microbial metabolism, as the dominant bioavailable metabolite of rutin and quercetin in dairy cows. The formation of 4-methylcatechol inhibited the microbial degradation of tyrosine to *p*-cresol, potentially through competitive inhibition of decarboxylation reactions. These new observations warrant further investigations on the mechanisms and potential benefits of rutin supplementation in feed for cattle.

Table 3.1. Source of chemical and reagents used in chemical analysis, LC-MS analysis, structural confirmation, and quantification.

Chemicals and reagents	Vendor
Acetonitrile (LC-MS grade), Formic acid (LC-MS grade), Hydrochloric acid, Water (LC-MS grade)	Fisher Scientific (Houston, TX)
Amino acid mixture (acidic), Amino acid mixture (basic), *tert*-Butyl Hydroxyquinose (tBHQ), Dansyl chloride (DC), Hippuric acid	Sigma-Aldrich (St. Louis, MO)
3,4-Dihydroxyphenylacetic acid (DHPAA), 2-Hydrazinoquinoline (HQ), Rutin, Triphenylphosphine (TPP)	Alfa Aesar (Tewksbury, MA)
2-2´-Dipyridyl disulfide (DPDS)	MP Biomedicals, LLC (Irvine, CA)
Fatty acids standards (C4-C22)	Nu-Chek Prep, Inc. (Elysian, MN)
Methanol (LC-MS grade)	Avantor performance materials (Radnor, PA)
4-Methylcatechol, Quercetin	Acros Organics (Fair Lawn, NJ)
3-O-methyl Quercetin/Isorhamnetin	Frontier Specialty Chemicals (Logan, UT)
4-O-methyl Quercetin/Tamarixetin	Cayman Chemical Company (Ann Arbor, MI)
Kaempferol	APExBIO (Houston, TX)

Table 3.2. Ingredient and nutrient content of the total mixed ration (TMR).

Component	Contribution
Ingredient, % of DM	
Corn silage	19.70
Corn, extra fine, rolled	10.60
Corn gluten	4.90
Alfalfa hay, chopped	5.00
Protein mix[1]	8.45
QLF commercial dairy mix[2]	2.75
Cottonseed, Fuzzy	3.20
Megalac[3]	0.40
Nutrient content, DM basis	
DM, %	55.8
Crude protein, %	16.4
Acid detergent fiber, %	17.3
Neutral detergent fiber, %	17.5
Total digestible nutrients, %	77.1
Net energy-lactation, Mcal/kg	1.72
Calcium, %	0.95
Phosphorus, %	0.41
Magnesium, %	0.37
Potassium, %	1.44
Sodium, %	0.50
Iron, ppm	276
Zinc, ppm	86.2
Copper, ppm	17.4
Manganese, ppm	66.5
Molybdenum, %	1.8
Sulfur, %	0.31
Chloride ion, %	0.58
Dietary cation anion difference[4], mEq/kg	227

[1] Extra fine rolled corn, 29.72%; soybean meal 47% protein, 17.50%; canola meal, 12.50%; amino plus (AG Processing, Inc., Omaha, NB), 8.75%; blood meal, 6.25%; calcium carbonate, 5.50%; sodium bicarbonate, 5.00%, distillers grain, 5.00%; WR Elite Dairy Micro (Vita Plus Corporation, Madison, WI), 2.50%; potassium carbonate, 2.00%; UltraMet (Vita Plus Corporation, Madison, WI), 2.00%; sodium chloride, 2.00%; urea 46% N, 1.25%; Rumensin 90 (Elanco Animal Health, Greenfield, IN), 0.03%.

[2] Molasses-based liquid supplement of soluble sugars. Quality Liquid Feeds, Dodgeville, WI.

[3] Arm & Hammer Animal Nutrition, Ewing, NJ.

[4] DCAD = (Na+K) - (Cl+S) according to Goff (2018).

Table 3.3. LC-MS data acquisition condition in a 10-minute run.

Target compounds	Column type	Mobile phase	MS detection mode
Amino acids (dansylated)	BEH C18	A: 0.1% formic acid in H_2O B: 0.1% formic acid in ACN	Positive
Fatty acids (HQ derivatization)	BEH C18	A: 2 mM NH_4OAc in water with 0.05% CH_3COOH B: 2 mM NH_4OAc in 95% ACN and 5% H_2O with 0.05% CH_3COOH	Positive
Hydrophilic metabolites	BEH Amide	A: 0.1% formic acid in H_2O B: 0.1% formic acid in ACN	Positive and negative
Rutin and quercetin metabolites	BEH C18	A: 0.1% formic acid in H_2O B: Methanol	Negative

Table 3.4. Identification of plasma, rumen, and urine metabolites in LC-MS analysis. The metabolites were detected in negative mode ($[M-H]^-$) or positive mode after the DC derivatization ($[M+DC]^+$).

Ion	Sample	Mode of ion detection	*m/z* of detected ion	Identity	Formula	Δppm	Database ID
I	Plasma Rumen	$[M-H]^-$	609.1454	Rutin	$C_{27}H_{30}O_{16}$	-0.3	HMDB0003249
II	Plasma Rumen	$[M-H]^-$	301.0351	Quercetin	$C_{15}H_{10}O_7$	1	HMDB0005794
III	Plasma	$[M-H]^-$	285.0361	Kaempferol	$C_{15}H_{10}O_6$	-2	HMDB0005801
IV	Plasma Urine	$[M-H]^-$	203.0012	4-Methylcatechol sulfate	$C_7H_8O_5S$	-0.9	HMDB0240459
V	Plasma Urine	$[M-H]^-$	187.0064	*p*-Cresol sulfate	$C_7H_8O_4S$	-0.5	HMDB0011635
VI	Plasma Urine Rumen	$[M-H]^-$	123.0448	4-Methylcatechol	$C_7H_8O_2$	-3	HMDB0000873
VII	Plasma Urine Rumen	$[M+DC]^-$	342.1166	*p*-Cresol	C_7H_8O	0.6	HMDB0001858
VIII	Urine	$[M-H]^-$	178.0506	Hippuric acid	$C_9H_9NO_3$	1	HMDB0000714
IX	Rumen	$[M-H]^-$	167.0343	DHPAA	$C_8H_8O_4$	-0.6	HMDB0001336
IX’	Rumen	$[M-H]^-$	123.0446	DHPAA (fragment)	$C_7H_8O_2$	0	
X	Rumen	$[M+DC]^+$	386.1061	4-Hydroxyphenylacetic acid	$C_8H_8O_3$	-0.3	HMDB0060390
XI	Rumen	$[M+DC]^+$	648.1838	Tyrosine	$C_9H_{11}NO_3$	0.8	HMDB0000158

Table 3.5. Kinetic parameters of quercetin in plasma. The values were calculated based on the concentrations of quercetin in hydrolyzed plasma samples.

Parameter	Quercetin
$AUC_{0\text{-}t}$ *(µmol/L*min)*	143.30
V_d *(L/kg)*	129.63
$t_{1/2}$ *(min)*	12.24
C_{max} *(µmol/L)*	1.70
t_{max} *(min)*	60
Cl (L/min/kg)	0.97

Table 3.6. Kinetic parameters of rutin, quercetin, and their microbial metabolites in rumen fluid.

	Rutin	Quercetin	3,4-Dihydroxyphenylacetic acid	4-Methylcatechol
$t_{1/2}$ *(min)*	10.89	14.62	60.65	48.22
C_{max} *(µmol/ml)*	156.42	71.16	181.21	10.09
t_{max} *(min)*	30	60	120	120

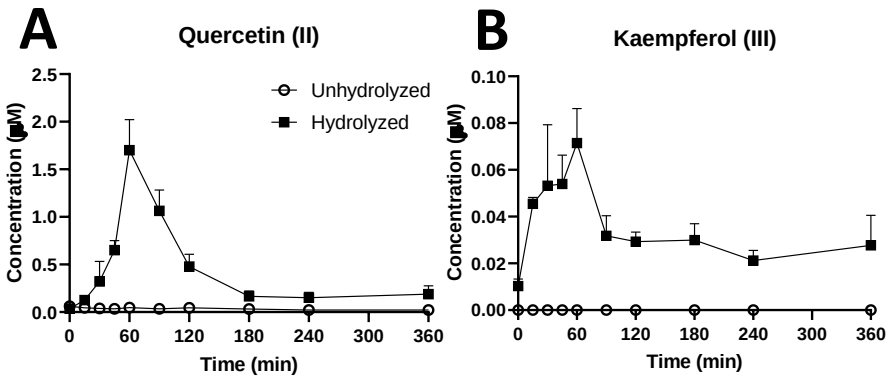

Figure 3.1. Concentrations of detectable flavonol metabolites of rutin in hydrolyzed and unhydrolyzed plasma. Acid hydrolysis was conducted to release flavonols from their respective conjugates in plasma. (**A**) Time course of quercetin (II), and (**B**) time course of kaempferol (III). The Roman Number refers to the ion IDs in Table 1. The concentrations are expressed as means ± SEMs.

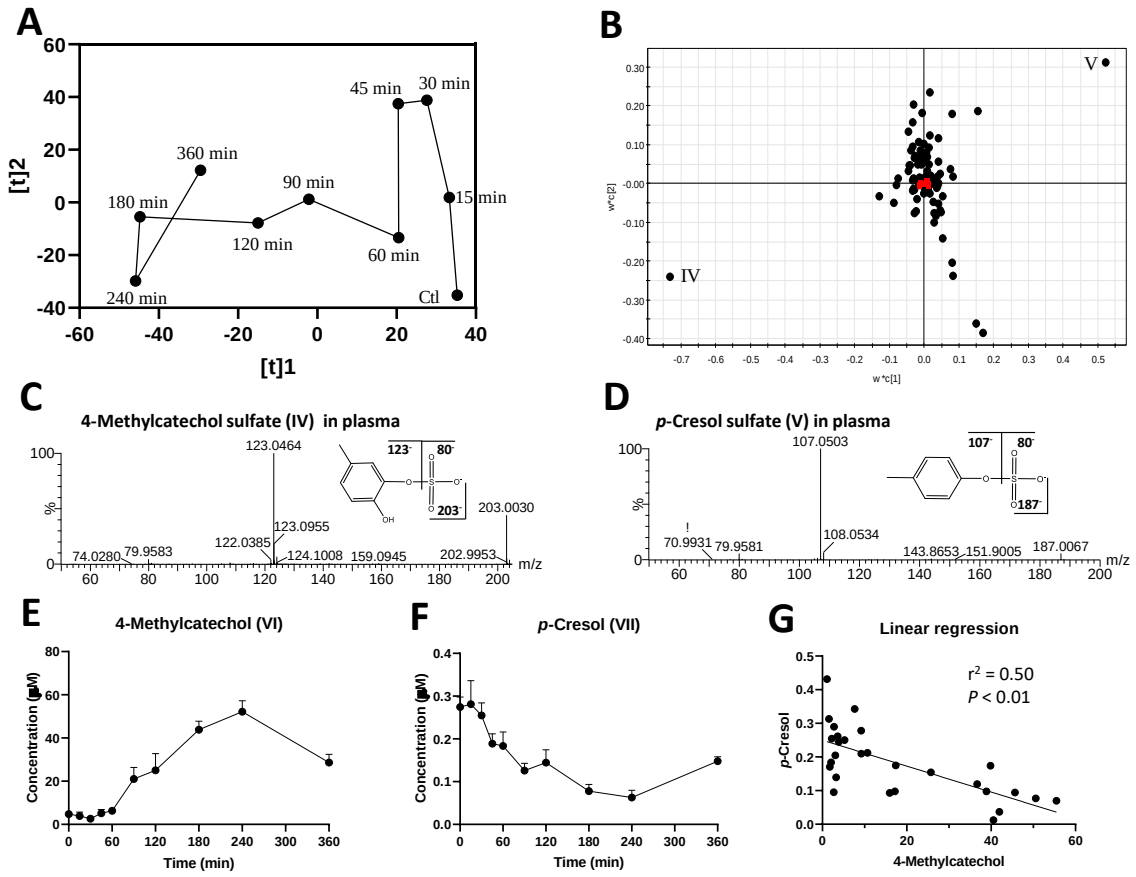

Figure 3.2. Identification and characterization of the most prominent changes in the plasma metabolome after the intraruminal rutin administration. (**A**) A scores plot of the PLS-DA model on plasma metabolome. The trajectory of treatment-elicited changes is comprised of the means of 4 samples at each time point in principal components 1 and 2. The distribution of individual samples is presented in Figure S1. (**B**) Loadings plot of the PLS-DA model. Two most prominent metabolites contributing to the separation of samples were labeled (IV-V), and their identities are listed in Table 1. (**C**) MS/MS fragmentogram of 4-methylcatechol sulfate (IV). (**D**) MS/MS fragmenogram of *p*-cresol sulfate (V). (**E**) Time course of 4-methylcatechol (VI), and (**F**) time course of *p*-cresol (VII) after acid hydrolysis procedure. The concentrations are expressed as means ± SEMs. (**G**) Pearson correlation and linear regression analyses of 4-methylcatechol and *p*-cresol in plasma.

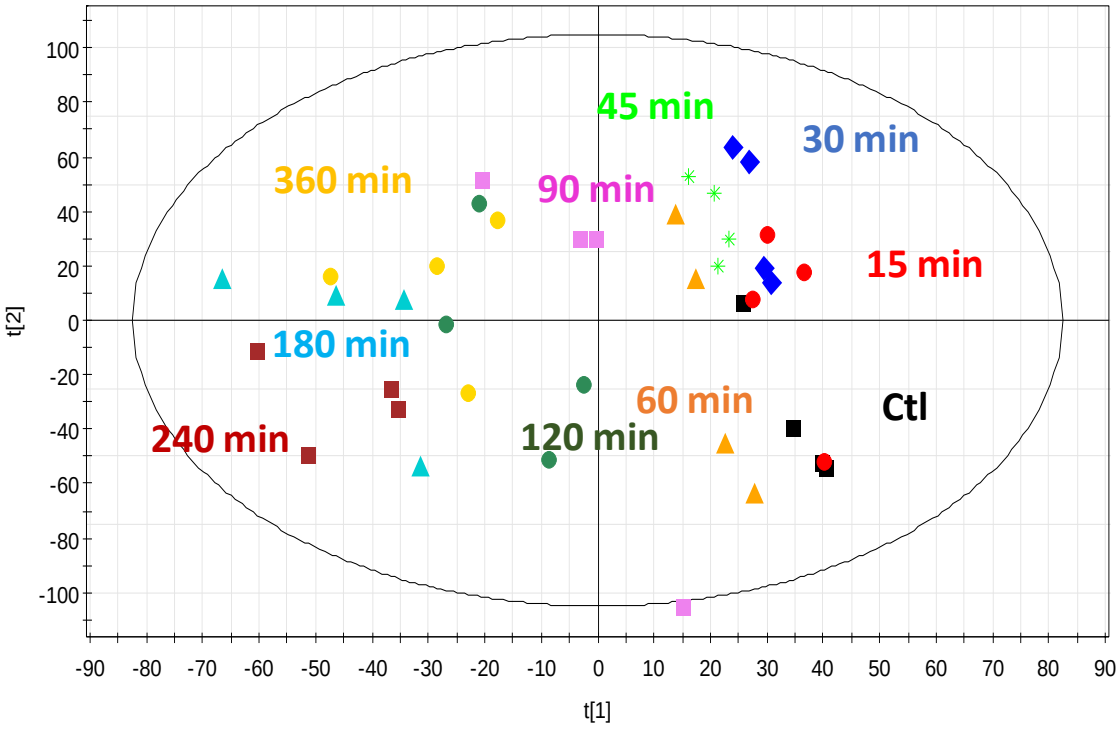

Figure 3.3. Scores plot of the serum samples after intraruminal rutin administration.

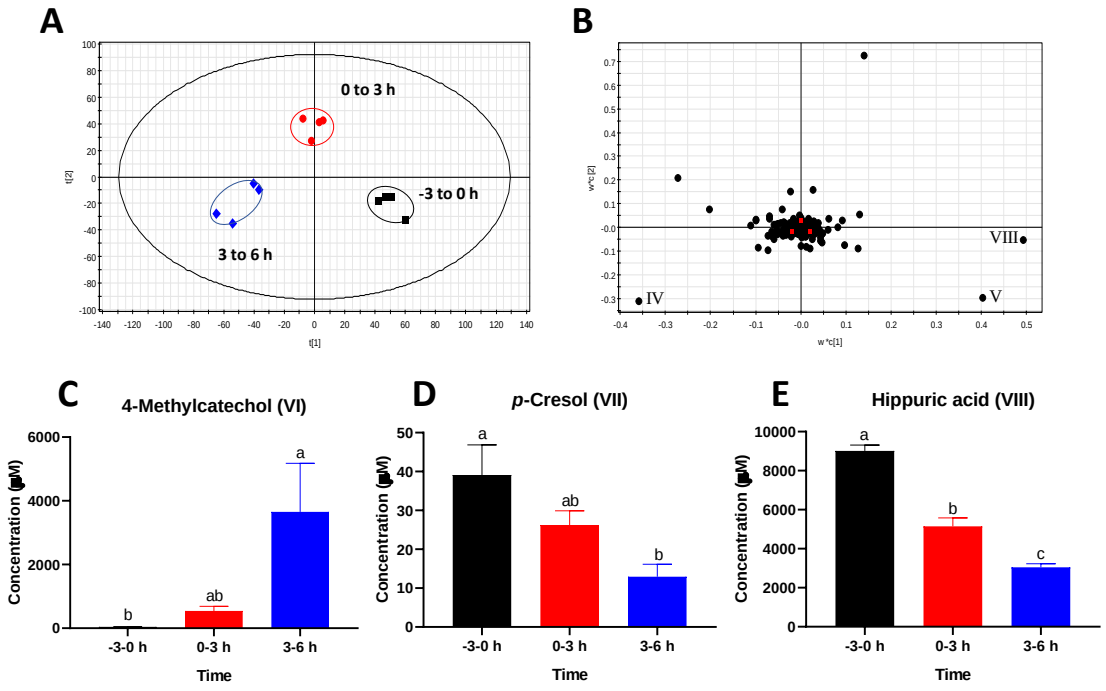

Figure 3.4. Identification and characterization of the most prominent changes in the urine metabolome after the intraruminal rutin administration. The LC-MS data of pre- and post-treatment of urine samples were processed by PLS-DA modeling. (**A**) A scores plot of the PLS-DA model. Three sample groups (n = 4/group) were circled. (**B**) Loadings plot of the PLS-DA model. Three most prominent metabolites contributing to the separation of samples were labeled (IV, V, and VIII), and their identities are listed in Table 1. Concentrations of (**C**) 4-methylcatechol (VI), (**D**) *p*-cresol (VII), and (**E**) hippuric acid (VIII) in urine. The concentrations are expressed as means ± SEMs. Different letters indicate significant difference ($P < 0.05$) among timepoints.

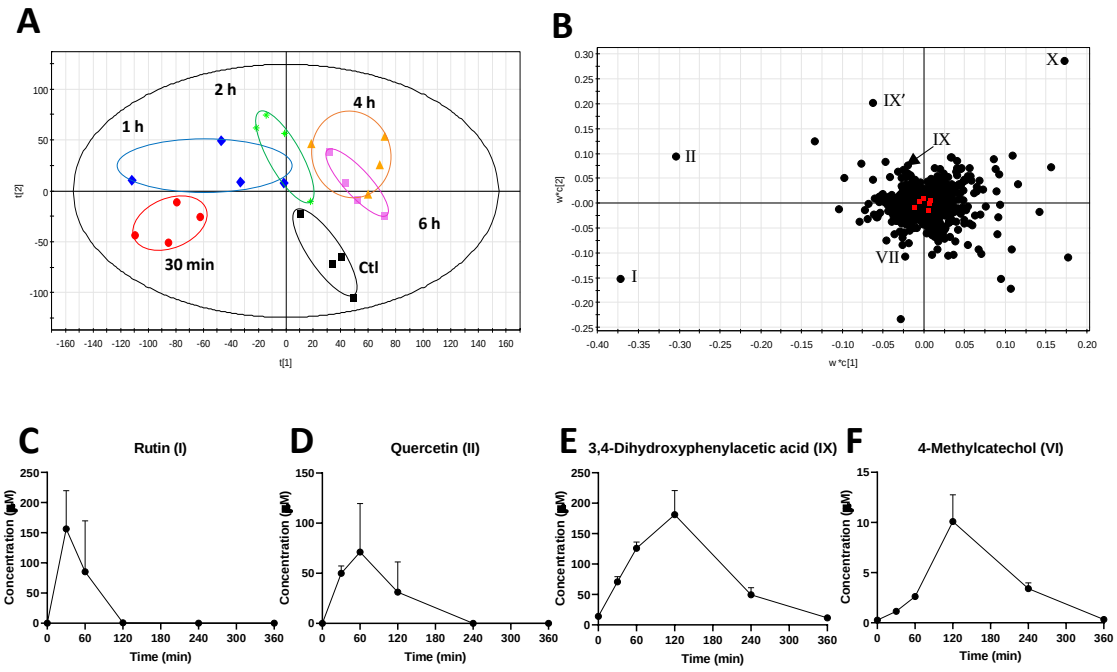

Figure 3.5. Identification and characterization of the most prominent changes in the rumen metabolome after the intraruminal rutin administration. Data from LC-MS analysis of rumen fluid extracts were processed by PLS-DA modeling. (**A**) Scores plot of the PLS-DA model on rumen metabolome. The samples in the same time point (n = 4) were circled. (**B**) Loadings plot of the PLS-DA model. The labeled markers (I, II, VII, IX, IX' and X) are the identified metabolites that contribute to the separation of samples. their identities are listed in Table 1. Time course of (**C**) rutin (I), (**D**) quercetin (II), (**E**) 3,4-dihydrophenylacetic acid (IX), and (**F**) 4-methylcatechol (VI) in rumen fluid. The concentrations are expressed as means ± SEMs.

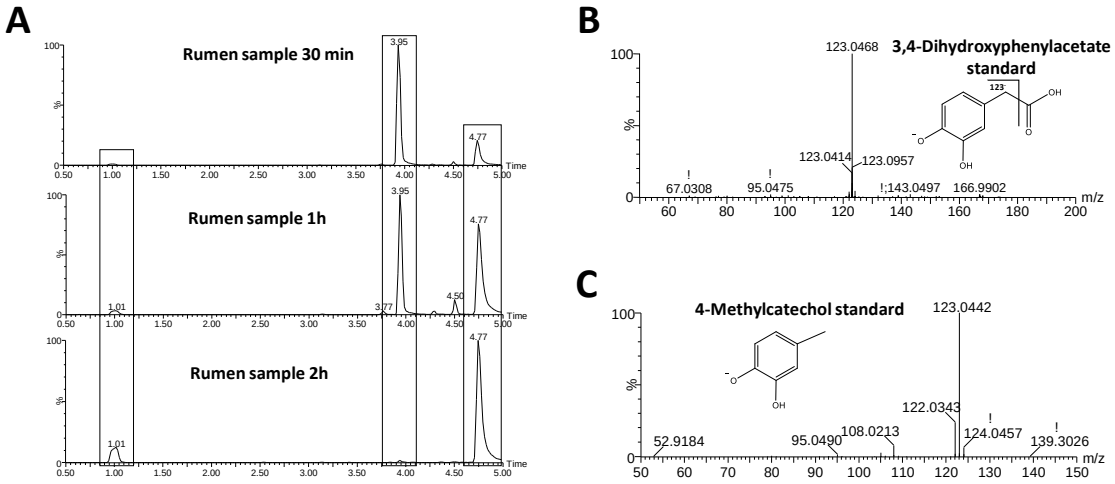

Figure 3.6. Identification of ruminal degradation of rutin in rumen fluid. (**A**) Extracted chromatography of rutin, quercetin, and DHPAA at 30 min, 1 h, and 2 h after intraruminal rutin administration. (**B**) MS/MS fragmentation of DHPAA standard, and (**C**) 4-methylcatechol standard.

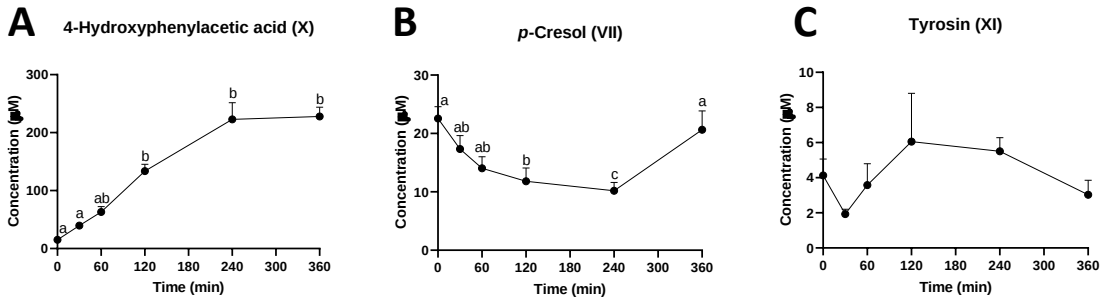

Figure 3.7. Concentrations of *p*-cresol and its precursors in rumen fluid. Time course of (**A**) 4-hydroxyphenylacetic acid (X), (**B**) *p*-cresol (VII), and (**C**) tyrosine (XI). The concentrations are expressed as means ± SEMs. Different letters indicate significant difference ($P < 0.05$) among timepoints.

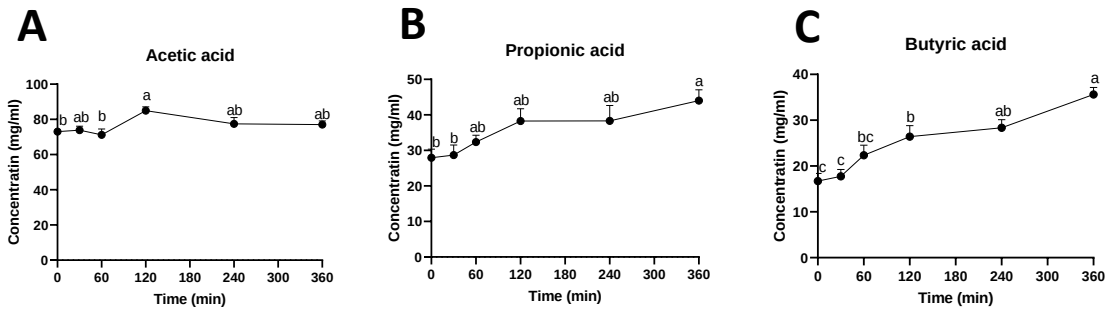

Figure 3.8. Concentrations of SCFAs in rumen fluid. Time course of (**A**) acetic acid, (**B**) propionic acid, and (**C**) butyric acid. The concentrations and ratios are expressed as means ± SEMs. Different letters indicate significant difference ($P < 0.05$) among timepoints.

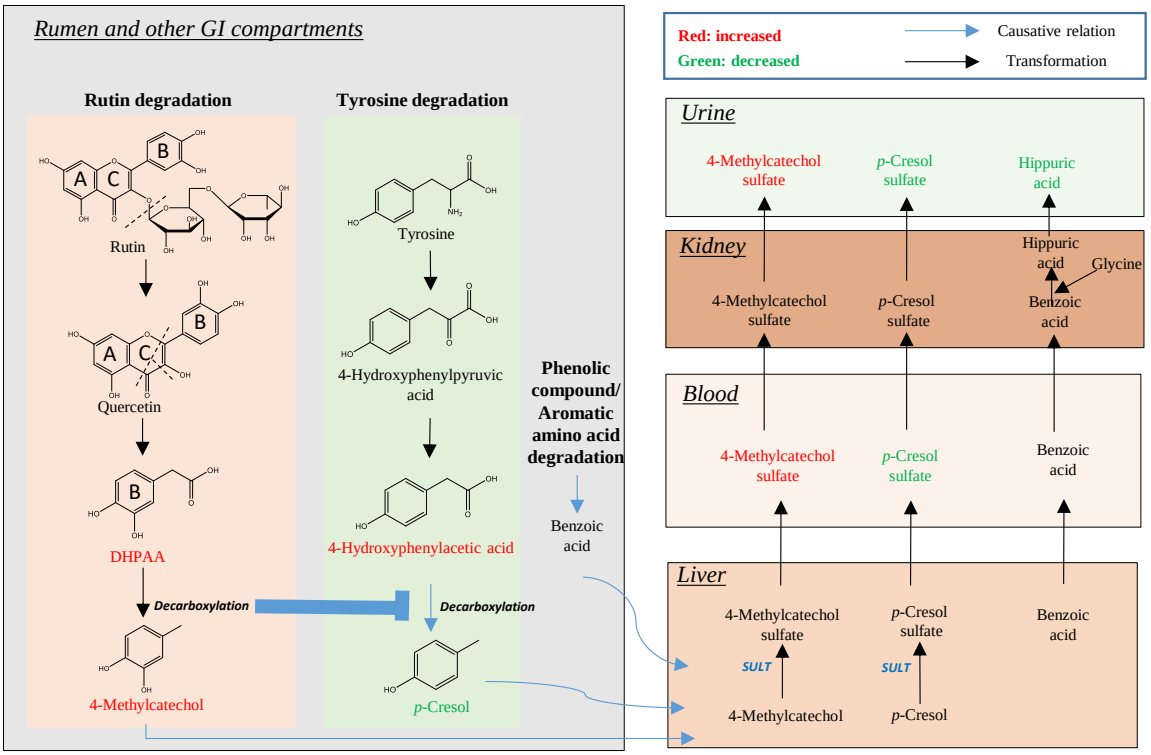

Figure 3.9. Summary of intrarumianl rutin-induced metabolic changes in dairy cow. Microbial metabolism in the rumen produces 4-methylcatechol and *p*-cresol as the bioavailable end products of rutin and tyrosine, respectively. Since these two degradation pathways share the same decarboxylation reaction, the conversion of DHPAA to 4-methylcatechol could inhibit the conversion of 4-hydroxyphenylacetic acid to *p*-cresol. These metabolic events in the rumen further affect the distribution of other rutin and tyrosine metabolites in the plasma and urine of dairy cows.

CHAPTER 4. METABOLOMIC FINGERPRINTING OF CHEMICAL EXPOSURE-INDUCED METABOLIC CHANGES IN PRODUCTION ANIMALS: A CASE STUDY ON OXIDIZED OIL ALTERED AMINO ACID METABOLISM IN NURSERY PIGS

4.1 SUMMARY

Oxidized lipids from rendering and recycling are an economic source of lipids in swine feeds. Negative effects of feeding oxidized lipids on pigs have been observed, but the underlying metabolic events of amino acid metabolism remain to be defined because amino acid plays a fundamental role in animal growth and health. In this study, oxidized corn oil-induced metabolic events on amino acid metabolism in weanling pigs were examined by the liquid chromatography-mass spectrometry (LC-MS)-based metabolomics and biochemical analyses. Feeding oxidized corn oil (OCO) decreased the level of tryptophan in serum, while, it increased nicotinamide adenine dinucleotide (NAD^+) and the gene expression levels in the tryptophan-NAD^+ metabolic pathway in the liver through transcriptional regulation. In contrast, feeding OCO increased the level of serum threonine through direct chemical interaction with the hepatic threonine catabolic enzyme activity. Moreover, OCO altered the redox system by stimulating a robust glutathione (GSH) synthesis and recycling reactions that process consumed the GSH precursor amino acids in the liver, including glutamic acid, methionine, and glycine. Overall, these results suggest that consuming oxidized oils can selectively modify the amino acid metabolism of pigs in different ways, which may negatively affect health and growth performance.

KEYWORDS: Oxidized lipids, Tryptophan, Threonine, Glutathione, Nursery pig

ABBREVIATIONS: AA, amino acid; ACN, acetonitrile; AMP, adenosine monophosphate; CCO, control corn oil; DC, dansyl chloride; DPDS, 2-2'-dipyridyl disulfide; FAA, free fatty acid; GCLC, glutamate-cysteine ligase catalytic subunit; GPX1, glutathione peroxidase 1; GSH, glutathione; GSSG, oxidized glutathione; GSR, glutathione-disulfide reductase; GSTA, glutathione s-transferase; HAAO, 3-hydroxyanthranilate 3,4-dioxygenase; HMDB, human metabolome database; HQ, 2-hydrazinoquinoline; IACUC, institutional animals care and use committee; IDO, indoleamine 2,3-dioxygenase; KYNU, Kynureninase; LC-MS, liquid chromatography-mass spectrometry; LOP, lipid oxidation products; MGST1, microsomal glutathione s-transferase 1; NAD^+, nicotinamide adenine dinucleotide; OCO, oxidized corn oil; PCA, principal components analysis; P-5-P, pyridoxal 5'-phosphate; PLS-DA, projection to latent structures-discriminant analysis; QPRT, quinolinate phosphoribosyltransferase; QTOFMS, quadrupole time of flight mass spectrometer; SEM, standard error mean; TDG, threonine dehydrogenase; TDH, threonine dehydratase; TDO, tryptophan 2,3-dioxygenase; TPP, triphenylphosphine; UPLC, ultra-performance liquid chromatography.

4.2 INTRODUCTION

Heavily-oxidized lipids from deep frying and heating practice in restaurants and the food processing industry have been widely used in animal feeds as an economical source of energy [252]. However, the unfavorable chemical and organoleptic properties of these recycled oxidized lipids, including rancidity, elevated acidity, and increased lipid oxidation products (LOPs) [115] could reduce feed intake and impair growth performance and health of production animals, especially young pigs under rapid growth [253-255]. In addition, the quality and organoleptic characteristics of meat products from animals that consumed these oils could be reduced. Diminished growth performances in animals fed these recycled oils have been associated with damaged physiological functions, such as impaired small intestinal function and increased hepatic lipid accumulation [253,255]. Moreover, the levels of unsaturated aldehydes, major secondary LOPs in heavily-oxidized lipids, had a strong correlation with compromised growth performance and feed intake in young pigs [256].

Compromised growth performance and health are recognized as responses to feeding oxidized lipids-induced negative impacts on nutrient metabolism to production animals since nutrient metabolism is an indispensable component of animal growth. The primary effect of oxidized lipids on nutrient metabolism is interrupted lipid metabolism, showing as increased hepatic lipids and increased expression of peroxisome proliferator-activated receptor alpha (PPARα) targeted genes in pigs and other species [253,257]. In contrast, the influences of feeding oxidized lipids on amino acid metabolism remain largely unexplored, partially because of the fact that the inclusion of oxidized lipids has little influence on amino acid and protein composition in feed. Amino acids are the building blocks of protein synthesis and the sources of functional molecules in energy metabolism, antioxidant system, neurotransmission, endocrine signaling, and many other biological activities [258]. Changes in amino acid homeostasis and metabolism could have a

fundamental impact on biological or physiological events related to growth performance and health.

Potential mechanisms of oxidized lipids-induced changes in amino acid metabolism are majorly classified by direct chemical interactions and indirect signaling transductions. Unsaturated aldehydes in frying oils interact directly with basic amino acids (BAA) by generating chemical bonds. This interaction affects the bioavailability and function of targeted BAA as well as the digestibility of BAA-containing proteins [259]. Some electrophilic LOPs can react with thiol-contained antioxidants, resulting in eliciting redox stress and glutathione (GSH) metabolism. In an indirect way, cyclic fatty in oxidized lipids functions as the ligands for the nuclear receptors PPARα that elicits a series of responses in regulating downstream amino acid metabolism through transcriptional regulation [260]. In fact, oxidized oil-induced metabolic events in amino acid metabolism were revealed in our previous mouse study, showing a decreased serum tryptophan concentration associated with stimulated hepatic tryptophan-nicotinamide adenine dinucleotide (NAD^+) biosynthesis pathway [128]. Similarly, the decreased serum tryptophan concentration was also observed in nursery pigs fed oxidized oil [121]. However, the mechanisms of oxidized lipids-induced changes in amino acid metabolism remain to be further examined. In this study, comprehensive metabolomes of serum and liver from nursery pigs fed oxidized corn oil (OCO) were characterized by the liquid chromatography-mass spectrometry (LC-MS)-based untargeted metabolomic analysis, targeted analysis, and biochemical analysis.

4.3 MATERIALS AND METHODS

4.3.1 Chemicals and reagents

The source of chemicals and reagents used in sample preparation, LC-MS analysis, structural confirmation, and quantification are enlisted in **Table 4.1**.

4.3.2 Animals, diets, and sample collection

The protocol of the feeding trial was reviewed and approved by the University of Minnesota Institutional Animal Care and Use Committee. The procedures of OCO preparation, diet formulation, and animal management have been described previously [121]. Briefly, OCO was prepared by heating control corn oil (CCO) at 185 °C for 12 h with an airflow rate of 12 L/min. The feeding trial was conducted at the University of Minnesota Southern Research and Outreach Center (Waseca, MN). A total of 128 barrows weaned at 19 days of age (initial BW = 6.3 ± 1.4 kg) were assigned to 8 blocks (4 pens/block and 4 pigs/pen) based on their body weight (BW). Pigs had *ad libitum* access to feed and water. Four pens in each block were assigned randomly to 4 isocaloric dietary treatments containing 9% CCO, 6% CCO + 3% OCO, 3% CCO + 6% OCO, and 9% OCO, respectively. The pig with the BW close to the mean pen BW on day 0 of feeding was selected as the focal pig in each pen (n = 32). On day 35 of feeding, focal pigs were euthanized, and blood and liver samples were collected. Serum was isolated, and samples were snap-frozen and stored at -80 °C for metabolite and biochemical analysis.

4.3.3 LC-MS-based metabolomics analysis

The procedures of sample preparation, sample analysis, and data analysis in metabolomics analysis were described as follows.

4.3.3.1 Sample preparation

Liver tissue samples were fractionated using a modified Bligh and Dyer method [158]. Briefly, 100 mg of liver sample was homogenized in 0.5 mL of methanol and then mixed with 0.5 mL of chloroform and 0.4 mL of water. After 10-min centrifugation at 18,000 × *g*, the upper aqueous fraction was harvested for hydrophilic metabolite analysis, and the organic fraction was dried under nitrogen and reconstituted in 0.5 mL n-butanol.

Serum samples were deproteinized and extracted by mixing 1 volume of serum with 19 volumes of 66% aqueous acetonitrile (ACN) and then centrifuged at 18,000 × *g* for 10 min to obtain the supernatants.

4.3.3.2 Chemical derivatization

For detecting the metabolites containing amino functional groups in their structures, the samples were derivatized with DC prior to the LC-MS analysis. Briefly, 5 µL of sample or amino acid standard was mixed with 5 µL of 50 µM d_5-tryptophan as internal standard, 50 µL of 10 mmol/L sodium carbonate, and 100 µL 3 mg/mL DC in acetone. The mixture was incubated at 60 °C for 15 min and centrifuged at 18,000 × *g* for 10 min, and the supernatant was transferred into an HPLC vial for LC-MS analysis. For detecting metabolites containing carboxyl group, the samples were derivatized with 2-2'-dipyridyl disulfide (DPDS), triphenylphosphine (TPP), and 2-hydrazinoquinoline (HQ) prior to the LC-MS analysis [224]. Briefly, 2 µL of sample or standard was added into 100 µL of freshly prepared ACN solution containing 1 mM DPDS, 1 mM TPP, 1 mM HQ, and 100 µM deuterated d_4-acetic acid as internal standard. The reaction mixture was incubated at 60 °C for 30 min, chilled on ice, and mixed with 100 µL of H_2O. This mixture was centrifuged at 18,000 × *g* for 10 min, and the supernatant was transferred into an HPLC vial for LC-MS analysis.

4.3.3.3 Conditions of LC-MS analysis

A 5 µL of aliquot prepared from serum and hepatic extracts was injected into an Acquity ultra-performance liquid chromatography-quadrupole time-of-flight mass spectrometry (UPLC-QTOFMS) system (Waters, Milford, MA), and separated in a UPLC column in a 10-min run at a flow rate of 0.5 mL/min. Detailed information on LC-MS acquisition conditions is provided (**Table 4.2**). The LC eluant was injected into a Xevo-G2-S QTOF mass spectrometry for accurate mass measurement and ion counting. Capillary voltage and cone voltage for electrospray

ionization was maintained at 3 kV and 30 V for positive mode detection, or at -3 kV and -35 V for negative mode detection, respectively. Source temperature and desolvation temperature were set at 120°C and 350°C, respectively. Nitrogen was used as both cone gas (50 L/h) and desolvation gas (600 L/h), and argon was used as collision gas. For accurate mass measurement, the mass spectrometer was calibrated with sodium formate solution with a range *m/z* of 50-1000 and monitored by the intermittent injection of the lock mass leucine encephalin ($[M + H]^+$ = 556.2771 *m/z* and $[M – H]^-$ = 554.2615 *m/z*) in real-time. Mass chromatograms and mass spectral data were acquired and processed by MassLynx software (Waters) in centroided format.

4.3.3.4 Characterization, quantification, and pathway analysis of metabolite markers

Chromatographic and spectral data of samples were analyzed using MarkerLynx™ software (Waters). A multivariate data matrix containing information on sample identity, ion identity [retention time (RT) and *m/z*], and ion abundance was generated through centroiding, deisotoping, filtering, peak recognition, and integration. The relative abundance of each ion was calculated by normalizing the single ion counts (SIC) *versus* total ion counts (TIC) in the whole chromatogram. The data matrix and sample list were further exported into SIMCA-P software (Umetrics, Kinnelon, NJ). Partial least squares-discriminant analysis (PLS-DA) on CCO, 3% OCO, 6% OCO, and 9% OCO fed pigs was conducted after data were transformed by mean-centering and *Pareto* scaling. The potential metabolite markers were identified by analyzing ions contributing to the principal components and to the separation of sample groups in the loadings scatter plot.

4.3.3.5 Marker characterization and quantification

The chemical identities of metabolite markers were determined by accurate mass measurement, using elemental composition analysis, by searching the Human Metabolome Database (HMDB), the Kyoto Encyclopedia of Genes and Genomes (KEGG), Metlin (https://metlin.scripps.edu/) and

comparisons with authentic standards if available. Individual metabolite concentrations were determined by fitting the ratio between the peak area of each metabolite and the peak area of the internal standard with a standard curve using QuanLynx^{TM} software (Waters).

4.3.4 Gene expression analysis

Total RNA from liver tissue was isolated using Trizol reagent from Invitrogen Life Technologies (Carlsbad, CA) according to the manufacturer's protocol. The cDNA was generated from 1 μg of total RNA using the High-Capacity cDNA Reverse Transcription Kit from Thermo Fisher Scientific (Wilmington, DE). The sequence of the primers used for the quantitative real-time polymerase chain reaction (qPCR) analysis of targeted genes was enlisted (**Table 4.3**), including tryptophan 2,3-dioxygenase (*TDO*), indoleamine 2,3-dioxygenase (*IDO2*), Kynureninase (*KYNU*), 3-hydroxyanthranilate 3,4-dioxygenase (*HAAO*), and quinolinate phosphoribosyltransferase (*QPRT*), glutathione peroxidase 1 (*GPX1*), glutathione-disulfide reductase (*GSR*), glutathione s-transferase (*GSTA*), microsomal glutathione s-transferase 1 (*MGST1*), and glutamate-cysteine ligase catalytic subunit (*GCLC*). The expression levels of targeted genes were measured by qPCR using SYBR Green PCR Master Mix in a StepOne Plus system from Applied Biosystems (Carlsbad, CA). β-actin (*ACTB*) was used as the reference gene, and the expression levels of genes were quantified using the comparative threshold cycle (CT) method.

4.3.5 *In vitro* analysis of threonine dehydratase (TDH) and threonine dehydrogenase (TDG) enzymatic activities

TDH activity was determined by an enzyme reaction assay. Pig liver homogenate was prepared using a modified method from Bird and Nunn [261]. Briefly, the liver sample was homogenized in ice-cold 0.1 M KH_2PO_4 buffer (pH 8.2, 2.5 vol/wt). The homogenate was centrifuged at 42,000 × *g* for 1h at 4 °C and the supernatant was collected. Hydrophilic compounds of CCO and CCO

were extracted by mixing oils with 90% isopropanol 1:1 v/v. After vortexed and centrifuged at 18,000 × *g* for 10 min, the aqueous phase was taken for further enzyme reaction assay. For determining the influence of OCO on TDH enzyme activity, a 20 µL of liver homogenate was mixed either with CCO (20 µL CCO extract), OCO (20 µL OCO extract), or solvent blank (20 µL 90% isopropanol), with reaction mix containing 0.1 M KH_2PO_4 (pH 8.2), 1 mM dithiothreitol (DTT), and 0.2 mM pyridoxal 5'-phosphate (P-5-P). The reaction started by adding threonine as the substrate to a final concentration of 0.2 M. The mixture was incubated at 37 °C for 0, 5, 10, 15, and 30 min. After the incubation, the reaction was stopped by adding ACN (10:1 v/v) to the reaction mix. The level of α-ketobutyrate production in the reaction system was measured by LC-MS targeted analysis.

TDG enzyme activity was determined using a threonine dehydrogenase assay kit from Biomedical Research Service & Clinical Application (Buffalo, NY). Briefly, the liver sample was homogenized with 1x Cell Lysis Solution. The homogenate was centrifuged at 14,000 × *g* for 5 min at 4 °C. The supernatant was harvested and stored at -80 °C for further analysis.
Before starting the enzyme reaction assay, lysate liver protein concentration was determined using a Pierce™ BCA Protein Assay Kit (Thermo Fisher Scientific, Waltham, MA). The lysate liver samples were further diluted to a recommended range of 0.5-2 mg/mL. For determining the enzyme activity of TDG in OCO or CCO-treated pigs, 10 µL of liver homogenates were mixed with either 50 µL Reaction Solution or Control Solution in a 96-well plate and mixed by a vortex. The plate was covered and incubated at 37 °C for 1 h. After the incubation, a 50 µL of 3% acetic acid was used to stop the reaction. A cherry red color change was measured by a Spectra Max 250 96-well plate reader from Molecular Devices (Sunnyvale, CA) at 492 nm. The TDG activity was defined in IU/L = ΔO.D. × 16.98

4.3.6 Statistical analysis

Statistical analysis of metabolomics parameters and gene expression levels was performed by one-way ANOVA followed by Tukey's post hoc test, in which the CCO group was considered as control and compared to 3%, 6%, and 9% OCO treatment groups using GraphPad Prism version 8.0.2 (La Jolla, CA). Results are presented as mean ± standard error mean (SEM). Differences between dietary treatments were considered significant if $P < 0.05$ and were considered a trend if the *P*-value was between 0.05 and 0.10.

4.4 RESULTS

4.4.1 Profiling serum free amino acids

To evaluate oxidized oil-induced metabolic events, serum free amino acids were quantified by the LC-MS since serum free amino acids pool directly reflects and indicate endogenous amino acid homeostasis. Quantitative analysis revealed that OCO selectively affected serum free amino acids, resulting in decreased concentrations of alanine, glutamic acid, and tryptophan, while the increased percentages of threonine, tyrosine, and ornithine in OCO treatments compared to CCO treatment (**Table 4.4**).

4.4.2 OCO-elicited metabolic changes in serum

Further investigations of OCO-elicited events on amino acid metabolism were detected by untargeted metabolomics, multivariate data analysis of serum metabolite in the scores plot of the PLS-DA model showed separations between OCO and CCO treatments, in particular the shift from OCO to 9% CCO treatments in the principal component 1 (PC) (**Figure 4.1A**). Major metabolites contributing to the separation between OCO and 9% CCO were identified in the loadings plot (**Figure 4.1B**) and their structural identities were characterized (**Table 4.5**). Except

for detected changes in amino acids in Table 4.4, OCO also increased 4-aminobutyraldehyde, acetylcholine, and serine.

For serum lipidomic profile, the separation between OCO and CCO was observed in the scores plot of the PLS-DA model by PC1 (**Figure 4.2A**), and individual lipid species were identified and labeled in the loadings plot indicating ions with higher abundance in CCO or OCO groups (**Figure 4.2B**). Among them, phosphatidylcholines (PCs) and triacylglycerols (TAGs) containing multi-polyunsaturated fatty acids were found with high abundance in the CCO group (**Table 4.8**), such as PC(16:0/22:5) and TAG(18:1/18:2/18:3) (**Figure 4.3A-B**), while cholesteryl ester and lysophosphatidylcholine (LysoPC), including LysoPC(18:0) and cholesteryl ester (18:2), were greater in the 9% OCO group than in the CCO group (**Figure 4.3C-D**). In general, concentrations of serum free fatty acids did not show dramatic changes across CCO and OCO groups (**Table 4.7**). The major species of saturated fatty acids and major species of unsaturated fatty acids, C16:0, C18:0, C18:1, and C18:2, do not show statistical significance between CCO and OCO treatments (**Figure 4.3E-H**).

4.4.3 Comprehensive analysis of hepatic metabolome

Free amino acids. Following the observations of changes in serum amino acid profile, hepatic free amino acids were also further quantified by LC-MS. Consistent with the limited impact of OCO on changes of free amino acids in serum, only hepatic glutamate was impacted by 9% OCO while taurine tended to be decreased (**Table 4.8**).

Metabolome. The scores plot of hepatic metabolome in the PLS-DA model showed a dose-dependent separation between OCO and CCO samples by PC1 (**Figure 4.4A**). Major metabolites contributing to the separation of OCO and 9% CCO groups in the hepatic metabolome model were characterized (**Figure 4.4B, Table 4.9**). Feeding OCO decreased the level of

taurodeoxycholic acid, malic acid, ascorbic acid, cysteine, methionine, alanine, and inosine, but increased the level of glutathione, adenosine monophosphate (AMP), GSH, oxidized glutathione (GSSG), and NAD^+ in the liver.

Lipidome. Similarly, a dose-dependent separation was observed from the scores plot of hepatic lipidomic analysis in the PLS-DA model by PC1 (**Figure 4.5A**). Ions contributed to the separations of CCO and OCO treatments were identified in a loadings plot, correspondingly (**Figure 4.5B, Table 4.10**). In particular, the relative abundance of octadecanoic acid (C18:0) increased in OCO than CCO treatments, indicating the OCO-induced fatty acid saturation process in the liver. Quantitative analysis showed that feeding OCO altered hepatic free fatty acids dramatically as a significant decrease in concentrations of short-chain fatty acids, palmitic acid (C16:0), and unsaturated long-chain fatty acids (C18:2), while saturated long-chain fatty acid octadecanoic acid (C18:0) increased (**Table 4.11, Figure 4.6**).

4.4.4 Effects of OCO on tryptophan-NAD^+ pathway

Following the observation of NAD^+ as OCO-responsive metabolites in the hepatic metabolome, comprehensive detection of OCO-elicited metabolic effects on tryptophan-NAD^+ pathway was examined through targeted analysis. An increase in hepatic NAD^+ concentration in 9% OCO treatment was observed (**Figure 4.7A**), however, the concentration of hepatic free tryptophan was not affected by OCO (**Table 4.5**). Genes encoding metabolizing enzymes involved in tryptophan-NAD^+ biosynthesis pathway were further evaluated by qPCR **(Figure 4.7B**). OCO increased gene expression levels of *TDO2, IDO2, KYNU, and QPRT* dose-dependently, suggesting OCO stimulated tryptophan-NAD^+ biosynthesis. In addition, metabolites involved in the synthesis of adenine dinucleotide moiety for NAD^+ biosynthesis including, adenosine, and inosine, were also increased by OCO treatments (**Figure 4.7C-E**).

4.4.5 Effects of OCO on threonine catabolism

TDG pathway. Following the observation of increased threonine as OCO-responsive metabolites in serum, hepatic threonine metabolism was further characterized by LC-MS-based targeted analysis and biochemical analysis. Hepatic threonine level was not altered by OCO (**Figure 4.8A**). Both enzyme activity and gene expression level of TDG had no statistical significance by OCO (**Figure 4.8B-C**), suggesting the OCO-induced little effects on the TDG pathway.

TDH pathway. In contrast to TDG, TDH regulated metabolic pathway was inhibited showing decreased major metabolites α-ketobutyrate (in all OCO doses) and α-aminobutyrate (9% OCO treatment) in OCO treated pigs compared to CCO treated pigs (**Figure 4.8D-E**). To further evaluate the influences of OCO and its hydrophilic compounds on TDH enzyme activity, an *in vitro* reaction assay was conducted with liver homogenate, substrates, and hydrophilic extracts of OCO, CCO as a sample control, and solvent control as the blank or background (**Figure 4.8F**). The concentration of α-ketobutyrate, the product of the TDH catalyzed reaction, was quantified for the evaluation of TDH enzymatic activity in threonine degradation process. A comparable level of α-ketobutyrate was observed in control, OCO extract, and blank at the first 5 min in reaction assays. In comparison to a linear increase of product in control and blank, OCO extracts reduced α-ketobutyrate significantly starting at 15 min to 30 min of reaction (**Figure 4.8F**), which indicates the hydrophilic compounds in OCO might directly inhibit the enzyme activity of TDH.

Other downstream metabolites in threonine degradation, such are propionic acid and pyruvate were decreased by OCO treatments (**Figure 4.8G-H**). Therefore, increased serum threonine might be attributed to the suppression of threonine catabolism by inhibiting TDH activity, which resulted in decreased concentrations of pyruvate and propionic acids (**Figure 4.8**), these downstream metabolites in threonine catabolic pathways might contribute to energy conversion.

4.4.6 Effects of OCO on GSH metabolism

Following the observation of decreased GSH and its precursor amino acids, cysteine, and methionine as OCO-responsive metabolites in the liver (**Table 4.9**), targeted LC-MS and biochemical analyses were conducted to evaluate GSH metabolism-related metabolites and gene expression levels. Concentrations of hepatic GSH and its oxidized form GSSG were increased under OCO treatment (**Figure 4.9A-B**). However, the ratio of hepatic GSH and GSSG was reduced by feeding OCO (**Figure 4.9C**). In addition, another marker of oxidative stress, pyroglutamate increased in the liver of pigs fed 9% OCO compared to CCO (**Figure 4.9D**). Hepatic gene expression of key enzymes in GSH synthesis, reduction, and antioxidant response was elevated by the 6% and 9% OCO treatments (**Figure 4.9E**).

Metabolites in the transmethylation cycle were further quantified since it generates methionine and cysteine as precursors for GSH synthesis. The results showed a generally decreased cystathionine, homocysteine, and S-adenosyl-homocysteine (SAH) (**Figure 4.10A-C**), but slightly increased S-adenosyl methionine (SAM) (**Figure 4.10D**).

4.5 DISCUSSION

The recycled lipids such as animal fats obtained from slaughterhouses, by-products of the biodiesel industry, and frying oils produced by food facilities are used as potential lipid sources added to feeds of livestock due to the low-cost property [262]. Correspondently, large quantities of LOPs compromised animal health and productive performance and triggered a series of metabolic events through interrupted amino acid metabolism. Although various animal feeding studies elucidated the negative effects of feeding oxidized lipids on animal performance, the causes of these compromised performances on how oxidized lipids affect metabolism particularly amino

acid metabolism are not well established. In the current study, the metabolic effects of feeding OCO to young animals was evaluated by a nursery pig feeding trial. Selective influence on amino acid profile and its related metabolic pathways were observed that partially revealed mechanisms of OCO-induced metabolic effects through several aspects, such as transcriptional regulation of LOP responsible genes, direct chemical reaction with proteins, and impacts on antioxidants in maintaining the homeostasis of the redox system as responses to oxidized lipid intake. The causes and significances of the altered metabolic pathway by OCO are summarized and discussed (**Figure 4.11**).

4.5.1 Influence of OCO-induced metabolic events on tryptophan-NAD^+ metabolism.

Growth performance. Tryptophan is an essential amino acid for most animals due to its synthesis cannot be achieved in the body. In swine diets, supplying adequate tryptophan is critical to improving the growth performance and health of pigs, especially for young piglets [263]. The NRC recommendations for the dietary tryptophan requirements are from 0.11 to 0.27% depending on the different growth stages of pigs [264]. In the current study, a 23-33% decrease in serum tryptophan was found in OCO-treated pigs (**Table 4.4**). However, OCO diets only slightly decreased growth performance and did not induce a significant decrease in feed intake compared to the CCO diet in our previous published manuscript which includes the growth performance data of pigs in our current study [121]. The reduced growth performance in pigs might be a consequence of an OCO-induced decrease in efficiency of converting feed to body mass or decreased tryptophan due to the important function of tryptophan on growth. The mechanism of the OCO-elicited decrease of animal growth and tryptophan metabolism needs further evaluation.

Tryptophan-NAD+ pathway. In addition to serving as building components for protein biosynthesis, tryptophan and its metabolites play important roles in various physiological events, including the regulations of appetite, stress responses, immunity, mood, and behaviors [265]. Over

95% of tryptophan ingested from the diet is metabolized in the liver through the kynurenine pathway to produce NAD^+, Acetyl-CoA, or other metabolites [265]; while, 1-2% of dietary tryptophan is utilized to synthesize serotonin which is a neurotransmitter in regulating mood, appetite, and gut functions; the rest of the dietary tryptophan is degraded into indoleacetic acid by the gut bacteria [266]. Therefore, the possible causes of the decrease in serum tryptophan might be enhanced endogenous tryptophan utilization for NAD^+ biosynthesis. Correspondingly, the comprehensive hepatic metabolome investigation observed the increased NAD^+ and AMP levels as biomarkers in the liver of OCO-fed pigs (**Figure 4.4, Table 4.7**), suggesting the elevated biosynthesis from tryptophan to NAD^+ driven by OCO. The subsequent targeted analysis confirmed this assumption showing as OCO-elicited increased hepatic gene expression levels of enzymes in the NAD^+ synthesis pathway (**Figure 4.7A-B**). Similar research observation was found in our previous mice study, the elevated hepatic tryptophan-NAD^+ pathway was identified as an oxidized soybean oil-induced metabolic response [128]. One potential cause in promoting the tryptophan-NAD^+ pathway is through transcriptional regulation by oxidized lipid-induced activation of PPARα, because some LOPs in oxidized oils act as agonists of PPARα and it can further stimulate the tryptophan-NAD^+ pathway that responses for oxidized lipid intake [257,267]. Consistent results in our current pigs and mice studies with the stimulated tryptophan-NAD^+ metabolism also indicate that the mechanism might be appropriate for other primates even though pigs and humans have a lower PPAR response compared to mice.

Significance of OCO-elicited NAD^+ metabolism and its related metabolic events. NAD^+ plays crucial biological functions in maintaining the redox equilibrium of the body. NAD^+/NADH are cofactors involved in many dehydrogenase-regulated reactions, which serve as protons/electrons transporters in biological reactions, especially its importance in fatty acid β-oxidation and aldehyde dehydrogenase (ALDH) involved reactions, the latter enzyme could neutralize oxidized lipid-derived reactive aldehydes and mitigate reactive oxygen species (ROS) [268]. Besides

nicotinamide adenine dinucleotide phosphate (NADP) and its reduced form NADPH are responsible to recover oxidized antioxidants, such as GSSG, and converting them to its reduced form GSH, which is an important mechanism for maintaining the redox balance and protecting against cytotoxicity from LOPs after consumed oxidized lipids [269,270]. Therefore, a series of metabolic events associated with promoting the tryptophan-NAD^+ pathway play major functions to mitigate the imbalance of the redox system through recruiting ALDH or GSH in neutralizing reactive aldehydes in OCO. However, OCO-elicited changes on other catabolic pathways of tryptophan, such as glutarate, serotonin, and melatonin, are still undefined, although over 95% of tryptophan is catabolized in the kynurenine pathway and 5% is used for other metabolites synthesis.

Purine metabolism. Meanwhile, increased AMP, adenosine, and inosine, the intermediate metabolites of purine catabolism [271], were observed in OCO treatments (**Figure 4.7C-E**), which contributed to the composition of adenine dinucleotide moiety that is the precursor used for NAD^+ synthesis. Therefore, feeding OCO promoted the production of adenosine and decreased purine degradation associated with the increase of NAD^+ production. However, the explanation of the mechanism requires further investigation.

DNA repair. LOPs, especially reactive aldehydes in oxidized lipid-induced DNA damage had been observed in many studies, which further produces mutagenic and carcinogenic effects [272]. Poly(ADP-ribose) polymerase 1 (PARP1) is responsible for repairing diverse types of DNA damage by transcriptional regulation. When DNA damage happened, the PARP1 is activated that uses NAD^+ as substrate for poly(ADP-ribose) (PAR) formation associated with nicotinamide releasing [273]. In our current study, the elevated production of NAD^+ from tryptophan in OCO-treated groups might be also responsible for DNA repair.

Overall, these observations suggest that the mobilization of free tryptophan might be a priority used for NAD^+ synthesis in the liver that is further utilized for LOPs neutralization and DNA repair compared to being utilized for other metabolic activities.

4.5.2 Influence of OCO-induced metabolic events on threonine metabolism

Threonine metabolism. Threonine is the second limiting amino acid in the swine diet which is extensively used for protein synthesis, in particular mucosal protein in the intestine [274,275]. In the current study, a 30% increase in serum threonine was observed as a biomarker of OCO-treated pigs (**Table 4.4**), however, hepatic threonine levels were not altered (**Figure 4.8A**). Except for the function of threonine used in protein synthesis, excessive blood threonine is transported into the liver and catabolized by major enzymes, threonine dehydrogenase (TDG), and threonine dehydratase (TDH).

TDG catalyzes threonine degradation by producing 2-amino-3-ketobutyrate, which is further cleaved to form glycine and acetyl-CoA **[276]**. In our current study, both enzymatic activity and gene expression of TDG did not show statistical significance by feeding OCO although slight changes were observed under OCO treatments (**Figure 4.8A-C**). Concentration changes of hepatic free fatty acids might be a potential cause that altered TDG expression, because some short-chain or long-chain fatty acids, such as β-hydroxybutyrate, lauric acid, myristic acid, palmitic acid, and stearic acid were found to have inhibitory functions on TDG activity in the liver of rat [277]. In our current study, an OCO-induced shift in hepatic free fatty acid profile was observed (**Table 4.9**), however, whether it is the biomarker for changing TDG expression needs further investigation.

TDH catalyzes threonine dehydration by producing α-ketobutyrate and ammonia. In the rat, TDH-regulated threonine irreversible oxidation is the dominant pathway for hepatic threonine catabolism, which accounts for ~ 65% of total oxidized threonine in rats and this reaction can be activated by glucagon [278]. However, the proportion of threonine oxidation through TDH was still not clear in pigs. In our current study, concentrations of α-ketobutyrate and α-aminobutyrate were decreased by OCO with ranges of 30-35% and 10-50%, respectively (**Figure 4.8C-D)**. One possible reason is that reactive aldehydes in oxidized lipids directly interact with enzymes and inhibit catalytic activity, this phenomenon was confirmed by *in vitro* incubation with hydrophilic phase extracted from OCO that significantly reduced α-ketobutyrate production as a response to the decreased catalytic function of TDH (**Figure 4.8E**). The methionine transsulfuration pathway also contributes to α-ketobutyrate production from the conversion of homocysteine to cystathionine [279]. However, cystathionine and homocysteine levels were not largely influenced by OCO treatment (**Figure 4.10A-B**).

Energy metabolism. The intermediate metabolite α-ketobutyrate can be finally converted into succinyl-CoA and it enters into the citric acid cycle leading to gluconeogenesis [280]. When feeding oxidized lipids to pigs, the inhibition of threonine oxidation in the TDH pathway might further block the energy metabolism by reducing gluconeogenesis from essential amino acids, but the underlying mechanisms still need to be explored.

4.5.3 Influence of OCO-induced metabolic events on GSH metabolism

Oxidative stress and antioxidants. Extensive research had been observed that incidents of oxidative stress are associated with the consumption of oxidized lipids in pigs [121,254], chickens [122,281,282], and rats [283-285]. As a result, decreases in endogenous antioxidants such as GSH or vitamin E were observed as notable markers, which are key factors for scavenging reactive oxygen species (ROS) in LOPs and sustaining the balance of the redox system. Although OCO

treatments increased hepatic both GSH and GSSG concentrations dose-dependently (**Figure 4.9A-B**), the ratio between GSH/GSSG decreased, suggesting the robustness of GSH metabolism for handling oxidized lipids. while the raised pyroglutamate concentration (**Figure 4.9C-D**) indicates accumulated oxidative stress in the liver after feeding OCO. Under normal conditions, GSH preserves a high level in the reduced form compared to its oxidized form GSSG in the cells that maintain a reduced redox environment, while a decreased GSH/GSSG ratio is commonly associated with liver metabolic stress [286]. On the other aspect, an increased concentration of pyroglutamate, the metabolites from γ-glutamylcysteine degradation, indicates that the limited cysteine was available to be utilized for GSH synthesis [287]. These phenomena can be characterized as OCO-induced more oxidative stress, but redox system balance was still maintained by promoting GSH metabolism. Except for the balance between GSH and GSSH, the vitamin also plays a pivotal role in the maintenance of redox balance. Vitamin E is not only able to reduce the ROS production from the oxidization of PUFAs such as hydroxyl radicals or lipid peroxides by direct interaction, but it can also restore oxidized GSH in its reduced form that contributes to the endogenous redox balance [288]. Our previous published data observed a decrease of serum α-tocopherol OCO fed pigs [121], the diminished vitamin E might be used to recycle GSH from GSSG with robust biotransformation that partially explained the elevated GSH concentration after feeding OCO.

GSH metabolism. The elevated gene expression levels of enzymes on GSH biosynthesis, GSSG reduction, and GSH conjugation to ROSs (**Figure 4.9E**) were observed as responses to OCO-induced GSH metabolism in the liver. Among these enzymes, GCLC catalyzes the first step of *de novo* GSH synthesis by converting glutamate and cysteine to γ-glutamylcysteine, which is a vital indicator of endogenous GSH [289]. Previous research found that the gene expression level of *GCLC* can be up-regulated by oxidant species and electrophiles especially exposed to the conditions of oxidant stress or glutathione deletion [290,291]. Increasing the transcriptional level of

GCLC is positively associated with its protein levels, and even this is a strong marker of the increase of cellular GSH [292]. The underlying mechanism of transcriptional regulation of GSH metabolism can go through the manipulation of antioxidant response element (ARE), activator protein-1, NF-E2 related factor 2 (Nrf2), or nuclear factor kappa B (NF-κB) pathways since LOPs in the oxidized lipids are considered as agonists in these pathways [293]. To prevent the accumulation of cellular toxic oxygen radicals from the oxidized lipids, GSH interacts with LOPs to form GSSG by glutathione peroxidase (GPX) in a selenium-dependent process. Afterward, GSSG can be reduced back to GSH catalyzed by glutathione reductase (GSR) using NADPH to form a redox cycle. Alternatively, some peroxides can be reduced through glutathione s-transferase (GST) regulated reactions, which happen in both microsome and cytosol [293]. In the current study, the stimulation of GSH metabolism-related genes and elevated concentration of GSH suggest that there is a robust antioxidant system to protect damages of cells from reactive oxygen species in OCO. In brief, these results indicate that consuming OCO did induce metabolic stress in the liver whereas the redox system is maintaining equilibrium status because of the regulatory functions of endogenous antioxidants that mitigate OCO-induced oxidative stress.

4.6 CONCLUSIONS

Overall, we examined feeding oxidized corn oil to young pigs induced a series of amino acid metabolism through metabolomic and biochemical-based analyses in this study. The promotion of the tryptophan-NAD^+ pathway is an important metabolic event in utilizing essential amino acids for vitamin synthesis, instead of protein synthesis, contributing to other metabolic activities, such as ROS mitigation and DNA repair, these reactions were stimulated by oxidized lipid-induced transcriptional regulation. Besides, OCO directly contributed to the increase of serum threonine, which might directly interact with the TDH enzyme to reduce threonine catabolism and methionine transsulfuration in the liver. Moreover, the accelerated synthesis and recycling of hepatic GSH by endogenous antioxidants as a self-protective mechanism after ingested oxidized

lipids to neutralize ROS generated by OCO. These observations elucidated oxidized lipid-elicited events on amino acid metabolism by multiple mechanisms.

Table 4.1. Source of chemicals and reagents used in chemical analysis, LC-MS analysis, structural confirmation, and quantification.

Chemicals and reagents	**Vendor**
Acetone (LC-MS grade), Acetonitrile (LC-MS grade), Ammonium formate, Chloroform, Formic acid (LC-MS grade), Isopropanol (LC-MS grade), Water (LC-MS grade)	Fisher Scientific (Houston, TX)
Adenosine, Adenosine-5-monophosphoric acid (AMP), 2-Hydrazinoquinoline (HQ), Inosine, Triphenylphosphine (TPP)	Alfa Aesar (Ward Hill, MA)
2-2´-Dipyridyl disulfide (DPDS)	MP Biomedicals, LLC (Irvine, CA)
Fatty acids standards (C4-C22)	Nu-Chek Prep, Inc. (Elysian, MN)
Amino acid standards, α-Amino-n-butyric acid, n-Butanol, Dithiothreitol, Dansyl chloride (DC), Glutathione oxidized (GSSG), Glutathione reduced (GSH), α-Ketobutyric acid, β-Nicotinamide adenine dinucleotide hydrate (NAD), Potassium phosphate monobasic (KH_2PO_4), Sodium carbonate (Na_2CO_3)	Sigma-Aldrich (St. Louis, MO)
Pyridoxal 5-phosphate	TCI America (New Brunswick, NJ)
L-Threonine	Acros Organics (Morris Plains, NJ)
d5-Tryptophan	Cambridge Isotope Laboratories (Tewksbury, MA)

Table 4.2. LC-MS data acquisition condition in a 10-minute run.

Target compounds	**Column type**	**Mobile phase**	**MS detection mode**
Hydrophobic metabolites & Amino acids (dansylated)	BEH C18	A: 0.1% formic acid in H_2O B: 0.1% formic acid in ACN	Positive and negative
Fatty acids (HQ derivatization)	BEH C18	A: 2 mM NH_4OAc in water with 0.05% CH_3COOH B: 2 mM NH_4OAc in 95% ACN and 5% H_2O with 0.05% CH_3COOH	Positive
Hydrophilic metabolites	BEH Amide	A: 0.1% formic acid in H_2O B: 0.1% formic acid in ACN	Positive and negative
Lipids	BEH C8	A: 0.1% formic acid and 10 mM NH_4HCO_2 in 60% H_2O and 40% ACN B: 0.1% formic acid NH_4HCO_2 in methanol	Positive

Table 4.3. The sequences of primers used in the real-time PCR analysis.

Gene	Forward primer (from 5' to 3')	Reverse primer (from 5' to 3')
TDO2	GAGAGTCCCTTACAACAGGAGAC	CATGTGGCTCTAAACCTGGAGT
IDO2	AGACGCAGCCCAAAGAGGTT	ACGGATGCTTTCTCCCCCAG
KYNU	ACCTGCCATCACAAAAGCTGG	TAGGAGCACCAGCAGGCAAA
HAAO	AGCAGCCACAGGGTATGTCC	CTTGGCAGCAGCACACGTAG
QPRT	GGAGCGGGTGGCCCTTAATA	GGTCGTACCTGTGGGAGGTG
TDG	TGGTGCCCATAGCAGAGTCG	TTGGGCTCTGGAACCTTGGG
GPX1	GGGGAGATCCTGAATTGCCT	GAAGAGCGGGTGAGCATTTG
GSR	TGCGTGAATGTCGGATGTGT	GTGTTCAGTCGGCTCACGTA
GSTA1	AGACTCAAGACCTGGATAAGT	AGGCCACCTTGGCATCTTTT
MGST1	AGCCCAGAATGACCTTG	ACGATTTGGCTGGGGAAGG
GCLC	CTGCCTGAGTACAAGCCCAA	CTCCTGTGCCGGATGTTTCT
ACTB	ATCGCCGACAGGATGCAGAA	ATCGCCGACAGGATGCAGAA

Table 4.4. Effects of OCO on serum free amino acids.

	Serum (μM)					Serum (%)				
	CCO	**3% OCO**	**6% OCO**	**9% OCO**	***p*-value**	**CCO**	**3% OCO**	**6% OCO**	**9% OCO**	***p*-value**
Ala	318.28[a]	286.11[ab]	301.56[ab]	254.21[b]	**0.04**	7.37	6.87	7.35	6.50	0.16
Arg*	116.35	124.96	117.11	108.43	0.46	2.66	3.03	2.85	2.74	0.24
Asn	83.96	68.88	71.28	72.15	0.84	1.88	1.67	1.71	1.74	0.94
Asp	25.98	22.64	23.49	20.19	0.45	0.59	0.54	0.57	0.51	0.67
Cit	39.06	41.38	42.73	42.21	0.96	0.91	0.98	1.05	1.09	0.78
Gln	453.09	381.13	411.00	390.04	0.18	10.45	9.24	10.02	10.03	0.51
Glu	474.78[a]	348.01[ab]	397.11[ab]	310.29[b]	**0.02**	10.89[a]	8.36[ab]	9.65[ab]	7.89[b]	**0.04**
Gly	1073.68	1073.73	1036.56	1018.71	0.85	24.99	25.85	25.14	26.28	0.82
His*	51.63	55.21	49.85	48.08	0.47	1.18	1.34	1.22	1.20	0.67
Iso/Leu*	204.66	197.58	209.91	180.88	0.40	4.68	4.77	5.10	4.58	0.38
Lys*	149.08	132.75	124.84	154.35	0.62	3.40	3.23	2.97	3.85	0.33
Met*	22.84	19.34	22.80	23.94	0.66	0.52	0.47	0.55	0.59	0.58
Orn	60.10	63.74	61.31	67.11	0.80	1.36	1.53	1.48	1.71	0.15
Phe*	124.66	131.40	124.30	114.91	0.36	2.87	3.21	3.04	2.92	0.36
Pro	278.39	269.86	275.09	253.78	0.50	6.43	6.50	6.69	6.46	0.72
Ser	215.06	233.19	205.54	219.91	0.71	4.94	5.67	4.95	5.57	0.25
Tau	228.05	227.05	181.05	204.54	0.85	5.18	5.47	4.28	5.23	0.80
Thr*	118.64	150.78	147.48	146.60	0.44	2.69	3.63	3.55	3.67	**0.06**
Trp*	43.06[a]	34.34[ab]	35.80[ab]	30.98[b]	**0.04**	0.99	0.84	0.86	0.78	**0.10**
Tyr	46.75	47.14	56.25	60.60	0.33	1.05	1.13	1.38	1.52	**0.07**
Val	215.99	232.79	230.90	203.55	0.60	4.95	5.63	5.59	5.15	0.38
Total	4344.06	4141.98	4125.95	3925.44	0.40					

*: Essential amino acids.

[abc]: Different superscripts in a column indicate significant difference between treatments ($P < 0.05$).

Table 4.5. Identification of OCO-induced changes in serum amino-contained metabolites.

Ions	Modes of Ion detection	*m/z* of detection	Identity	Formula	Δppm	Database ID
Is	$[M+DC]^+$	323.1053	Alanine*	$C_3H_7NO_2$	4.0	HMDB0000161
IIs	[M+DC]+	381.1110	Glutamate*	$C_5H_9NO_4$	2.6	HMDB0060475
IIIs	$[M+DC]^+$	438.1478	Tryptophan*	$C_{11}H_{12}N_2O_2$	2.3	HMDB0030396
IVs	$[M+DC]^+$	460.1648	Carnosine*	$C_9H_{14}N_4O_3$	0.4	HMDB0000033
Vs	$[M+DC]^+$	353.1160	Threonine*	$C_4H_9NO_3$	3.1	HMDB0000167
VIs	$[M+DC]^+$	321.1262	4-Aminobutyraldehyde	C_4H_9NO	3.4	HMDB0001080
VIIs	$[M+DC]^+$	379.1682	Acetylcholine	$C_7H_{15}NO_2$	2.6	HMDB0000895
VIIIs	$[M+DC]^+$	339.1004	Serine*	$C_3H_7NO_3$	3.2	HMDB0000187

*: confirmed by authentic standards.

Table 4.6. Identification of OCO-induced changes in serum lipidome.

Ions	Modes of Ion detection	*m/z* of detection	Identity	Formula
Is_L	$[M+H]^+$	758.5710	PC(16:0/18:2)	$C_{42}H_{80}NO_8P$
IIs_L	[M+H]+	808.5885	PC(16:0/22:5)	$C_{46}H_{82}NO_8P$
$IIIs_L$	$[M+H]^+$	782.5719	PC(18:1/18:3)	$C_{44}H_{80}NO_8P$
IVs_L	$[M+H]^+$	786.6028	PC(18:1/18:1)	$C_{44}H_{84}NO_8P$
Vs_L	$[M+NH_4]^+$	898.7894	TAG(18:1/18:2/18:2)	$C_{57}H_{100}O_6$
VIs_L	$[M+NH_4]^+$	872.7738	TAG(16:0/18:1/18:3)	$C_{55}H_{98}O_6$
$VIIs_L$	$[M+NH_4]^+$	896.7744	TAG(18:1/18:2/18:3)	$C_{57}H_{98}O_6$
$VIIIs_L$	$[M+H]^+$	810.6028	PC(18:0/20:4)	$C_{46}H_{84}NO_8P$
IXs_L	$[M+H]^+$	666.6211	Cholesteryl ester 18:2	$C_{45}H_{76}O_2$
Xs_L	$[M+H]^+$	524.3726	LysoPC(18:0)	$C_{26}H_{54}NO_7P$
XIs_L	$[M+H]^+$	671.6766	Cholesteryl ester 20:5	$C_{47}H_{74}O_2$

Table 4.7. Concentrations of serum fatty acids

	Serum (µg/mL)				
	CCO	**3% OCO**	**6% OCO**	**9% OCO**	***p*-value**
C4:0	0.07	0.11	0.17	0.07	0.63
C6:0	0.01	0.01	0.02	0.01	0.71
C8:0	0.00	0.00	0.00	0.00	0.12
C12:0	0.01	0.00	0.02	0.01	0.22
C16:0	50.35	51.19	55.84	51.53	0.19
C16:1	0.00	0.00	0.00	0.01	0.48
C18:0	52.99	53.58	56.97	54.16	0.49
C18:1	2.14	2.06	1.55	1.92	0.79
C18:2	12.83	9.88	8.99	7.77	0.20
C20:0	1.16	1.15	1.15	0.97	0.61

Table 4.8. Effects of OCO on liver free amino acids.

	Liver (µg/g)				
	CCO	**3% OCO**	**6% OCO**	**9% OCO**	***p*-value**
Ala	365.06	282.77	303.11	244.25	0.08
Arg*	13.15	12.17	11.62	11.17	0.43
Asn	48.51	43.31	29.30	32.94	0.43
Asp	142.97	139.10	181.06	136.20	0.66
Cit	16.40	16.36	16.40	16.34	0.78
Gln	511.72	492.27	460.03	498.40	0.84
Glu	857.75[a]	679.85[ab]	678.47[ab]	656.06[b]	**0.04**
Gly	381.55	330.16	277.69	314.18	0.15
His*	33.44	30.95	26.95	26.97	0.28
Iso/Leu*	46.28	39.06	35.96	36.42	0.47
Lys*	46.49	33.36	27.22	34.37	0.35
Met*	12.94	11.83	11.35	11.36	0.23
Orn	18.91	17.26	14.41	15.97	0.66
Phe*	21.32	19.27	15.91	17.84	0.52
Pro	77.74	62.21	59.64	53.64	0.11
Ser	183.84	154.37	126.14	145.87	0.53
Tau	375.98	317.94	225.26	706.08	**0.09**
Thr*	31.25	30.27	27.42	26.56	0.78
Trp*	12.94	12.71	12.66	12.71	0.79
Tyr	23.54	19.94	17.02	18.69	0.34
Val	40.26	33.67	30.27	30.55	0.38
Total	3262.04	2781.83	2587.88	3046.56	0.23

*: Essential amino acids.

[abc]: Different superscripts in a column indicate significant difference between treatments ($P < 0.05$).

Table 4.9. Identification of OCO-induced changes in hepatic metabolites.

Ions	Modes of Ion detection	*m/z* of detection	Formula	Identity	Δppm	Database ID
I_L	$[M-H]^-$	498.2887	$C_{26}H_{45}NO_6S$	Taurodeoxycholic acid	-0.4	HMDB0000896
II_L	$[M+HQ]^+$	382.1027	$C_6H_{12}N_2O_4S_2$	Cysteine	5.2	HMDB0000574
III_L	$[M+HQ]^+$	291.1295	$C_5H_{11}NO_2S$	Methionine*	5.5	HMDB0000696
IV_L	$[M-H]^-$	133.0133	$C_4H_5O_5$	Malic acid	3	HMDB0000156
V_L	$[M-H]^-$	175.0235	$C_6H_8O_6$	Ascorbic acid*	-4.5	HMDB0000044
VI_L	$[M-DC]^+$	323.1055	$C_3H_7NO_2$	Alanine*	-3.4	HMDB0000161
VII_L	$[M-H]^-$	267.0727	$C_{10}H_{12}N_4O_5$	Inosine*	-0.07	HMDB0000195
$VIII_L$	$[M-H]^-$	306.0758	$C_{10}H_{17}N_3O_6S$	Glutathione*	-4.8	HMDB0000125
IX_L	$[M-H]^-$	346.0551	$C_{10}H_{14}N_5O_7P$	Adenosine monophosphate*	-0.6	HMDB0000045
X_L	$[M-H]^-$	611.1444	$C_{20}H_{32}N_6O_{12}S_2$	Oxidized glutathione*	0.7	HMDB0003337
XI_L	$[M-H]^+$	664.1164	$C_{21}H_{27}N_7O_{14}P_2$	NAD*	-0.07	HMDB0000902

*: confirmed by authentic standards.

Table 4.10. Identification of CCO-induced changes in hepatic lipidomes.

Ions	Modes of Ion detection	*m/z* of detection	Identity	Formula
I_{LL}	$[M+H]^+$	758.5693	PC(16:0/18:2)	$C_{42}H_{80}NO_8P$
II_{LL}	$[M+NH_4]^+$	896.7720	TAG(18:2/18:2/18:2)	$C_{57}H_{98}O_6$
III_{LL}	$[M+NH_4]^+$	898.7871	TAG(16:0/18:0/20:5)	$C_{57}H_{100}O_6$
IV_{LL}	$[M+H]^+$	784.5854	PC(18:1/18:2)	$C_{44}H_{82}NO_8P$
V_{LL}	$[M+H]^+$	782.5701	PC(16:0/20:4)	$C_{44}H_{80}NO_8P$
VI_{LL}	$[M+H]^+$	808.5856	PC(16:0/22:5)	$C_{46}H_{82}NO_8P$
VII_{LL}	$[M+H]^+$	788.6170	PC(18:0/18:1)	$C_{44}H_{86}NO_8P$
$VIII_{LL}$	$[M+HQ]^+$	398.3160	Palmitic acid (C16:0)	$C_{16}H_{32}O_2$
IX_{LL}	$[M+HQ]^+$	426.3477	Octadecanoic acid (18:0)	$C_{18}H_{36}O_2$
X_{LL}	$[M+H]^+$	760.5854	PC(16:0/18:1)	$C_{26}H_{54}NO_7P$
XI_{LL}	$[M+H]^+$	836.6184	PC(18:0/22:5)	$C_{48}H_{86}NO_8P$

Table 4.11. Concentrations of hepatic fatty acids.

	Liver (µg/g)				
	CCO	**3% OCO**	**6% OCO**	**9% OCO**	***p*-value**
C4:0	0.62[a]	0.40[b]	0.26[c]	0.16[c]	**< 0.01**
C6:0	0.02[a]	0.01[b]	0.01[b]	0.01[b]	**< 0.01**
C8:0	0.14[a]	0.08[b]	0.03[bc]	0.02[c]	**< 0.01**
C12:0	4.91	2.81	4.28	3.38	0.33
C16:0	174.93[a]	150.78[ab]	123.87[b]	96.46[c]	**< 0.01**
C16:1	0.05	0.06	0.03	0.04	0.54
C18:0	375.13[c]	508.11[a]	475.88[ab]	412.95[b]	**< 0.01**
C18:1	12.73	9.00	9.85	10.88	0.45
C18:2	999.01[a]	556.29[b]	595.01[bc]	466.17[c]	**< 0.01**
C20:0	0.80[b]	1.51[a]	0.89[ab]	0.87[ab]	**0.02**

[abc]: Different superscripts in a column indicate significant difference between treatments ($P < 0.05$).

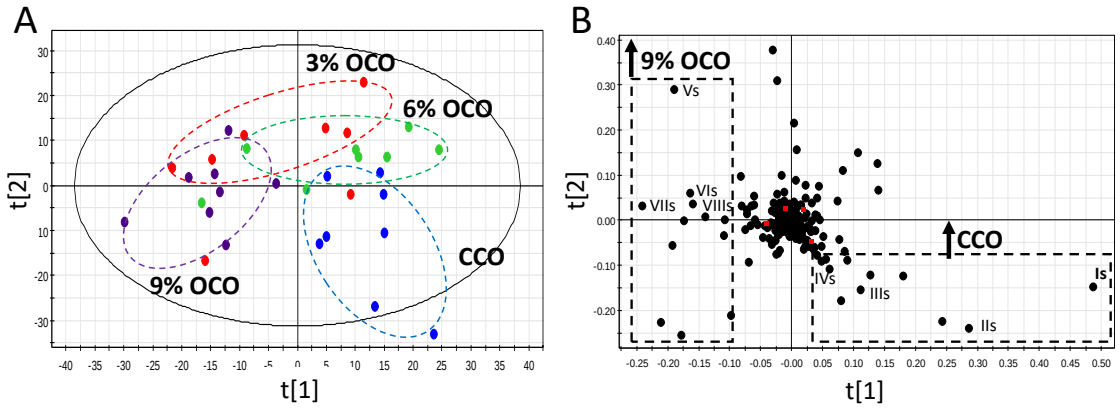

Figure 4.1 Profiling OCO-induced changes in serum amino acids. Serum amino-contained metabolites were conducted by LC-MS-based untargeted analysis and the data was processed by multivariate data analysis shown in the PLS-DA modeling. (A) Scores plot of the PLS-DA model on serum samples. (B) Loadings plot of the PLS-DA model on serum samples.

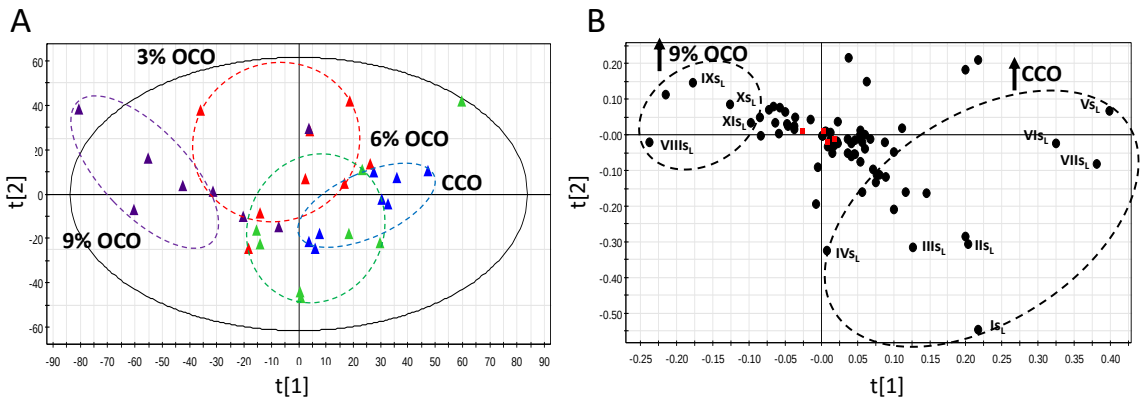

Figure 4.2 Influence of feeding OCO in serum lipidome. Serum lipidome was conducted by LC-MS-based untargeted analysis and the data was processed by multivariate data analysis shown in the PLS-DA modeling. (A) Scores plot of the PLS-DA model on serum lipidome. (B) Loadings plot of the PLS-DA model on serum lipidome.

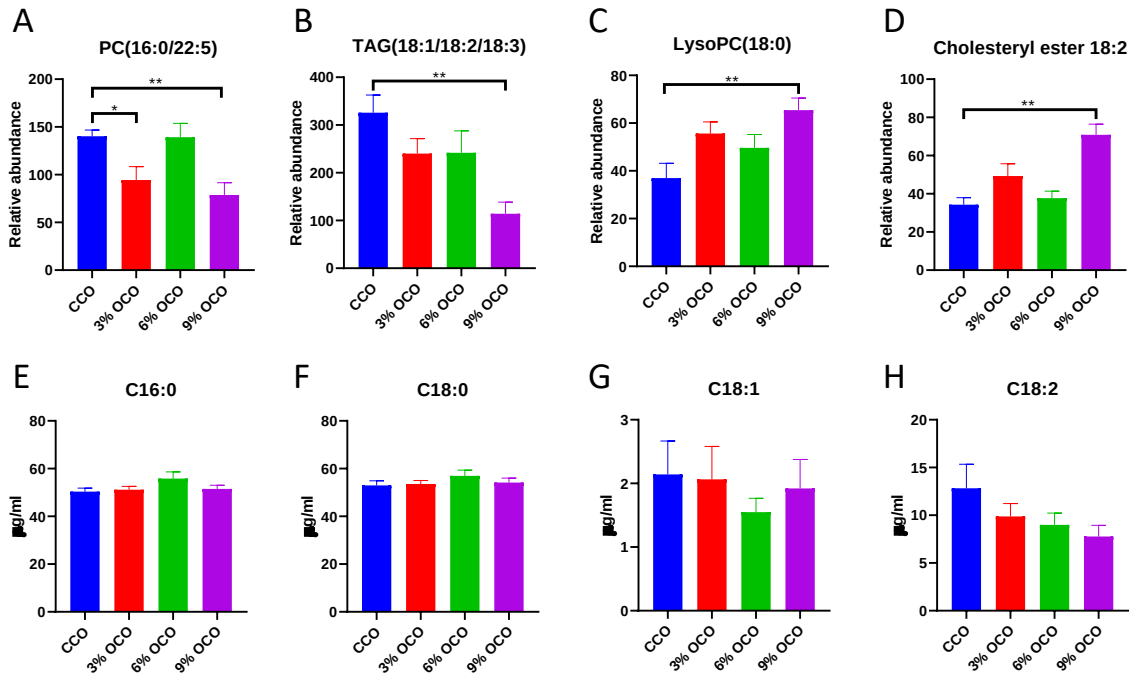

Figure 4.3 Individual lipid species in the serum. Major lipid species influenced by feeding OCO in multivariate modeling were identified. The relative abundance of major lipid species are expressed as the ratios between their ion counts and the total ion counts recorded by the MS detector. (A) PC(16:0/22:5). (B) TAG(18:1/18:2/18:3). (C) LysoPC(18:0). (D) Cholesteryl ester 18:2. Quantification of free fatty acids in the serum was conducted. (E) Concentration of C16:0. (F) Concentration of C18:0. (G) Concentration of C18:1. (H) Concentration of C18:2. Value = mean ± SEM (n = 8 pigs/group). The statistical difference between CCO and OCO treatments was labeled as * or ** to indicate $P < 0.05$ or $P < 0.01$ from one-way ANOVA followed by the Tukey post hoc test.

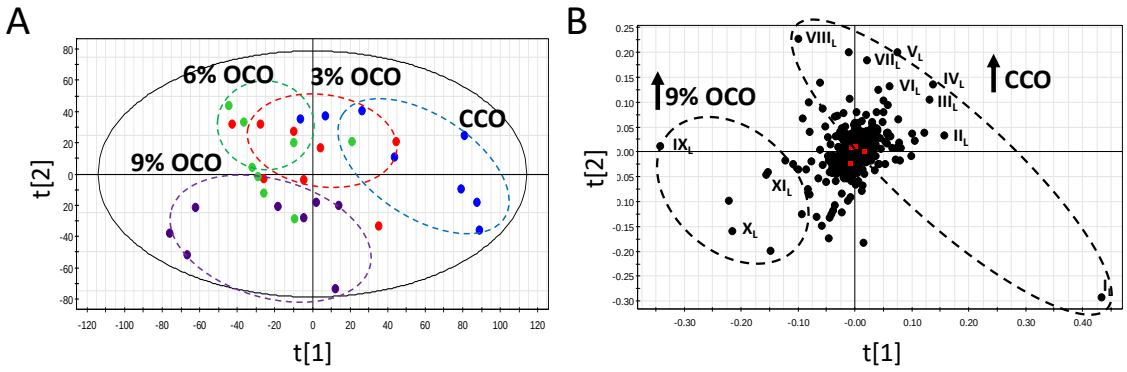

Figure 4.4 Influence of feeding OCO in hepatic metabolome. Hepatic metabolome was conducted by LC-MS-based untargeted analysis and the data was processed by multivariate data analysis shown in the PLS-DA modeling. (A) Scores plot of the PLS-DA model on liver samples. (B) Loadings plot of the PLS-DA model on liver samples.

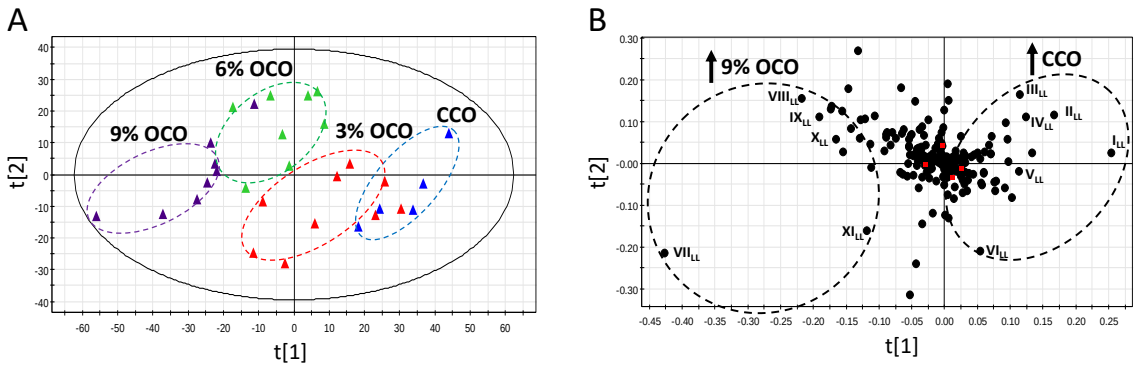

Figure 4.5 Influence of feeding OCO in hepatic lipidome. Hepatic metabolome was conducted by LC-MS-based untargeted analysis and the data was processed by multivariate data analysis shown in the PLS-DA modeling. (A) Scores plot of the PLS-DA model on liver lipidome. (B) Loadings plot of the PLS-DA model on liver lipidome.

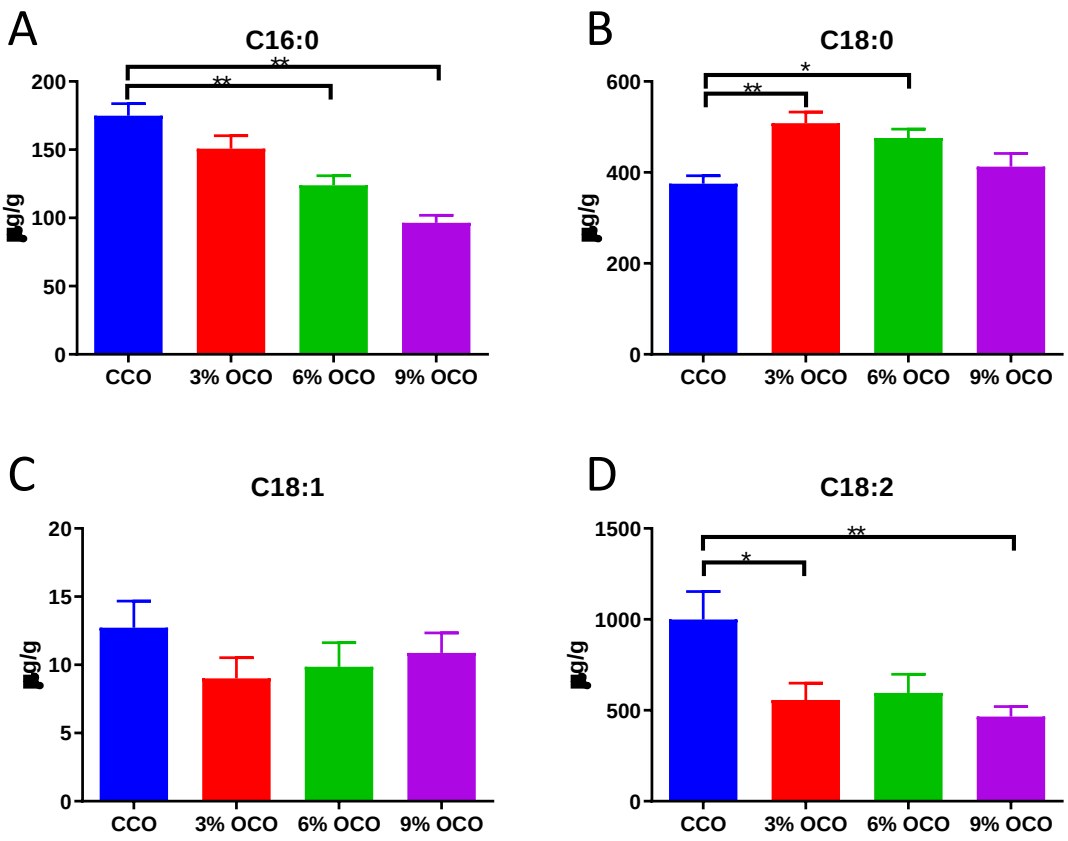

Figure 4.6 Concentrations of individual fatty acids in the liver. Major fatty acids in the liver were quantified. (A) Concentrations of C16:0. (B) Concentrations of C18:0. (C) Concentrations of C18:1. (D) Concentrations of C18:2. Value = mean ± SEM (n = 8 pigs/group). The statistical difference between CCO and OCO treatments was labeled as * or ** to indicate $P < 0.05$ or $P < 0.01$ from one-way ANOVA followed by the Tukey post hoc test.

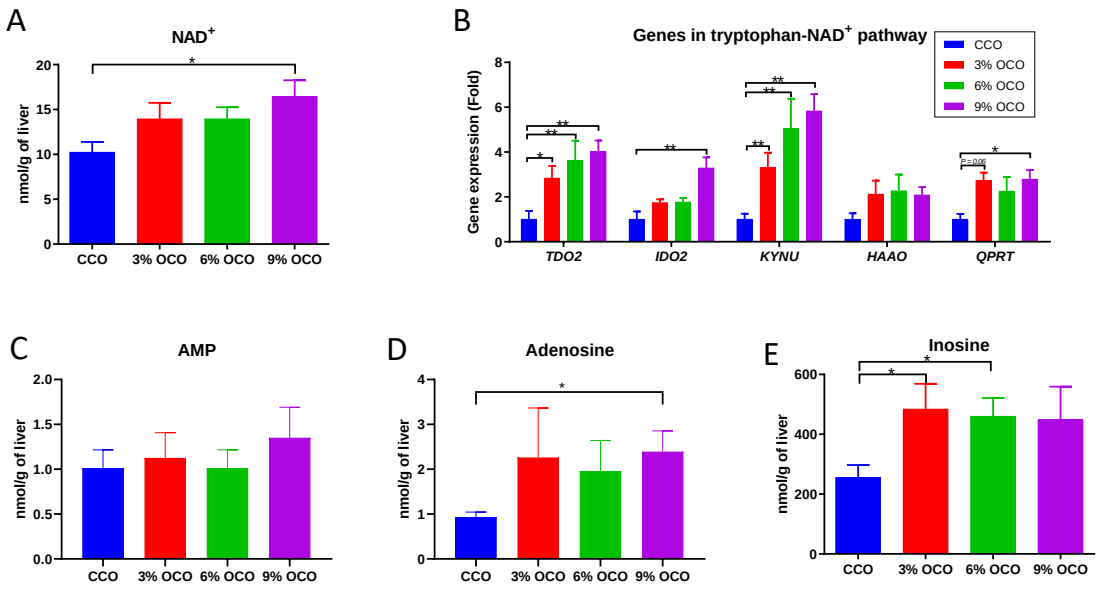

Figure 4.7 Effects of OCO on hepatic tryptophan-NAD$^+$ pathway. (A) Concentrations of hepatic NAD$^+$. (B) Hepatic gene expression level of enzymes in the tryptophan-NAD$^+$ pathway. The average expression level of genes in CCO samples is artificially set as 1. (C) Concentration of hepatic AMP. (D) Concentrations of hepatic adenosine. (E) Concentrations of hepatic Inosine in OCO and CCO treated pigs. Value = mean ± SEM (n = 8 pigs/group). The statistical difference between CCO and OCO treatments was labeled as * or ** to indicate $P < 0.05$ or $P < 0.01$ from one-way ANOVA followed by the Tukey post hoc test.

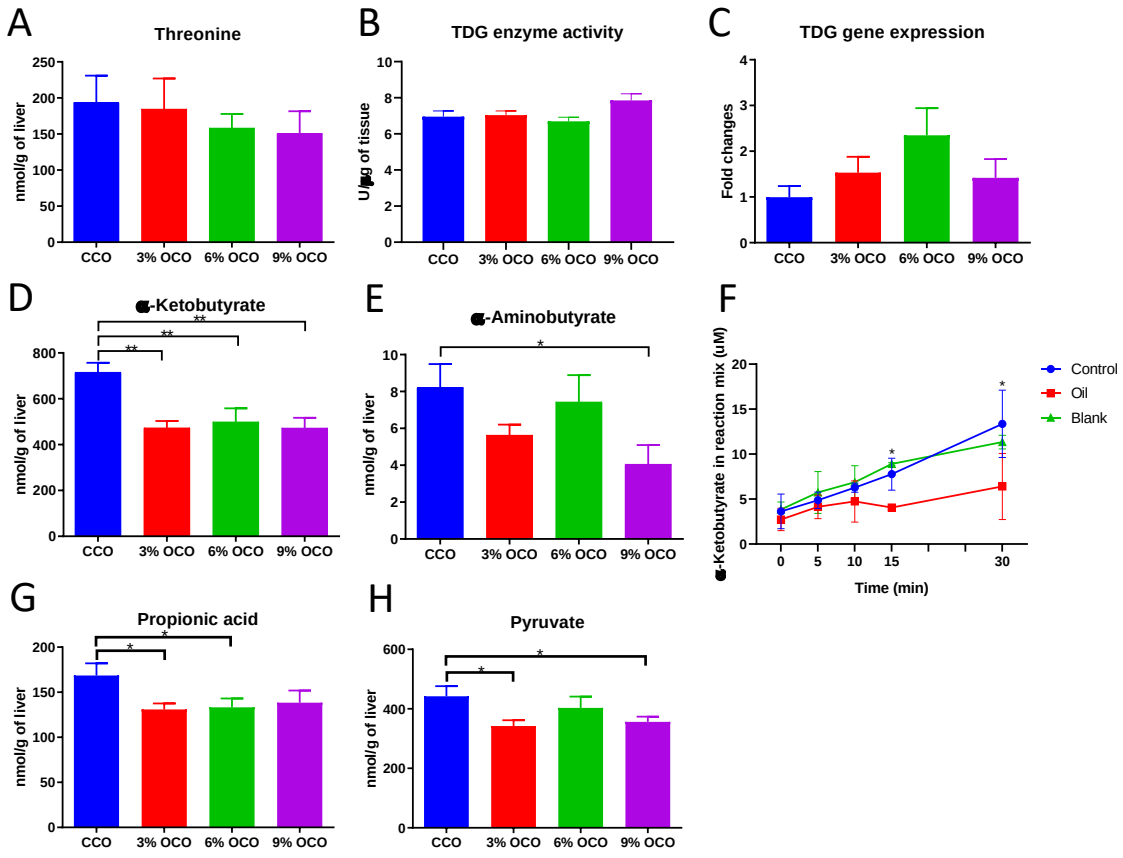

Figure 4.8 Effects of OCO on hepatic threonine catabolism. (A) Concentrations of hepatic threonine. (B) TDG enzyme activity. (C) Gene expression level of TDG. (D) Concentrations of hepatic α-ketobutyrate. (E) Concentrations of hepatic α-aminobutyrate. (F) α-ketobutyrate level after *in vitro* incubation of pig liver homogenate with or without polar phase of OCO, or extraction solution as blank control. Value = mean ± SEM. The statistical difference between CCO and OCO treatments was labeled as * or ** to indicate $P < 0.05$ or $P < 0.01$ from one-way ANOVA followed by the Tukey post hoc test.

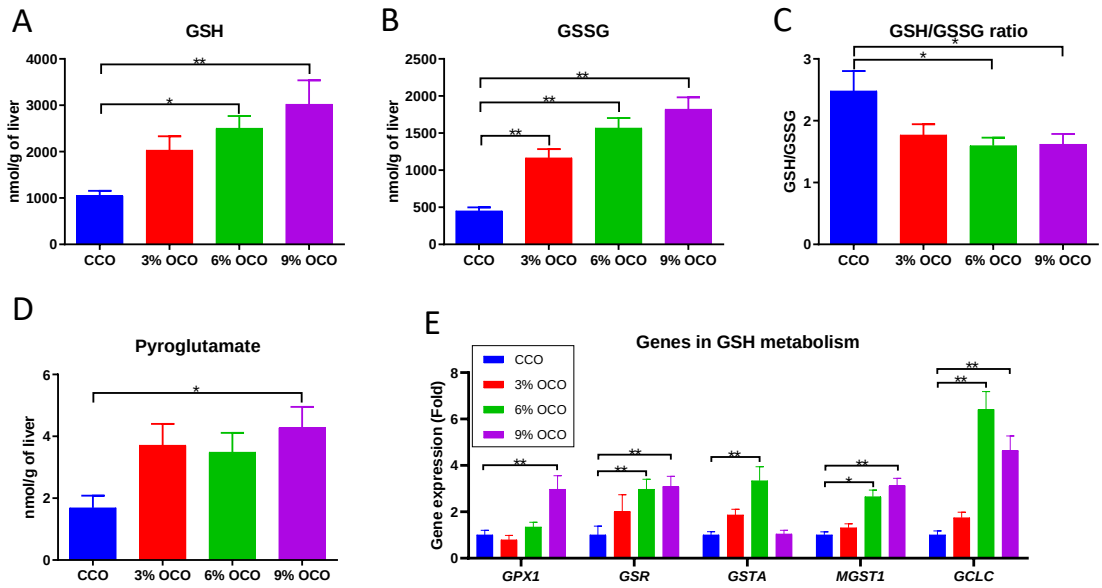

Figure 4.9 Effects of OCO on hepatic glutathione metabolism. (A) Gene expression level of enzymes in GSH metabolism. (B) Concentrations of GSH. (C) Concentrations of GSSG. (D) GSH to GSSG ratio. (E) Concentrations of pyroglutamate in OCO and CCO treated pigs. Value = mean ± SEM (n = 8 pigs/group). The statistical difference between CCO and OCO treatments was labeled as * or ** to indicate $P < 0.05$ or $P < 0.01$ from one-way ANOVA followed by the Tukey post hoc test.

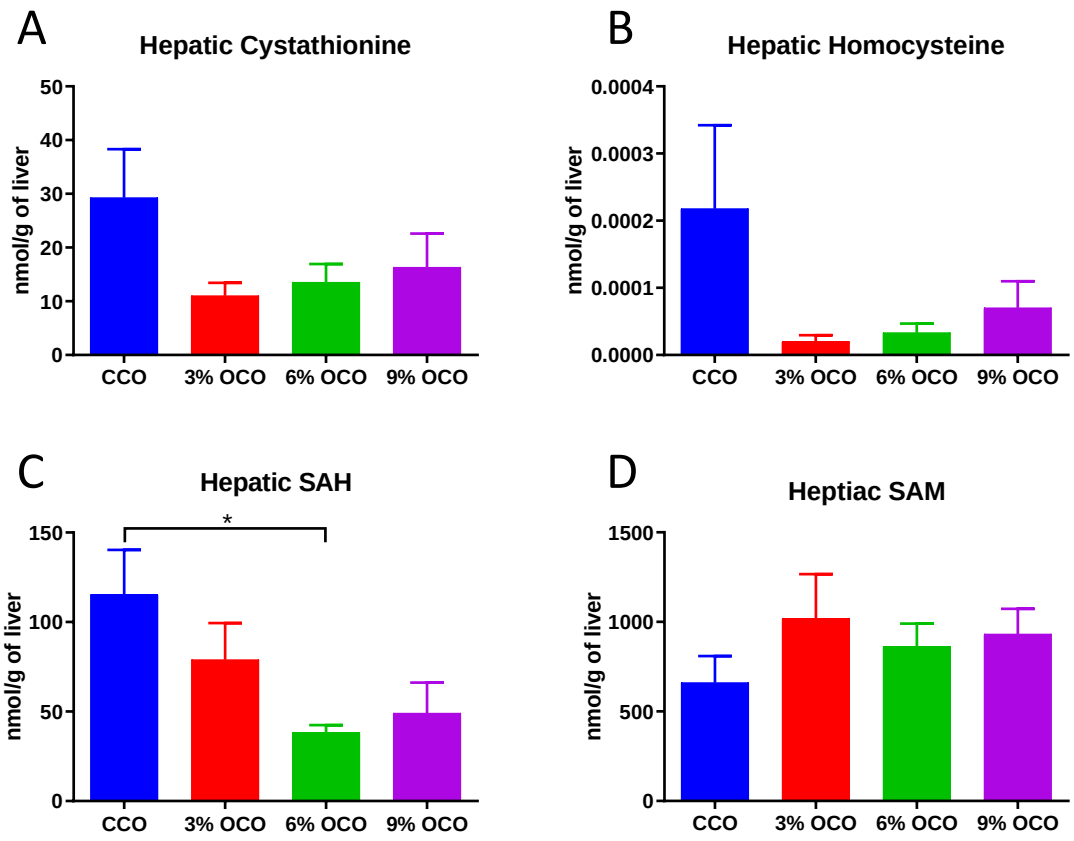

Figure 4.10 Effects of OCO on methyltransferase pathway. (A) Concentrations of cystathionine. (B) Concentrations of homocysteine. (C) Concentrations of SAH. (D) Concentrations of SAM in OCO and CCO treated pigs. Value = mean ± SEM (n = 8 pigs/group). The statistical difference between CCO and OCO treatments was labeled as * or ** to indicate $P < 0.05$ or $P < 0.01$ from one-way ANOVA followed by the Tukey post hoc test.

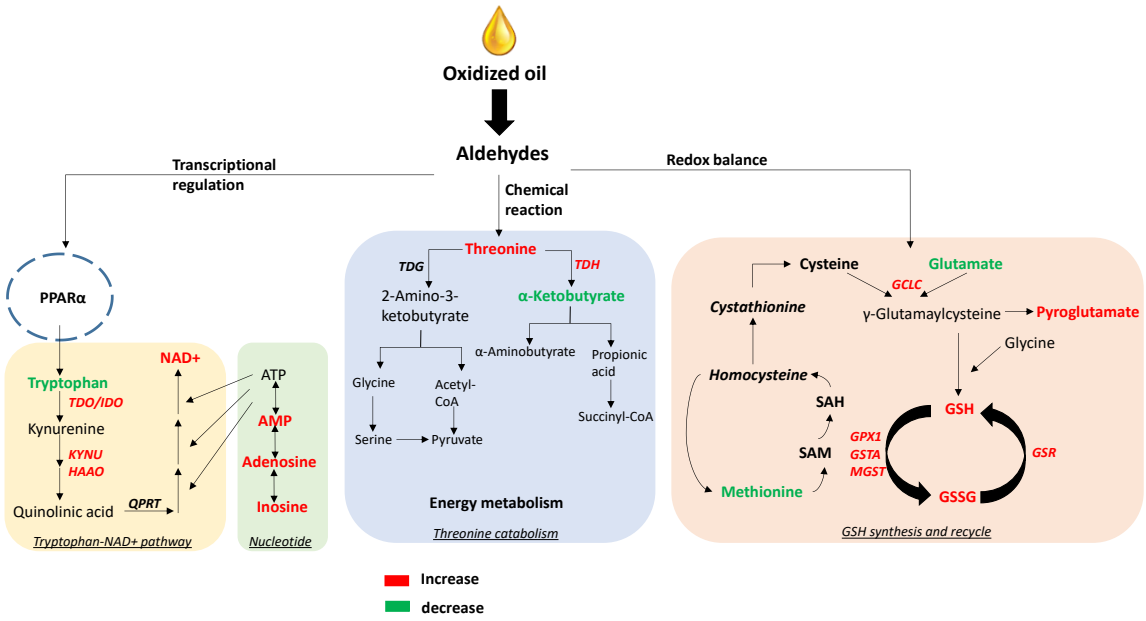

Figure 4.11 Summary of OCO-elicited metabolic changes in amino acid metabolism. Selective changes in blood tryptophan, threonine, glutamate, and glycine concentrations were good indicators for altered metabolism as responses to ingestion of oxidized lipids. Promoted tryptophan-NAD^+ synthesis pathway and GSH synthesis and recycling, inhibited threonine degradation were OCO-induced major metabolic events.

SUMMARY AND PERSPECTIVE

In our current studies, extensive metabolic changes in production animals were revealed by LC-MS-based metabolomics fingerprinting, which includes lipids, plant polyphenols, and amino acid metabolisms in various types of samples. Metabolomics fingerprinting allows us to detect the end-products of a complex biological system and decipher genetic selection and chemical exposure-induced interactions in production animals. Besides, rapid detection and quantification of thousands of metabolites in a tiny piece of biological sample help us to uncover a more complete picture of system-wide metabolism. Although metabolomics is widely used in biomedical, plant, and nutritional research, applications of metabolomics to assist with the phenotypic characterization of production animals are still limited.

Metabolomics is not only a key technique to directly assess economic traits in production animals, such as their growth performance, feed efficiency, and milk production, but it can further provide guidance on disease diagnosis, animal health assessment, animal production, characterization, and biomarker discovery. Therefore, a more complete description of phenotype in production animals can be achieved through metabolomics fingerprinting. Since the animal selection and breeding works in production animals require fast, effective, and quantitative phenotyping, metabolomics consents to these requirements with earlier, less invasively, and lower cost than other current techniques. In general, metabolomics fingerprinting is an effective approach and promising technique for evaluating the growth performance, health, and product quality of production animals.

REFERENCES

1. Alexandratos NaBJ. World agriculture to 2030/2050. In: Nations FaAOotU, ed. Vol 12-03. ESA Working Paper 2012:160 p.
2. Blayney DP. *The changing landscape of US milk production.* 2004.
3. United States Department of Agriculture E, Statistics and Market Information System. Milk Production - National Agricultural Statistics Service (NASS). 2021.
4. Cole JB, VanRaden PM. Symposium review: Possibilities in an age of genomics: The future of selection indices1. *Journal of dairy science*. 2018/04/01/ 2018;101(4):3686-3701.
5. Tokach MD, Goodband BD, O'Quinn TG. Performance-enhancing technologies in swine production. *Animal Frontiers.* 2016;6(4):15-21.
6. Losinger WC. Feed-conversion ratio of finisher pigs in the USA. *Preventive veterinary medicine.* Oct 9 1998;36(4):287-305.
7. Pierozan CR, Agostini PS, Gasa J, et al. Factors affecting the daily feed intake and feed conversion ratio of pigs in grow-finishing units: the case of a company. *Porcine Health Management.* 2016/03/01 2016;2(1):7.
8. United States Department of Agriculture E, Statistics and Market Information System. Poultry Production and Value - Final Estimates 2019.
9. Knowles TG, Kestin SC, Haslam SM, et al. Leg disorders in broiler chickens: prevalence, risk factors and prevention. *PLoS One.* Feb 6 2008;3(2):e1545.
10. Schmidt CJ, Persia ME, Feierstein E, Kingham B, Saylor WW. Comparison of a modern broiler line and a heritage line unselected since the 1950s. *Poultry science.* Dec 2009;88(12):2610-2619.
11. Council NC. U.S. Broliser Performance. 2011; http://www.nationalchickencouncil.org/about-the-industry/statistics/u-s-broiler-performance/. Accessed January 30, 2014.
12. Kidd MT, Anderson KE. Laying hens in the U.S. market: An appraisal of trends from the beginning of the 20th century to present1. *Journal of Applied Poultry Research.* 2019/12/01/ 2019;28(4):771-784.
13. Zaheer K. An Updated Review on Chicken Eggs: Production, Consumption, Management Aspects and Nutritional Benefits to Human Health. *Food and Nutrition Sciences.* 2015;Vol.06No.13:13.
14. Gerzilov V, Datková V, Mihaylova S, Bozakova N. EFFECT OF POULTRY HOUSING SYSTEMS ON EGG PRODUCTION. 2012.

15. Pelletier N, Ibarburu M, Xin H. Comparison of the environmental footprint of the egg industry in the United States in 1960 and 2010. *Poultry science.* 02/01 2014;93:241-255.
16. Jovel J, Dieleman LA, Kao D, Mason AL, Wine E. Chapter 10 - The Human Gut Microbiome in Health and Disease. In: Nagarajan M, ed. *Metagenomics*: Academic Press; 2018:197-213.
17. Turnbaugh PJ, Ley RE, Mahowald MA, Magrini V, Mardis ER, Gordon JI. An obesity-associated gut microbiome with increased capacity for energy harvest. *Nature.* Dec 21 2006;444(7122):1027-1031.
18. Wen L, Ley RE, Volchkov PY, et al. Innate immunity and intestinal microbiota in the development of Type 1 diabetes. *Nature.* Oct 23 2008;455(7216):1109-1113.
19. Frank DN, St Amand AL, Feldman RA, Boedeker EC, Harpaz N, Pace NR. Molecular-phylogenetic characterization of microbial community imbalances in human inflammatory bowel diseases. *Proceedings of the National Academy of Sciences of the United States of America.* Aug 21 2007;104(34):13780-13785.
20. Honda K, Littman DR. The microbiome in infectious disease and inflammation. *Annual review of immunology.* 2012;30:759-795.
21. Brulc JM, Antonopoulos DA, Miller MEB, et al. Gene-centric metagenomics of the fiber-adherent bovine rumen microbiome reveals forage specific glycoside hydrolases. *Proceedings of the National Academy of Sciences of the United States of America.* 2009;106(6):1948-1953.
22. Isaacson R, Kim HB. The intestinal microbiome of the pig. *Animal health research reviews.* Jun 2012;13(1):100-109.
23. Qu A, Brulc JM, Wilson MK, et al. Comparative metagenomics reveals host specific metavirulomes and horizontal gene transfer elements in the chicken cecum microbiome. *PLoS One.* Aug 13 2008;3(8):e2945.
24. Gonçalves P, Martel F. Butyrate and colorectal cancer: the role of butyrate transport. *Current drug metabolism.* Nov 2013;14(9):994-1008.
25. Donohoe DR, Garge N, Zhang X, et al. The microbiome and butyrate regulate energy metabolism and autophagy in the mammalian colon. *Cell metabolism.* May 4 2011;13(5):517-526.
26. Topping DL, Clifton PM. Short-chain fatty acids and human colonic function: roles of resistant starch and nonstarch polysaccharides. *Physiological reviews.* Jul 2001;81(3):1031-1064.

27. Puertollano E, Kolida S, Yaqoob P. Biological significance of short-chain fatty acid metabolism by the intestinal microbiome. *Current opinion in clinical nutrition and metabolic care.* Mar 2014;17(2):139-144.
28. Burkholder KM, Thompson KL, Einstein ME, Applegate TJ, Patterson JA. Influence of stressors on normal intestinal microbiota, intestinal morphology, and susceptibility to Salmonella enteritidis colonization in broilers. *Poultry science.* Sep 2008;87(9):1734-1741.
29. Schmidt B, Mulder IE, Musk CC, et al. Establishment of normal gut microbiota is compromised under excessive hygiene conditions. *PLoS One.* 2011;6(12):e28284.
30. Treyer A, Müsch A. Hepatocyte polarity. *Comprehensive Physiology.* Jan 2013;3(1):243-287.
31. Foroutan A, Guo AC, Vazquez-Fresno R, et al. Chemical Composition of Commercial Cow's Milk. *Journal of agricultural and food chemistry.* 2019/05/01 2019;67(17):4897-4914.
32. Miller GD, Jarvis JK, McBean LD. *Handbook of dairy foods and nutrition.* CRC press; 2006.
33. Devlin TM. Textbook of biochemistry: with clinical correlations. 2006.
34. Boulpaep EL, Boron WF, Caplan MJ, et al. Medical physiology: a cellular and molecular approach. 2009.
35. Devlin TM. *Textbook of biochemistry with clinical correlations.* John Wiley & Sons; 2010.
36. Vighi G, Marcucci F, Sensi L, Di Cara G, Frati F. Allergy and the gastrointestinal system. *Clin Exp Immunol.* 2008;153 Suppl 1(Suppl 1):3-6.
37. Celi P, Cowieson AJ, Fru-Nji F, Steinert RE, Kluenter AM, Verlhac V. Gastrointestinal functionality in animal nutrition and health: New opportunities for sustainable animal production. *Animal Feed Science and Technology.* 2017/12/01/ 2017;234:88-100.
38. Klasing KC. Nutritional modulation of resistance to infectious diseases. *Poultry science.* Aug 1998;77(8):1119-1125.
39. Chauhan SS, Celi P, Ponnampalam EN, Leury BJ, Liu F, Dunshea FR. Antioxidant Dynamics in the Live Animal and Implications for Ruminant Health and Product (Meat/Milk) Quality: Role of Vitamin E and Selenium. *Animal Production Science.* 2014;54:1525-1536.
40. Pluske JR. Feed- and feed additives-related aspects of gut health and development in weanling pigs. *Journal of Animal Science and Biotechnology.* 2013/01/07 2013;4(1):1.
41. Starkey JD. Triennial Growth Symposium--A role for vitamin D in skeletal muscle development and growth. *Journal of animal science.* Mar 2014;92(3):887-892.

42. Van Loo J. How chicory fructans contribute to zootechnical performance and well-being in livestock and companion animals. *J Nutr.* Nov 2007;137(11 Suppl):2594s-2597s.
43. Hoste H, Torres-Acosta JF, Sandoval-Castro CA, et al. Tannin containing legumes as a model for nutraceuticals against digestive parasites in livestock. *Veterinary parasitology.* Aug 15 2015;212(1-2):5-17.
44. Chauhan SS, Celi P, Fahri FT, Leury BJ, Dunshea FR. Dietary antioxidants at supranutritional doses modulate skeletal muscle heat shock protein and inflammatory gene expression in sheep exposed to heat stress. *Journal of animal science.* Nov 2014;92(11):4897-4908.
45. Yeoman CJ, White BA. Gastrointestinal tract microbiota and probiotics in production animals. *Annual review of animal biosciences.* Feb 2014;2:469-486.
46. de Lange CFM, Pluske J, Gong J, Nyachoti CM. Strategic use of feed ingredients and feed additives to stimulate gut health and development in young pigs. *Livestock Science.* 2010/09/01/ 2010;134(1):124-134.
47. McNeil NI. The contribution of the large intestine to energy supplies in man. *The American journal of clinical nutrition.* Feb 1984;39(2):338-342.
48. Flint HJ, Bayer EA. Plant cell wall breakdown by anaerobic microorganisms from the Mammalian digestive tract. *Annals of the New York Academy of Sciences.* Mar 2008;1125:280-288.
49. Kim HB, Borewicz K, White BA, et al. Longitudinal investigation of the age-related bacterial diversity in the feces of commercial pigs. *Veterinary microbiology.* Nov 21 2011;153(1-2):124-133.
50. Lamendella R, Domingo JW, Ghosh S, Martinson J, Oerther DB. Comparative fecal metagenomics unveils unique functional capacity of the swine gut. *BMC microbiology.* May 15 2011;11:103.
51. Panda AK, Rao SVR, Raju MVLN, Sunder GS. Effect of Butyric Acid on Performance, Gastrointestinal Tract Health and Carcass Characteristics in Broiler Chickens. *Asian-Australas J Anim Sci.* 7 2009;22(7):1026-1031.
52. Rossi R, Pastorelli G, Cannata S, Corino C. Recent advances in the use of fatty acids as supplements in pig diets: A review. *Animal Feed Science and Technology.* 2010/11/25/ 2010;162(1):1-11.
53. Alkhalf A, Alhaj M, Al-Homidan I. Influence of probiotic supplementation on blood parameters and growth performance in broiler chickens. *Saudi J Biol Sci.* 2010;17(3):219-225.

54. Kutlu HR, Forbes JM. Changes in growth and blood parameters in heat-stressed broiler chicks in response to dietary ascorbic acid. *Livestock Production Science.* 1993/11/01/ 1993;36(4):335-350.
55. Carrillo JA, Bai Y, He Y, et al. Growth curve, blood parameters and carcass traits of grass-fed Angus steers. *Animal : an international journal of animal bioscience.* 2021/11/01/ 2021;15(11):100381.
56. Hellwing ALF, Tauson A-H, Skrede A. Blood parameters in growing pigs fed increasing levels of bacterial protein meal. *Acta Vet Scand.* 2007;49(1):33-33.
57. Whitehead MW, Hawkes ND, Hainsworth I, Kingham JG. A prospective study of the causes of notably raised aspartate aminotransferase of liver origin. *Gut.* Jul 1999;45(1):129-133.
58. Nguyen P, Leray V, Diez M, et al. Liver lipid metabolism. *Journal of animal physiology and animal nutrition.* Jun 2008;92(3):272-283.
59. Wu G. Chapter 27 - Management of metabolic disorders (including metabolic diseases) in ruminant and nonruminant animals. In: Bazer FW, Lamb GC, Wu G, eds. *Animal Agriculture*: Academic Press; 2020:471-491.
60. Brew K, Vanaman TC, Hill RL. The role of alpha-lactalbumin and the A protein in lactose synthetase: a unique mechanism for the control of a biological reaction. *Proceedings of the National Academy of Sciences of the United States of America.* 1968;59(2):491-497.
61. Linzell JL. Mechanism of Secretion of the Aqueous Phase of Milk. *Journal of dairy science.* 1972/09/01/ 1972;55(9):1316-1322.
62. Davoodi SH, Shahbazi R, Esmaeili S, et al. Health-Related Aspects of Milk Proteins. *Iran J Pharm Res.* Summer 2016;15(3):573-591.
63. Newburg D, Neubauer S, Jensen R. Handbook of milk composition. *ed. Jensen RG, Academic Press, San Diego.* 1995:273-349.
64. Mather IH, Keenan TW. Origin and secretion of milk lipids. *Journal of mammary gland biology and neoplasia.* Jul 1998;3(3):259-273.
65. Hazel LN. THE GENETIC BASIS FOR CONSTRUCTING SELECTION INDEXES. *Genetics.* 1943;28(6):476-490.
66. Leal SM. Genetics and Analysis of Quantitative Traits. *Am J Hum Genet.* 2001;68(2):548-549.
67. Miglior F, Fleming A, Malchiodi F, Brito LF, Martin P, Baes CF. A 100-Year Review: Identification and genetic selection of economically important traits in dairy cattle. *Journal of dairy science.* Dec 2017;100(12):10251-10271.

68. Meluzzi A, Sirri F. Welfare of broiler chickens. *Italian Journal of Animal Science.* 2009/01/01 2009;8(sup1):161-173.
69. Paxton H, Anthony NB, Corr SA, Hutchinson JR. The effects of selective breeding on the architectural properties of the pelvic limb in broiler chickens: a comparative study across modern and ancestral populations. *J Anat.* 2010;217(2):153-166.
70. Jones DR, Anderson KE, Davis GS. The effects of genetic selection on production parameters of single comb White Leghorn hens. *Poultry science.* Aug 2001;80(8):1139-1143.
71. Knol EF, Nielsen B, Knap PW. Genomic selection in commercial pig breeding. *Animal Frontiers.* 2016;6(1):15-22.
72. Young CW. Review of Regional Project NC-2. *Journal of dairy science.* 1977/03/01/ 1977;60(3):493-498.
73. Cousillas-Boam G, Weber WJ, Benjamin A, et al. Effect of Holstein genotype on innate immune and metabolic responses of heifers to lipopolysaccharide (LPS) administration. *Domestic animal endocrinology.* 2019;70:106374.
74. Lippolis JD, Putz EJ, Reinhardt TA, Casas E, Weber WJ, Crooker BA. Effect of Holstein genotype on immune response to an intramammary Escherichia coli challenge. *Journal of dairy science.* Jun 2022;105(6):5435-5448.
75. Weber WJ, Wallace CR, Hansen LB, Chester-Jones H, Crooker BA. Effects of Genetic Selection for Milk Yield on Somatotropin, Insulin-Like Growth Factor-I, and Placental Lactogen in Holstein Cows. 2007;90(7):3314-3325.
76. Hansen LB. Consequences of selection for milk yield from a geneticist's viewpoint. *Journal of dairy science.* May 2000;83(5):1145-1150.
77. Ma L, Sonstegard TS, Cole JB, et al. Genome changes due to artificial selection in U.S. Holstein cattle. *BMC Genomics.* 2019/02/11 2019;20(1):128.
78. Mahoney CB, Hansen LB, Young CW, Marx GD, Reneau JK. Health care of Holsteins selected for large or small body size. *Journal of dairy science.* Dec 1986;69(12):3131-3139.
79. Rogers GW, Banos G, Sander-Nielsen U. Genetic Correlations Among Protein Yield, Productive Life, and Type Traits from the United States and Diseases Other than Mastitis from Denmark and Sweden. *Journal of dairy science.* 1999;82(6):1331-1338.
80. Lucy MC. Reproductive loss in high-producing dairy cattle: where will it end? *Journal of dairy science.* Jun 2001;84(6):1277-1293.
81. Oltenacu P, Broom D. The impact of genetic selection for increased milk yield on the welfare of dairy cows. *Animal Welfare.* 05/01 2010;19.

82. Dobson H, Smith R, Royal M, Knight C, Sheldon I. The high-producing dairy cow and its reproductive performance. *Reprod Domest Anim.* 2007;42 Suppl 2(Suppl 2):17-23.
83. Nebel RL, McGilliard ML. Interactions of high milk yield and reproductive performance in dairy cows. *Journal of dairy science.* Oct 1993;76(10):3257-3268.
84. Beerda B, Ouweltjes W, Sebek LB, Windig JJ, Veerkamp RF. Effects of genotype by environment interactions on milk yield, energy balance, and protein balance. *Journal of dairy science.* Jan 2007;90(1):219-228.
85. Grummer RR. Impact of changes in organic nutrient metabolism on feeding the transition dairy cow. *Journal of animal science.* Sep 1995;73(9):2820-2833.
86. Drackley JK. Biology of Dairy Cows During the Transition Period: the Final Frontier? *Journal of dairy science.* 1999;82(11):2259-2273.
87. Bell AW. Regulation of organic nutrient metabolism during transition from late pregnancy to early lactation. *Journal of animal science.* Sep 1995;73(9):2804-2819.
88. Bertoni G, Trevisi E, Lombardelli R. Some new aspects of nutrition, health conditions and fertility of intensively reared dairy cows. 2009;8(4):491.
89. Friggens NC, Ridder C, Lovendahl P. On the use of milk composition measures to predict the energy balance of dairy cows. *Journal of dairy science.* Dec 2007;90(12):5453-5467.
90. Xu C, Wang Z, Liu G, et al. Metabolic Characteristic of the Liver of Dairy Cows during Ketosis Based on Comparative Proteomics. *Asian-Australas J Anim Sci.* 7 2008;21(7):1003-1010.
91. Melendez P, Marin MP, Robles J, Rios C, Duchens M, Archbald L. Relationship between serum nonesterified fatty acids at calving and the incidence of periparturient diseases in Holstein dairy cows. *Theriogenology.* Oct 1 2009;72(6):826-833.
92. Ospina PA, Nydam DV, Stokol T, Overton TR. Evaluation of nonesterified fatty acids and beta-hydroxybutyrate in transition dairy cattle in the northeastern United States: Critical thresholds for prediction of clinical diseases. *Journal of dairy science.* Feb 2010;93(2):546-554.
93. Goff JP, Horst RL. Physiological Changes at Parturition and Their Relationship to Metabolic Disorders. *Journal of dairy science.* 1997;80(7):1260-1268.
94. Drackley JK, Dann HM, Douglas N, et al. Physiological and pathological adaptations in dairy cows that may increase susceptibility to periparturient diseases and disorders. *Italian Journal of Animal Science.* 2005/01/01 2005;4(4):323-344.
95. Tan B, Yin Y, Liu Z, et al. Dietary L-arginine supplementation increases muscle gain and reduces body fat mass in growing-finishing pigs. *Amino acids.* May 2009;37(1):169-175.

96. Kim SW, Wu G. Dietary arginine supplementation enhances the growth of milk-fed young pigs. *J Nutr.* Mar 2004;134(3):625-630.
97. Han Y-K, Thacker PA. Influence of Energy Level and Glycine Supplementation on Performance, Nutrient Digestibility and Egg Quality in Laying Hens. *Asian-australasian Journal of Animal Sciences.* 2011;24:1447-1455.
98. Mazinani M, Naserian AA, Rude BJ, Tahmasbi AM, Valizadeh R. Effects of feeding rumen-protected amino acids on the performance of feedlot calves. *J Adv Vet Anim Res.* 2020;7(2):229-233.
99. Sies H, Cadenas E. Oxidative stress: damage to intact cells and organs. *Philosophical transactions of the Royal Society of London. Series B, Biological sciences.* Dec 17 1985;311(1152):617-631.
100. Gutteridge JM. Lipid peroxidation and antioxidants as biomarkers of tissue damage. *Clinical Chemistry.* 1995;41(12):1819-1828.
101. Miyazawa T, Burdeos GC, Itaya M, Nakagawa K. Vitamin E: Regulatory Redox Interactions. Apr 2019;71(4):430-441.
102. Retsky KL, Freeman MW, Frei B. Ascorbic acid oxidation product(s) protect human low density lipoprotein against atherogenic modification. Anti- rather than prooxidant activity of vitamin C in the presence of transition metal ions. *The Journal of biological chemistry.* Jan 15 1993;268(2):1304-1309.
103. Moeini MM, Karami H, Mikaeili E. Effect of selenium and vitamin E supplementation during the late pregnancy on reproductive indices and milk production in heifers. *Animal reproduction science.* Aug 2009;114(1-3):109-114.
104. Lu T, Harper A, Dibner J, et al. Supplementing antioxidants to pigs fed diets high in oxidants: II. Effects on carcass characteristics, meat quality, and fatty acid profile. *Journal of animal science.* 11/03 2014;92.
105. Silva-Guillen YV, Arellano C, Boyd RD, Martinez G, van Heugten E. Growth performance, oxidative stress and immune status of newly weaned pigs fed peroxidized lipids with or without supplemental vitamin E or polyphenols. *Journal of Animal Science and Biotechnology.* 2020/03/05 2020;11(1):22.
106. Jiang W, Zhang L, Shan A. The effect of vitamin E on laying performance and egg quality in laying hens fed corn dried distillers grains with solubles. *Poultry science.* Nov 2013;92(11):2956-2964.

107. Muneendra K, Vinod K, Debashis R, Raju K, Shalini V. Application of herbal feed additives in animal nutrition - a review. *International Journal of Livestock Research.* 2014;4(9):1-8.
108. Erlund I. Review of the flavonoids quercetin, hesperetin, and naringenin. Dietary sources, bioactivities, bioavailability, and epidemiology. *Nutrition Research.* 2004/10/01/ 2004;24(10):851-874.
109. Stoldt AK, Derno M, Nürnberg G, et al. Effects of a 6-wk intraduodenal supplementation with quercetin on energy metabolism and indicators of liver damage in periparturient dairy cows. *Journal of dairy science.* Jul 2015;98(7):4509-4520.
110. Pettigrew JE, Jr., and R. L. Moser. Fat in swine nutrition. *Butterworth-Heinemann: Boston.* 1991:133-146.
111. NRA NRA. Survey Says: A snapshot of rendering *rendermagazine.* April 2011.
112. Seppanen CM, Saari Csallany A. Formation of 4-hydroxynonenal, a toxic aldehyde, in soybean oil at frying temperature. *Journal of the American Oil Chemists' Society.* 2002/10/01 2002;79(10):1033-1038.
113. Han IH, Csallany AS. Formation of Toxic α,β-Unsaturated 4-Hydroxy-Aldehydes in Thermally Oxidized Fatty Acid Methyl Esters. *Journal of the American Oil Chemists' Society.* 2009/03/01 2009;86(3):253-260.
114. Frankel EN. Lipid oxidation: Mechanisms, products and biological significance. *Journal of the American Oil Chemists' Society.* 1984/12/01 1984;61(12):1908-1917.
115. Zhang Q, Saleh AS, Chen J, Shen Q. Chemical alterations taken place during deep-fat frying based on certain reaction products: a review. *Chemistry and physics of lipids.* Sep 2012;165(6):662-681.
116. Chang SS, Peterson RJ, Ho C-T. Chemical reactions involved in the deep-fat frying of foods1. *Journal of the American Oil Chemists' Society.* 1978/10/01 1978;55(10):718-727.
117. Bergan JG, Draper HH. Absorption and metabolism of 1-14C-methyl linoleate hydroperoxide. *Lipids.* 1970/12/01 1970;5(12):976-982.
118. Kanazawa K, Kanazawa E, Natake M. Uptake of secondary autoxidation products of linoleic acid by the rat. *Lipids.* Jul 1985;20(7):412-419.
119. Porsgaard T, Zhang H, Nielsen RG, Høy C-E. Absorption in rats of rapeseed, soybean, and sunflower oils before and following moderate heating. *Lipids.* 1999/07/01 1999;34(7):727-732.

120. Hung YT, Hanson AR, Shurson GC, Urriola PE. Peroxidized lipids reduce growth performance of poultry and swine: A meta-analysis. *Animal Feed Science and Technology.* 2017/09/01/ 2017;231:47-58.
121. Hanson AR, Urriola PE, Wang L, Johnston LJ, Chen C, Shurson GC. Dietary peroxidized maize oil affects the growth performance and antioxidant status of nursery pigs. *Animal Feed Science and Technology.* 2016/06/01/ 2016;216:251-261.
122. Wang SY, Bottje W, Maynard P, Dibner J, Shermer W. Effect of Santoquin and oxidized fat on liver and intestinal glutathione in broilers. *Poultry science.* 1997;76(7):961-967.
123. Zhang W, Xiao S, Lee EJ, Ahn DU. Consumption of oxidized oil increases oxidative stress in broilers and affects the quality of breast meat. *Journal of agricultural and food chemistry.* Feb 9 2011;59(3):969-974.
124. Dibner JJ, Atwell CA, Kitchell ML, Shermer WD, Ivey FJ. Feeding of oxidized fats to broilers and swine: effects on enterocyte turnover, hepatocyte proliferation and the gut associated lymphoid tissue. *Animal Feed Science and Technology.* 1996/10/01/ 1996;62(1):1-13.
125. Sulzle A, Hirche F, Eder K. Thermally oxidized dietary fat upregulates the expression of target genes of PPAR alpha in rat liver. *J Nutr.* Jun 2004;134(6):1375-1383.
126. Koch A, Konig B, Spielmann J, Leitner A, Stangl GI, Eder K. Thermally oxidized oil increases the expression of insulin-induced genes and inhibits activation of sterol regulatory element-binding protein-2 in rat liver. *J Nutr.* Sep 2007;137(9):2018-2023.
127. Ashida H, Kanazawa K, Minamoto S, Danno G, Natake M. Effect of orally administered secondary autoxidation products of linoleic acid on carbohydrate metabolism in rat liver. *Archives of biochemistry and biophysics.* Nov 15 1987;259(1):114-123.
128. Wang L, Yao D, Urriola PE, et al. Identification of activation of tryptophan-NAD(+) pathway as a prominent metabolic response to thermally oxidized oil through metabolomics-guided biochemical analysis. *The Journal of nutritional biochemistry.* Jul 2018;57:255-267.
129. Loudon KMW, Tarr G, Pethick DW, et al. The Use of Biochemical Measurements to Identify Pre-Slaughter Stress in Pasture Finished Beef Cattle. *Animals (Basel).* 2019;9(8):503.
130. Gracie S, Pennell C, Ekman-Ordeberg G, et al. An integrated systems biology approach to the study of preterm birth using "-omic" technology - a guideline for research. *BMC Pregnancy and Childbirth.* 2011/10/12 2011;11(1):71.

131. Patti GJ, Yanes O, Siuzdak G. Innovation: Metabolomics: the apogee of the omics trilogy. *Nature reviews. Molecular cell biology.* Mar 22 2012;13(4):263-269.
132. Fiehn O. Metabolomics--the link between genotypes and phenotypes. *Plant molecular biology.* Jan 2002;48(1-2):155-171.
133. Ioannidis JP, Khoury MJ. Improving validation practices in "omics" research. *Science (New York, N.Y.).* Dec 2 2011;334(6060):1230-1232.
134. Fitzpatrick AM, Park Y, Brown LA, Jones DP. Children with severe asthma have unique oxidative stress-associated metabolomic profiles. *The Journal of allergy and clinical immunology.* Jan 2014;133(1):258-261.e251-258.
135. Barderas MG, Laborde CM, Posada M, et al. Metabolomic Profiling for Identification of Novel Potential Biomarkers in Cardiovascular Diseases. *Journal of Biomedicine and Biotechnology.* 2011/01/02 2011;2011:790132.
136. Wang X, Yang B, Sun H, Zhang A. Pattern recognition approaches and computational systems tools for ultra performance liquid chromatography-mass spectrometry-based comprehensive metabolomic profiling and pathways analysis of biological data sets. *Analytical chemistry.* Jan 3 2012;84(1):428-439.
137. Turi KN, Romick-Rosendale L, Ryckman KK, Hartert TV. A review of metabolomics approaches and their application in identifying causal pathways of childhood asthma. *The Journal of allergy and clinical immunology.* 2018;141(4):1191-1201.
138. Beckonert O, Keun HC, Ebbels TM, et al. Metabolic profiling, metabolomic and metabonomic procedures for NMR spectroscopy of urine, plasma, serum and tissue extracts. *Nature protocols.* 2007;2(11):2692-2703.
139. Alonso A, Marsal S, Julià A. Analytical methods in untargeted metabolomics: state of the art in 2015. *Frontiers in bioengineering and biotechnology.* 2015;3:23.
140. Veenstra TD. Metabolomics: the final frontier? *Genome medicine.* Apr 30 2012;4(4):40.
141. Zhang A, Sun H, Wang P, Han Y, Wang X. Modern analytical techniques in metabolomics analysis. *The Analyst.* Jan 21 2012;137(2):293-300.
142. Trygg J, Holmes E, Lundstedt T. Chemometrics in metabonomics. *Journal of proteome research.* Feb 2007;6(2):469-479.
143. Goldansaz SA, Guo AC, Sajed T, Steele MA, Plastow GS, Wishart DS. Livestock metabolomics and the livestock metabolome: A systematic review. *PLOS ONE.* 2017;12(5):e0177675.
144. Wishart DS. Metabolomics: applications to food science and nutrition research. *Trends in food science & technology.* 2008;19(9):482-493.

145. Jalali A, Hatamie A, Saferpour T, Khajeamiri A, Safa T, Buazar F. Impact of Pharmaceutical Impurities in Ecstasy Tablets: Gas Chromatography-Mass Spectrometry Study. *Iran J Pharm Res.* Winter 2016;15(1):221-229.
146. Karisa B, Thomson J, Wang Z, et al. Plasma metabolites associated with residual feed intake and other productivity performance traits in beef cattle. *Livestock Science.* 2014;165:200-211.
147. Melzer N, Wittenburg D, Hartwig S, et al. Investigating associations between milk metabolite profiles and milk traits of Holstein cows. *Journal of dairy science.* Mar 2013;96(3):1521-1534.
148. Abarghuei MJ, Rouzbehan Y, Salem A, Zamiri MJ. Nitrogen balance, blood metabolites and milk fatty acid composition of dairy cows fed pomegranate-peel extract. *Livestock Science.* 2014;164:72-80.
149. LeBlanc SJ, Leslie KE, Duffield TF. Metabolic predictors of displaced abomasum in dairy cattle. *Journal of dairy science.* Jan 2005;88(1):159-170.
150. Chapinal N, Carson ME, LeBlanc SJ, et al. The association of serum metabolites in the transition period with milk production and early-lactation reproductive performance. *Journal of dairy science.* Mar 2012;95(3):1301-1309.
151. Merrifield CA, Lewis M, Claus SP, et al. A metabolic system-wide characterisation of the pig: a model for human physiology. *Molecular bioSystems.* Sep 2011;7(9):2577-2588.
152. Brito LF, Bedere N, Douhard F, et al. Review: Genetic selection of high-yielding dairy cattle toward sustainable farming systems in a rapidly changing world. *Animal : an international journal of animal bioscience.* 2021/12/01/ 2021;15:100292.
153. Bobe G, Young JW, Beitz DC. Invited Review: Pathology, Etiology, Prevention, and Treatment of Fatty Liver in Dairy Cows. *Journal of dairy science.* 2004;87(10):3105-3124.
154. Jorritsma R, Jorritsma H, Schukken YH, Bartlett PC, Wensing T, Wentink GH. Prevalence and indicators of post partum fatty infiltration of the liver in nine commercial dairy herds in The Netherlands. *Livestock Production Science.* 2001/02/01/ 2001;68(1):53-60.
155. Grummer RR. Nutritional and management strategies for the prevention of fatty liver in dairy cattle. *Veterinary journal (London, England : 1997).* Apr 2008;176(1):10-20.
156. Gan L, Xiang W, Xie B, Yu L. Molecular mechanisms of fatty liver in obesity. 2015;9(3):275-287.
157. Carriquiry M, Weber WJ, Dahlen CR, Lamb GC, Baumgard LH, Crooker BA. Production response of multiparous Holstein cows treated with bovine somatotropin and fed diets enriched with n-3 or n-6 fatty acids. *Journal of dairy science.* Oct 2009;92(10):4852-4864.

158. Bligh EG, Dyer WJ. A RAPID METHOD OF TOTAL LIPID EXTRACTION AND PURIFICATION. *Canadian Journal of Biochemistry and Physiology.* 1959/08/01 1959;37(8):911-917.
159. Kim D, Langmead B, Salzberg SL. HISAT: a fast spliced aligner with low memory requirements. Apr 2015;12(4):357-360.
160. Li H, Handsaker B, Wysoker A, et al. The Sequence Alignment/Map format and SAMtools. *Bioinformatics.* 2009;25(16):2078-2079.
161. Bray NL, Pimentel H, Melsted P, Pachter L. Near-optimal probabilistic RNA-seq quantification. *Nature Biotechnology.* 2016/05/01 2016;34(5):525-527.
162. Imhasly S, Naegeli H, Baumann S, et al. Metabolomic biomarkers correlating with hepatic lipidosis in dairy cows. *BMC veterinary research.* Jun 2 2014;10:122.
163. Mann JP, Furse S, Snowden SG, et al. Plasma lipidomics distinguishes NASH and fibrosis from simple fatty liver in children. *medRxiv.* 2020:2020.2004.2018.20070417.
164. Chocian G, Chabowski A, Zendzian-Piotrowska M, Harasim E, Łukaszuk B, Górski J. High fat diet induces ceramide and sphingomyelin formation in rat's liver nuclei. *Molecular and cellular biochemistry.* Jul 2010;340(1-2):125-131.
165. Law S-H, Chan M-L, Marathe GK, Parveen F, Chen C-H, Ke L-Y. An Updated Review of Lysophosphatidylcholine Metabolism in Human Diseases. *Int J Mol Sci.* 2019;20(5):1149.
166. Agren JJ, Kurvinen JP, Kuksis A. Isolation of very low density lipoprotein phospholipids enriched in ethanolamine phospholipids from rats injected with Triton WR 1339. *Biochimica et biophysica acta.* May 1 2005;1734(1):34-43.
167. Yao ZM, Vance DE. The active synthesis of phosphatidylcholine is required for very low density lipoprotein secretion from rat hepatocytes. *The Journal of biological chemistry.* Feb 25 1988;263(6):2998-3004.
168. Verkade HJ, Fast DG, Rusinol AE, Scraba DG, Vance DE. Impaired biosynthesis of phosphatidylcholine causes a decrease in the number of very low density lipoprotein particles in the Golgi but not in the endoplasmic reticulum of rat liver. *The Journal of biological chemistry.* Nov 25 1993;268(33):24990-24996.
169. Fast DG, Vance DE. Nascent VLDL phospholipid composition is altered when phosphatidylcholine biosynthesis is inhibited: evidence for a novel mechanism that regulates VLDL secretion. *Biochimica et biophysica acta.* Sep 14 1995;1258(2):159-168.
170. Vance DE. Physiological roles of phosphatidylethanolamine N-methyltransferase. *Biochimica et biophysica acta.* Mar 2013;1831(3):626-632.

171. Henneberry AL, McMaster CR. Cloning and expression of a human choline/ethanolaminephosphotransferase: synthesis of phosphatidylcholine and phosphatidylethanolamine. *The Biochemical journal.* Apr 15 1999;339 (Pt 2):291-298.
172. Henneberry AL, Wistow G, McMaster CR. Cloning, genomic organization, and characterization of a human cholinephosphotransferase. *The Journal of biological chemistry.* Sep 22 2000;275(38):29808-29815.
173. Aoyama C, Ohtani A, Ishidate K. Expression and characterization of the active molecular forms of choline/ethanolamine kinase-alpha and -beta in mouse tissues, including carbon tetrachloride-induced liver. *The Biochemical journal.* May 1 2002;363(Pt 3):777-784.
174. Ridgway ND, Lagace TA. Regulation of the CDP-choline pathway by sterol regulatory element binding proteins involves transcriptional and post-transcriptional mechanisms. *The Biochemical journal.* 2003;372(Pt 3):811-819.
175. Chatterjee D, Mukherjee S, Das SK. Regulation of cholinephosphotransferase by thyroid hormone. *Biochemical and biophysical research communications.* Apr 13 2001;282(4):861-864.
176. Zeisel SH, da Costa K-A. Choline: an essential nutrient for public health. *Nutr Rev.* 2009;67(11):615-623.
177. Sivanesan S, Taylor A, Zhang J, Bakovic M. Betaine and Choline Improve Lipid Homeostasis in Obesity by Participation in Mitochondrial Oxidative Demethylation. *Frontiers in Nutrition.* 2018-July-10 2018;5(61).
178. Reo NV, Adinehzadeh M, Foy BD. Kinetic analyses of liver phosphatidylcholine and phosphatidylethanolamine biosynthesis using (13)C NMR spectroscopy. *Biochimica et biophysica acta.* Feb 28 2002;1580(2-3):171-188.
179. Sundler R, Akesson B. Regulation of phospholipid biosynthesis in isolated rat hepatocytes. Effect of different substrates. *The Journal of biological chemistry.* May 10 1975;250(9):3359-3367.
180. Mason TM. The Role of Factors that Regulate the Synthesis and Secretion of Very-Low-Density Lipoprotein by Hepatocytes. *Critical Reviews in Clinical Laboratory Sciences.* 1998/01/01 1998;35(6):461-487.
181. Bernabucci U, Ronchi B, Basirico L, et al. Abundance of mRNA of apolipoprotein b100, apolipoprotein e, and microsomal triglyceride transfer protein in liver from periparturient dairy cows. *Journal of dairy science.* Sep 2004;87(9):2881-2888.
182. Sundaram M, Yao Z. Recent progress in understanding protein and lipid factors affecting hepatic VLDL assembly and secretion. *Nutr Metab (Lond).* Apr 27 2010;7:35.

183. Go G-W, Mani A. Low-density lipoprotein receptor (LDLR) family orchestrates cholesterol homeostasis. *Yale J Biol Med.* 2012;85(1):19-28.
184. Magnusson B, Asp L, Boström P, et al. Adipocyte differentiation-related protein promotes fatty acid storage in cytosolic triglycerides and inhibits secretion of very low-density lipoproteins. *Arteriosclerosis, thrombosis, and vascular biology.* Jul 2006;26(7):1566-1571.
185. Katoh N. Relevance of apolipoproteins in the development of fatty liver and fatty liver-related peripartum diseases in dairy cows. *The Journal of veterinary medical science.* Apr 2002;64(4):293-307.
186. Liu L, Li X, Li Y, et al. Effects of nonesterified fatty acids on the synthesis and assembly of very low density lipoprotein in bovine hepatocytes in vitro. *Journal of dairy science.* 2014/03/01/ 2014;97(3):1328-1335.
187. Kersten S, Stienstra R. The role and regulation of the peroxisome proliferator activated receptor alpha in human liver. *Biochimie.* 2017/05/01/ 2017;136:75-84.
188. Grabacka M, Pierzchalska M, Dean M, Reiss K. Regulation of Ketone Body Metabolism and the Role of PPARα. *Int J Mol Sci.* 2016;17(12):2093.
189. Porstmann T, Griffiths B, Chung YL, et al. PKB/Akt induces transcription of enzymes involved in cholesterol and fatty acid biosynthesis via activation of SREBP. *Oncogene.* Sep 29 2005;24(43):6465-6481.
190. Shimomura I, Bashmakov Y, Ikemoto S, Horton JD, Brown MS, Goldstein JL. Insulin selectively increases SREBP-1c mRNA in the livers of rats with streptozotocin-induced diabetes. *Proceedings of the National Academy of Sciences of the United States of America.* 1999;96(24):13656-13661.
191. Du X, Shen T, Wang H, et al. Adaptations of hepatic lipid metabolism and mitochondria in dairy cows with mild fatty liver. *Journal of dairy science.* 2018/10/01/ 2018;101(10):9544-9558.
192. Zhu Y, Liu G, Du X, et al. Expression patterns of hepatic genes involved in lipid metabolism in cows with subclinical or clinical ketosis. *Journal of dairy science.* 2019/02/01/ 2019;102(2):1725-1735.
193. Browning JD, Horton JD. Molecular mediators of hepatic steatosis and liver injury. *The Journal of clinical investigation.* Jul 2004;114(2):147-152.
194. Corbin KD, Zeisel SH. Choline metabolism provides novel insights into nonalcoholic fatty liver disease and its progression. *Current opinion in gastroenterology.* 2012;28(2):159-165.

195. Buchman AL. The addition of choline to parenteral nutrition. *Gastroenterology.* Nov 2009;137(5 Suppl):S119-128.

196. Johnson AR, Craciunescu CN, Guo Z, et al. Deletion of murine choline dehydrogenase results in diminished sperm motility. *FASEB journal : official publication of the Federation of American Societies for Experimental Biology.* Aug 2010;24(8):2752-2761.

197. Teng YW, Mehedint MG, Garrow TA, Zeisel SH. Deletion of betaine-homocysteine S-methyltransferase in mice perturbs choline and 1-carbon metabolism, resulting in fatty liver and hepatocellular carcinomas. *The Journal of biological chemistry.* Oct 21 2011;286(42):36258-36267.

198. Zom RL, van Baal J, Goselink RM, Bakker JA, de Veth MJ, van Vuuren AM. Effect of rumen-protected choline on performance, blood metabolites, and hepatic triacylglycerols of periparturient dairy cattle. *Journal of dairy science.* Aug 2011;94(8):4016-4027.

199. Goselink RM, van Baal J, Widjaja HC, et al. Effect of rumen-protected choline supplementation on liver and adipose gene expression during the transition period in dairy cattle. *Journal of dairy science.* Feb 2013;96(2):1102-1116.

200. Chandler TL, White HM. Choline and methionine differentially alter methyl carbon metabolism in bovine neonatal hepatocytes. *PloS one.* 2017;12(2):e0171080-e0171080.

201. Hartwell JR, Cecava MJ, Donkin SS. Impact of dietary rumen undegradable protein and rumen-protected choline on intake, peripartum liver triacylglyceride, plasma metabolites and milk production in transition dairy cows. *Journal of dairy science.* Dec 2000;83(12):2907-2917.

202. Piepenbrink MS, Overton TR. Liver metabolism and production of cows fed increasing amounts of rumen-protected choline during the periparturient period. *Journal of dairy science.* May 2003;86(5):1722-1733.

203. Zahra LC, Duffield TF, Leslie KE, Overton TR, Putnam D, LeBlanc SJ. Effects of rumen-protected choline and monensin on milk production and metabolism of periparturient dairy cows. *Journal of dairy science.* Dec 2006;89(12):4808-4818.

204. Panche AN, Diwan AD, Chandra SR. Flavonoids: an overview. *Journal of nutritional science.* 2016;5:e47.

205. Middleton E, Jr., Kandaswami C, Theoharides TC. The effects of plant flavonoids on mammalian cells: implications for inflammation, heart disease, and cancer. *Pharmacological reviews.* Dec 2000;52(4):673-751.

206. Cui K, Guo XD, Tu Y, Zhang NF, Ma T, Diao QY. Effect of dietary supplementation of rutin on lactation performance, ruminal fermentation and metabolism in dairy cows. *Journal of animal physiology and animal nutrition.* Dec 2015;99(6):1065-1073.

207. Gruse J, Görs S, Tuchscherer A, et al. The Effects of Oral Quercetin Supplementation on Splanchnic Glucose Metabolism in 1-Week-Old Calves Depend on Diet after Birth. *The Journal of Nutrition.* 2015;145(11):2486-2495.

208. Oskoueian E, Abdullah N, Oskoueian A. Effects of Flavonoids on Rumen Fermentation Activity, Methane Production, and Microbial Population. *BioMed Research International.* 2013/09/24 2013;2013:349129.

209. Maciej J, Schäff CT, Kanitz E, et al. Short communication: Effects of oral flavonoid supplementation on the metabolic and antioxidative status of newborn dairy calves. *Journal of dairy science.* Jan 2016;99(1):805-811.

210. Gohlke A, Ingelmann CJ, Nürnberg G, et al. Influence of 4-week intraduodenal supplementation of quercetin on performance, glucose metabolism, and mRNA abundance of genes related to glucose metabolism and antioxidative status in dairy cows. *Journal of dairy science.* 2013;96(11):6986-7000.

211. Lee KM, Hwang MK, Lee DE, Lee KW, Lee HJ. Protective Effect of Quercetin against Arsenite-Induced COX-2 Expression by Targeting PI3K in Rat Liver Epithelial Cells. *Journal of agricultural and food chemistry.* 2010/05/12 2010;58(9):5815-5820.

212. Endale M, Park SC, Kim S, et al. Quercetin disrupts tyrosine-phosphorylated phosphatidylinositol 3-kinase and myeloid differentiation factor-88 association, and inhibits MAPK/AP-1 and IKK/NF-κB-induced inflammatory mediators production in RAW 264.7 cells. *Immunobiology.* Dec 2013;218(12):1452-1467.

213. Muthian G, Bright JJ. Quercetin, a flavonoid phytoestrogen, ameliorates experimental allergic encephalomyelitis by blocking IL-12 signaling through JAK-STAT pathway in T lymphocyte. *Journal of clinical immunology.* Sep 2004;24(5):542-552.

214. Zhang M, Swarts SG, Yin L, et al. Antioxidant properties of quercetin. *Advances in experimental medicine and biology.* 2011;701:283-289.

215. Xu D, Hu M-J, Wang Y-Q, Cui Y-L. Antioxidant Activities of Quercetin and Its Complexes for Medicinal Application. *Molecules.* 2019;24(6):1123.

216. Ader P, Wessmann A, Wolffram S. Bioavailability and metabolism of the flavonol quercetin in the pig. *Free radical biology & medicine.* Apr 1 2000;28(7):1056-1067.

217. Reinboth M, Wolffram S, Abraham G, Ungemach FR, Cermak R. Oral bioavailability of quercetin from different quercetin glycosides in dogs. *The British journal of nutrition.* Jul 2010;104(2):198-203.
218. Bokkenheuser VD, Shackleton CH, Winter J. Hydrolysis of dietary flavonoid glycosides by strains of intestinal Bacteroides from humans. *The Biochemical journal.* 1987;248(3):953-956.
219. Shin K-C, Nam H-K, Oh D-K. Hydrolysis of Flavanone Glycosides by β-Glucosidase from Pyrococcus furiosus and Its Application to the Production of Flavanone Aglycones from Citrus Extracts. *Journal of agricultural and food chemistry.* 2013/11/27 2013;61(47):11532-11540.
220. Berger LM, Wein S, Blank R, Metges CC, Wolffram S. Bioavailability of the flavonol quercetin in cows after intraruminal application of quercetin aglycone and rutin. *Journal of dairy science.* Sep 2012;95(9):5047-5055.
221. Berger LM, Blank R, Zorn F, Wein S, Metges CC, Wolffram S. Ruminal degradation of quercetin and its influence on fermentation in ruminants. *Journal of dairy science.* Aug 2015;98(8):5688-5698.
222. Hertog MGL, Hollman PCH, Venema DP. Optimization of a quantitative HPLC determination of potentially anticarcinogenic flavonoids in vegetables and fruits. *Journal of agricultural and food chemistry.* 1992/09/01 1992;40(9):1591-1598.
223. Wang L, Urriola PE, Luo ZH, et al. Metabolomics revealed diurnal heat stress and zinc supplementation-induced changes in amino acid, lipid, and microbial metabolism. *Physiological reports.* Jan 2016;4(1).
224. Lu Y, Yao D, Chen C. 2-Hydrazinoquinoline as a Derivatization Agent for LC-MS-Based Metabolomic Investigation of Diabetic Ketoacidosis. *Metabolites.* Oct 31 2013;3(4):993-1010.
225. Zhang Y, Huo M, Zhou J, Xie S. PKSolver: An add-in program for pharmacokinetic and pharmacodynamic data analysis in Microsoft Excel. *Computer methods and programs in biomedicine.* Sep 2010;99(3):306-314.
226. Feng X, Li Y, Brobbey Oppong M, Qiu F. Insights into the intestinal bacterial metabolism of flavonoids and the bioactivities of their microbe-derived ring cleavage metabolites. *Drug Metabolism Reviews.* 2018/07/03 2018;50(3):343-356.
227. Feliciano RP, Boeres A, Massacessi L, et al. Identification and quantification of novel cranberry-derived plasma and urinary (poly)phenols. *Archives of biochemistry and biophysics.* 2016/06/01/ 2016;599:31-41.

228. Gläßer G, Graefe EU, Struck F, Veit M, Gebhardt R. Comparison of antioxidative capacities and inhibitory effects on cholesterol biosynthesis of quercetin and potential metabolites. *Phytomedicine.* 2002/01/01/ 2002;9(1):33-40.
229. Boots AW, Haenen GRMM, den Hartog GJM, Bast A. Oxidative damage shifts from lipid peroxidation to thiol arylation by catechol-containing antioxidants. *Biochimica et Biophysica Acta (BBA) - Molecular and Cell Biology of Lipids.* 2002/08/08/ 2002;1583(3):279-284.
230. Pourová J, Najmanová I, Vopršalová M, et al. Two flavonoid metabolites, 3,4-dihydroxyphenylacetic acid and 4-methylcatechol, relax arteries ex vivo and decrease blood pressure in vivo. *Vascul Pharmacol.* 2018/12// 2018;111:36-43.
231. Applová L, Karlíčková J, Warncke P, et al. 4-Methylcatechol, a Flavonoid Metabolite with Potent Antiplatelet Effects. *Molecular nutrition & food research.* 2019;63(20):1900261.
232. Yasuoka MM, Monteiro BM, Fantinato-Neto P, et al. Transient Pulmonary Artery Hypertension in Holstein Neonate Calves. *Animals (Basel).* 2020;10(12):2277.
233. Lübke T, Damme M. Lysosomal sulfatases: a growing family*. *Biochemical Journal.* 2020;477(20):3963-3983.
234. Cheng K-J, Jones GA, Simpson FJ, Bryant MP. Isolation and identification of rumen bacteria capable of anaerobic rutin degradation. *Canadian Journal of Microbiology.* 1969;15(12):1365-1371.
235. Bryant MP, Small N. The anaerobic monotrichous butyric acid-producing curved rod-shaped bacteria of the rumen. *Journal of bacteriology.* Jul 1956;72(1):16-21.
236. Krishnamurty HG, Cheng KJ, Jones GA, Simpson FJ, Watkin JE. Identification of products produced by the anaerobic degradation of rutin and related flavonoids by Butyrivibrio sp. C3. *Can J Microbiol.* Aug 1970;16(8):759-767.
237. Winter J, Moore LH, Dowell VR, Jr., Bokkenheuser VD. C-ring cleavage of flavonoids by human intestinal bacteria. *Appl Environ Microbiol.* 1989;55(5):1203-1208.
238. Krumholz LR, Crawford RL, Hemling ME, Bryant MP. Metabolism of gallate and phloroglucinol in Eubacterium oxidoreducens via 3-hydroxy-5-oxohexanoate. *Journal of bacteriology.* May 1987;169(5):1886-1890.
239. Simpson FJ, Jones GA, Wolin EA. Anaerobic degradation of some bioflavonoids by microflora of the rumen. *Can J Microbiol.* Aug 1969;15(8):972-974.
240. Saito Y, Sato T, Nomoto K, Tsuji H. Identification of phenol- and p-cresol-producing intestinal bacteria by using media supplemented with tyrosine and its metabolites. *FEMS Microbiol Ecol.* Sep 1 2018;94(9).

241. Roediger WE, Babidge W. Human colonocyte detoxification. *Gut.* Dec 1997;41(6):731-734.
242. Selmer T, Andrei PI. p-Hydroxyphenylacetate decarboxylase from Clostridium difficile. *European Journal of Biochemistry.* 2001;268(5):1363-1372.
243. Saito Y, Sato T, Nomoto K, Tsuji H. Identification of phenol- and p-cresol-producing intestinal bacteria by using media supplemented with tyrosine and its metabolites. *FEMS Microbiology Ecology.* 2018;94(9).
244. Yokoyama MT, Carlson JR. Production of Skatole and para-Cresol by a Rumen Lactobacillus sp. *Appl Environ Microbiol.* 1981;41(1):71-76.
245. Yokoyama MT, Carlson JR. Production of Skatole and para-Cresol by a Rumen Lactobacillus sp. *Appl Environ Microbiol.* Jan 1981;41(1):71-76.
246. Selmer T, Andrei PI. p-Hydroxyphenylacetate decarboxylase from Clostridium difficile. A novel glycyl radical enzyme catalysing the formation of p-cresol. *Eur J Biochem.* Mar 2001;268(5):1363-1372.
247. Zhou Y, Zhang N, Arikawa AY, Chen C. Inhibitory Effects of Green Tea Polyphenols on Microbial Metabolism of Aromatic Amino Acids in Humans Revealed by Metabolomic Analysis. *Metabolites.* 2019;9(5):96.
248. Andriamihaja M, Lan A, Beaumont M, et al. The deleterious metabolic and genotoxic effects of the bacterial metabolite p-cresol on colonic epithelial cells. *Free radical biology & medicine.* Aug 2015;85:219-227.
249. Shiba T, Kawakami K, Sasaki T, et al. Effects of intestinal bacteria-derived p-cresyl sulfate on Th1-type immune response in vivo and in vitro. *Toxicology and applied pharmacology.* Jan 15 2014;274(2):191-199.
250. Meijers BK, Van Kerckhoven S, Verbeke K, et al. The uremic retention solute p-cresyl sulfate and markers of endothelial damage. *American journal of kidney diseases : the official journal of the National Kidney Foundation.* Nov 2009;54(5):891-901.
251. Borhan MS, Capareda S, Mukhtar S, Faulkner WB, McGee R, Parnell CB. Comparison of seasonal phenol and p-cresol emissions from ground-level area sources in a dairy operation in central Texas. *Journal of the Air & Waste Management Association.* 2012/04/01 2012;62(4):381-392.
252. Canakci M. The potential of restaurant waste lipids as biodiesel feedstocks. *Bioresource Technology.* 2007/01/01/ 2007;98(1):183-190.
253. Liu P, Chen C, Kerr BJ, Weber TE, Johnston LJ, Shurson GC. Influence of thermally oxidized vegetable oils and animal fats on growth performance, liver gene expression, and

liver and serum cholesterol and triglycerides in young pigs. *Journal of animal science.* Jul 2014;92(7):2960-2970.

254. Boler DD, Fernandez-Duenas DM, Kutzler LW, et al. Effects of oxidized corn oil and a synthetic antioxidant blend on performance, oxidative status of tissues, and fresh meat quality in finishing barrows. *Journal of animal science.* Dec 2012;90(13):5159-5169.

255. Rosero DS, Odle J, Moeser AJ, Boyd RD, van Heugten E. Peroxidised dietary lipids impair intestinal function and morphology of the small intestine villi of nursery pigs in a dose-dependent manner. *The British journal of nutrition.* Dec 28 2015;114(12):1985-1992.

256. Yuan J, Kerr BJ, Curry SM, Chen C. Identification of C9-C11 unsaturated aldehydes as prediction markers of growth and feed intake for non-ruminant animals fed oxidized soybean oil. *Journal of Animal Science and Biotechnology.* 2020/05/08 2020;11(1):49.

257. Chao PM, Yang MF, Tseng YN, Chang KM, Lu KS, Huang CJ. Peroxisome proliferation in liver of rats fed oxidized frying oil. *Journal of nutritional science and vitaminology.* Oct 2005;51(5):361-368.

258. Wu G. Amino acids: metabolism, functions, and nutrition. *Amino acids.* May 2009;37(1):1-17.

259. Obando M, Papastergiadis A, Li S, De Meulenaer B. Impact of Lipid and Protein Co-oxidation on Digestibility of Dairy Proteins in Oil-in-Water (O/W) Emulsions. *Journal of agricultural and food chemistry.* 2015/11/11 2015;63(44):9820-9830.

260. Mol M, Regazzoni L, Altomare A, et al. Enzymatic and non-enzymatic detoxification of 4-hydroxynonenal: Methodological aspects and biological consequences. *Free radical biology & medicine.* Oct 2017;111:328-344.

261. Bird MI, Nunn PB. Metabolic homoeostasis of L-threonine in the normally-fed rat. Importance of liver threonine dehydrogenase activity. *Biochem J.* Sep 15 1983;214(3):687-694.

262. Kerr BJ, Kellner TA, Shurson GC. Characteristics of lipids and their feeding value in swine diets. *J Anim Sci Biotechnol.* 2015;6(1):30.

263. Jansman AJ, van Diepen JT, Melchior D. The effect of diet composition on tryptophan requirement of young piglets. *Journal of animal science.* Mar 2010;88(3):1017-1027.

264. NRC. *Nutrient Requirements of Swine.* 10th ed. Washington, DC: National Academy Press; 1998.

265. Palego L, Betti L, Rossi A, Giannaccini G. Tryptophan Biochemistry: Structural, Nutritional, Metabolic, and Medical Aspects in Humans. *J Amino Acids.* 2016;2016:8952520-8952520.

266. Michael AF, Drummond KN, Doeden D, Anderson JA, Good RA. TRYPTOPHAN METABOLISM IN MAN. *The Journal of clinical investigation.* 1964;43(9):1730-1746.
267. Shin M, Ohnishi M, Iguchi S, Sano K, Umezawa C. Peroxisome-proliferator regulates key enzymes of the tryptophan-NAD+ pathway. *Toxicology and applied pharmacology.* Jul 1 1999;158(1):71-80.
268. Tagnon MD, Simeon KO. Aldehyde dehydrogenases may modulate signaling by lipid peroxidation-derived bioactive aldehydes. *Plant Signal Behav.* 2017;12(11):e1387707-e1387707.
269. Kirsch M, De Groot H. NAD(P)H, a directly operating antioxidant? *FASEB journal : official publication of the Federation of American Societies for Experimental Biology.* Jul 2001;15(9):1569-1574.
270. Kamat JP, Devasagayam TP. Methylene blue plus light-induced lipid peroxidation in rat liver microsomes: inhibition by nicotinamide (vitamin B3) and other antioxidants. *Chemico-biological interactions.* Jan 5 1996;99(1-3):1-16.
271. Carter CE. Metabolism of purines and pyrimidines. *Annual review of biochemistry.* 1956;25:123-146.
272. Gentile F, Arcaro A, Pizzimenti S, et al. DNA damage by lipid peroxidation products: implications in cancer, inflammation and autoimmunity. *AIMS Genet.* 2017;4(2):103-137.
273. Ray Chaudhuri A, Nussenzweig A. The multifaceted roles of PARP1 in DNA repair and chromatin remodelling. *Nature Reviews Molecular Cell Biology.* 2017/10/01 2017;18(10):610-621.
274. Saldana CI, Knabe DA, Owen KQ, Burgoon KG, Gregg EJ. Digestible threonine requirements of starter and finisher pigs. *Journal of animal science.* Jan 1994;72(1):144-150.
275. Schaart MW, Schierbeek H, van der Schoor SR, et al. Threonine utilization is high in the intestine of piglets. *J Nutr.* Apr 2005;135(4):765-770.
276. Bird MI, Nunn PB. Metabolic homoeostasis of L-threonine in the normally-fed rat. Importance of liver threonine dehydrogenase activity. *The Biochemical journal.* 1983;214(3):687-694.
277. Guerranti R, Pagani R, Neri S, Errico SV, Leoncini R, Marinello E. Inhibition and regulation of rat liver L-threonine dehydrogenase by different fatty acids and their derivatives. *Biochimica et biophysica acta.* Nov 7 2001;1568(1):45-52.

278. House JD, Hall BN, Brosnan JT. Threonine metabolism in isolated rat hepatocytes. *American Journal of Physiology-Endocrinology and Metabolism.* 2001;281(6):E1300-E1307.
279. Meister A. *Biochemistry of the Amino acids* Vol II. New York: Academic Press; 1965.
280. Mak WW, Pitot HC. Increase of L-serine dehydratase activity under gluconeogenic conditions in adult-rat hepatocytes cultured on collagen gel/nylon mesh. *Biochemical Journal.* 1981;198(3):499-504.
281. Anjum MI, Alam MZ, Mirza IH. Effect of Non-oxidized and Oxidized Soybean Oil Supplemented with Two Levels of Antioxidant on Broiler Performance. *Asian-Australas J Anim Sci.* 5 2002;15(5):713-720.
282. Engberg RM, Lauridsen C, Jensen SK, Jakobsen K. Inclusion of Oxidized Vegetable Oil in Broiler Diets. Its Influence on Nutrient Balance and on the Antioxidative Status of Broilers. *Poultry science.* 1996;75(8):1003-1011.
283. Yoshida H, Kajimoto G. Effect of dietary vitamin E on the toxicity of autoxidized oil to rats. *Annals of nutrition & metabolism.* 1989;33(3):153-161.
284. Liu JF, Huang CJ. Dietary oxidized frying oil enhances tissue alpha-tocopherol depletion and radioisotope tracer excretion in vitamin E-deficient rats. *J Nutr.* Sep 1996;126(9):2227-2235.
285. Ammouche A, Rouaki F, Bitam A, Bellal MM. Effect of ingestion of thermally oxidized sunflower oil on the fatty acid composition and antioxidant enzymes of rat liver and brain in development. *Annals of nutrition & metabolism.* 2002;46(6):268-275.
286. Denno R, Takabayashi A, Sugano M, et al. The ratio of reduced glutathione/oxidized glutathione is maintained in the liver during short-term hepatic hypoxia. *Journal of Gastroenterology.* June 01 1995;30(3):338-346.
287. Metges CC, Yu YM, Cai W, et al. Oxoproline kinetics and oxoproline urinary excretion during glycine- or sulfur amino acid-free diets in humans. *American journal of physiology. Endocrinology and metabolism.* May 2000;278(5):E868-876.
288. Shang F, Lu M, Dudek E, Reddan J, Taylor A. Vitamin C and vitamin E restore the resistance of GSH-depleted lens cells to H2O2. *Free Radical Biology and Medicine.* 2003/03/01/ 2003;34(5):521-530.
289. Meister A. Glutathione, metabolism and function via the gamma-glutamyl cycle. *Life sciences.* Jul 15 1974;15(2):177-190.
290. Tian L, Shi MM, Forman HJ. Increased transcription of the regulatory subunit of gamma-glutamylcysteine synthetase in rat lung epithelial L2 cells exposed to oxidative stress or

glutathione depletion. *Archives of biochemistry and biophysics.* Jun 1 1997;342(1):126-133.

291. Shi MM, Iwamoto T, Forman HJ. gamma-Glutamylcysteine synthetase and GSH increase in quinone-induced oxidative stress in BPAEC. *The American journal of physiology.* Oct 1994;267(4 Pt 1):L414-421.

292. Krzywanski DM, Dickinson DA, Iles KE, et al. Variable regulation of glutamate cysteine ligase subunit proteins affects glutathione biosynthesis in response to oxidative stress. *Archives of biochemistry and biophysics.* Mar 1 2004;423(1):116-125.

293. Lu SC. Regulation of glutathione synthesis. *Mol Aspects Med.* Feb-Apr 2009;30(1-2):42-59.

APPENDIX

Appendix A. Scores plot of serum lipidomes of UH and CH cows.

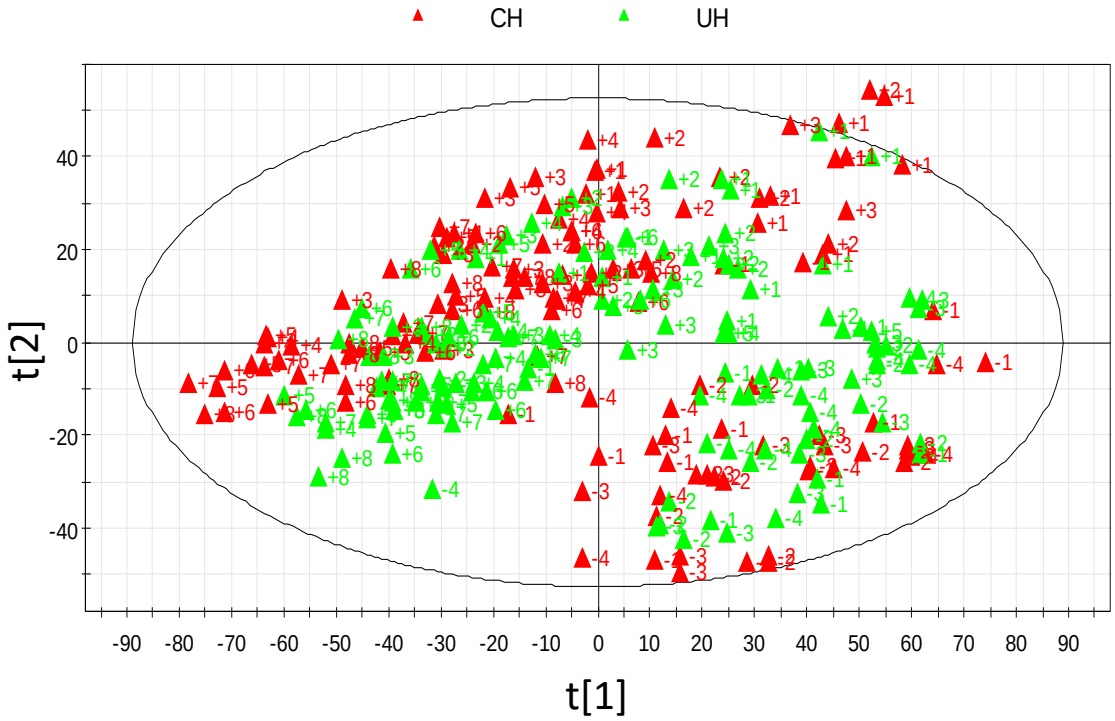

Appendix B. Scores plot and loadings plot of hepatic lipidomes of UH and CH cows.

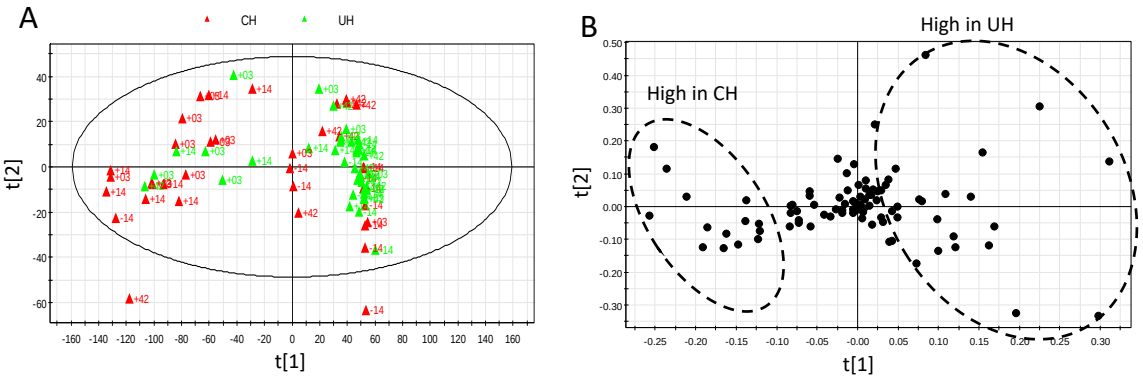

Appendix C. Scores plot of hepatic metabolome of UH and CH cows.